

# The role of Msi2 in adult and embryonic hematopoiesis

Luisa de Andrés Aguayo

---

DOCTORAL THESIS UPF - 2017

DIRECTOR

Dr. Thomas Graf

GENE REGULATION, STEM CELLS AND CANCER  
DEPARTMENT, CENTER FOR GENOMIC REGULATION  
(CRG), BARCELONA





*A mi familia*



## **AGRADECIMIENTOS**

Esta tesis no sólo representa el trabajo llevado a cabo en los últimos cinco años en el laboratorio, sino que también representa para mí la síntesis de los trece años que he estado trabajando en el laboratorio de Thomas. Trece años que han pasado volando pero que, echando la vista atrás, han sido una parte muy importante de mi vida. Durante esta etapa he conocido a mucha gente con la que probablemente haya entablado una amistad que durará toda la vida, también he conocido a gente de la cual me quedará el recuerdo de haber pasado buenos momentos y, también hay que reconocerlo, no tan buenos. Sea como sea espero no dejarme a nadie en los agradecimientos, y si así pasa que vayan por delante mis disculpas.

Para empezar, no hay duda que mi más sincero agradecimiento va para Thomas. Thomas for you is my sincere thanks for all these years that we have spent together. I'm really grateful for giving me the opportunity to work in this project because you knew that I was eager to continue the work of Florencio. All this time you have trust on me and you have let me know that I was able to do it. I appreciate your compliments but also your criticisms, in fact these have turn out to be much more useful than I could imagine. By your side, I have learned to critically approach my research, to communicate more efficiently and to discern the good from the bad of other's work. I have learned that despite our ups and downs, you have always had your door open to talk and you have been willing to listen to me, no matter what happened. And last but not least, I want to thank you as well for being so kind and patience and understanding in certain moments of my life, especially since Mario was born and I had to invest most of my energy in taking care of him.

Mi agradecimiento, muy especial en este caso, también va para Florencio. La verdad es que es difícil encontrar las palabras para expresar lo que has significado para mí. Fuiste el primero en confiar en mí cuando me seleccionaste para trabajar en el laboratorio de Thomas y a pesar de que apenas me conocías, enseguida me hiciste

partícipe de tu proyecto y me diste una responsabilidad que al principio me pareció que me iba grande. Aprendí contigo muchas de las cosas que años después me han permitido desarrollar mi trabajo en el laboratorio, entre ellas el orden, la rigurosidad en el trabajo, la tenacidad para conseguir algo y sobre todo...el sentido del humor. Pero no sólo eso, de lo que más he aprendido es de tu actitud ante la vida, tu capacidad de luchar ante las adversidades, y sobretodo, de no perder la sonrisa y tu sentido del humor a pesar de lo que pueda suceder. Te agradezco también que me hayas abierto las puertas de tu casa, y que haya podido conocer a tu maravillosa familia: a Sonsoles, a tus niñas, Ana y Elena, a tus padres y a tu hermana. Gracias por las tardes en vuestra casa y por esas cenas tan ricas!

Special thanks go to all the past and present members of the Graf's lab: Cathy, Huafeng, Matthias, Jinhang, Alexis, Lars, Fanny, Vanessa, Maribel, Paco, Francesca, Alessandro, Eric, Sabrina, Thien, Bruno, Jose, Tian, Ralph, Carolina and Toni. And sorry to the ones that I forgot to include, unfortunately my memory has always played tricks on me.

I would like to thank also to all the people that I have met during these years in the CRG.

També vull agrair a l'Imma la seva feina amb els estudiants, ja que ens facilita enormement la nostra. Sobretot per no cansar-se de recordar-me tot allò que oblidó (un i altre cop) i pels riures compartits.

A la Gemma per estar allà sempre, “para un roto y para un descosido”, i per les seves paraules de suport i xerrades al lavabo quan cap de les dues estàvem passant els millor moments de la nostra vida.

A Juan, Luciano y Pura, como miembros de mi comité de tesis, por haberme apoyado y aconsejado durante estos cinco años. Gracias por estar ahí!

También quiero agradecer a mi Vanessinha, que a pesar de los años sigue estando ahí, con sus mensajes de apoyo y su cariño. Para mí eres un ejemplo de tenacidad y de lucha por nunca rendirte ante nada y por ser capaz de dar tanto a tanta gente.

Por último y no menos importante, quiero agradecer a mi familia todo su apoyo. En estos últimos cinco años han coincidido los dos eventos más transformadores y trascendentales de mi vida, la muerte de mi padre y el nacimiento de mi hijo. Desafortunadamente fue en este mismo orden, con lo que Mario, mi hijo, no tuvo la oportunidad de conocer a su abuelo, porque estoy segura de que le hubiese enseñado, como hizo conmigo, el amor por la vida y la curiosidad por aprender. De mi padre aprendí a ir más allá y a cuestionarme y, sobretodo a mirar con escepticismo, todo lo que nos rodea. Así que en parte esta tesis es gracias a él también. También me siento agradecida por haber tenido la oportunidad de vivir la maternidad con alguien tan especial como mi hijo. Para mí es otro proyecto, obviamente mucho más importante que nada de lo que pueda hacer, y que durará toda la vida. Y por supuesto, está de más decir que agradezco a mi madre todo lo que ha sido y será capaz de hacer por mí y por mi familia, y su amor y apoyo incondicional a pesar de todo. Es un ejemplo para mí, aunque muchas veces no se lo demuestre. Gracias Anita, Julia y Daniel, por estar ahí y ayudarme y apoyarme siempre. Tengo la suerte de tener tres hermanos estupendos!





# CONTENTS

THESIS ABSTRACT.....	xi
RESUMEN DE TESIS .....	xiii
PREFACE.....	xv
PART I INTRODUCTION .....	1
1    Background.....	3
1.1    The HSC: a historical perspective .....	3
1.2    Characterization of primitive cells in the hematopoietic hierarchy. ....	6
2    Hematopoietic Stem Cell generation and maintenance .....	14
2.1    Embryonic origin of hematopoiesis.....	14
2.2    The adult HSC .....	18
HSC niche cells and regulators. ....	24
The Wnt pathway .....	27
The PI3K/Akt/mTORC1 pathway.....	31
3    The role of Musashi 2 in murine hematopoiesis.....	38
3.1    The identification of Msi2 in mouse HSCs .....	38
3.2    Msi2 in mouse models of leukemia.....	42
3.3    Mechanisms of Musashi action .....	43
PART II RESULTS .....	49
Chapter 1.....	51
Musashi 2 is a regulator of the hematopoietic stem cell compartment identified by a retroviral insertion screen and knockout mice	
Chapter 2.....	133

Characterization of the hematopoietic system during embryo  
development in Msi2 deficient mice

Chapter 3.....	151
Msi2 targets and their role in the regenerating hematopoietic system	
PART III DISCUSSION .....	179
REFERENCES .....	191

## THESIS ABSTRACT

The life-long production of blood cells is enabled by hematopoietic stem and progenitor cells (HSPC) residing in the bone marrow. An understanding of the genes that control how HSPCs work to sustain the continued production of blood cells will enable new techniques to expand them for life-saving transplantation therapies. We have used a retroviral integration screen to search for novel genes that regulate hematopoietic stem cell (HSC) function. One of the genes found was Musashi 2 (Msi2), an RNA binding protein that can act as a translational inhibitor. A gene trap mouse model that inactivates the gene shows that Msi2 is more highly expressed in long term (LT) and short term (ST) HSCs as well as in lymphoid myeloid primed progenitors (LMPPs), but much less in intermediate progenitors and mature cells. Mice lacking Msi2 are fully viable up to more than a year but exhibit severe defects in primitive precursors. Cell cycle and gene expression analyses suggest that the main hematopoietic defect in Msi2 defective mice consists in a decreased proliferation capacity of ST-HSCs and LMPPs. Moreover, HSCs lacking Msi2 are severely impaired in competitive repopulation experiments. We further found that Msi2 is expressed during embryo development in the CD41+ cells in the Aorta-Gonada Mesonephros (AGM), most probably corresponding to the earliest emerging HSCs. Also deficient Msi2 embryos have a decrease in the number of fetal liver HSPCs. Lastly, our experiments show that Msi2 deficient HSPCs have a defect in the Wnt and PTEN/PI3K/Akt pathways that could explain the phenotype

observed. Altogether, my thesis provides novel insight in to the role and mechanism of action of Musashi-2 in mouse HSPCs.

## **RESUMEN DE TESIS**

La producción de células sanguíneas a lo largo de toda la vida se lleva a cabo gracias a las células madre hematopoyéticas y células progenitoras (HSPC) que residen en la médula ósea. El estudio de los genes que controlan cómo estas HSPCs trabajan para sostener la producción continua de las células de la sangre permitirán el desarrollo de nuevos protocolos basados en la expansión ‘in vitro’ de estas células para terapias de trasplante. Hemos utilizado un cribado basado en el fenómeno de integración retroviral para buscar nuevos genes que regulan la función de células madre hematopoyéticas (HSC). Uno de los genes encontrados fue Musashi 2 (Msi2), una proteína de unión a ARN que puede actuar como un inhibidor de la traducción. El modelo de ratón desarrollado mediante “gene-trap” y que inactiva el gen, muestra que Msi2 está más expresado en HSCs de largo plazo (LT-HSC) y corto plazo (ST-HSC), así como en los progenitores linfoides-mieloides (LMPP), y su expresión disminuye en progenitores intermedios y células maduras. Los ratones deficientes para Msi2 son completamente viables, pero presentan defectos importantes en los precursores primitivos que se agravan con la edad. El análisis de ciclo celular y de expresión génica sugieren que el principal defecto hematopoyético en ratones con esta deficiencia consiste en una disminución de la capacidad de proliferación de ST-HSCs y LMPPs. Además, las HSCs con déficit de Msi2 no son capaces de repoblar la médula ósea cuando se transplantan junto a médula procedente de ratones “wild-type”. También hemos observado que Msi2 se expresa durante el desarrollo

del embrión en las células CD41 + de la Aorta-Gonada Mesonefros (AGM), correspondiendo muy probablemente a las HSCs emergentes. Además los embriones deficientes para Msi2 tienen una disminución en el número de HSPC en hígado fetal. Por último, nuestros experimentos muestran que un déficit de Msi2 en las HSPCs provoca un defecto en las vías Wnt y PTEN / PI3K / Akt; esto podría explicar el fenotipo observado en estos ratones. En conjunto, mi tesis proporciona una nueva perspectiva sobre el papel y el mecanismo de acción de Musashi-2 en HSPCs de ratón.

## **PREFACE**

This thesis provides novel insights into the mechanism by which Msi2 regulates self-renewal and function in mouse hematopoietic stem cells (HSCs).

## PART I INTRODUCTION



## **1 BACKGROUND**

Hematopoiesis is the process by which blood cells are formed. The production of these cells relies on a rare population of multipotent hematopoietic stem cells (HSCs) that is able to produce trillions of blood cells during mammal's lifespan. The HSCs have the capacity to self-renew (in order to maintain the HSCs pool intact) or divide into increasingly lineage-restricted myeloid, erythroid and lymphoid intermediates which undergo massive proliferation and sequential differentiation to produce mature blood cells. The hematopoietic system represents a continuum of cells with changing phenotype and properties as they progress from stem to differentiated cells.

### **1.1 The HSC: a historical perspective**

Although the discovery of hematopoietic stem cell has been historically credited to James Till and Ernest McCulloch in 1963, the use of the term can be traced back to the late 19<sup>th</sup> century, when the German physician and hematologist Artur Pappenheim drew the first genealogy of hematopoiesis that positioned a precursor cell ("Stammzelle") at the center and stated that this cell was capable of giving rise to both red and white blood cells (Figure 1)<sup>1</sup> .

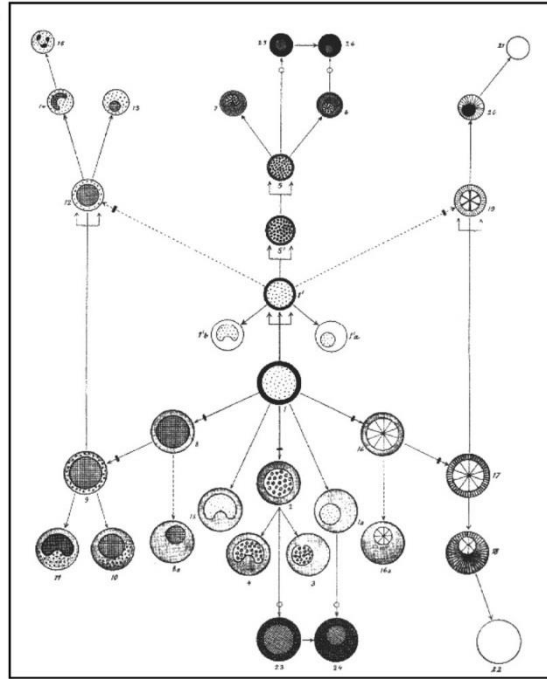


**Figure 1.** Artur Pappenheim's view of hematopoiesis from 1905. The cell in the center is the hypothesized common progenitor of the entire blood system. Pappenheim called this cell, among other terms, the stem cell. Adapted from Ramalho-Santos et al. (2007)<sup>1</sup>

Due to limitations of the experimental methods available at that time, the debate about the existence of a common hematopoietic stem cell continued for several decades, being the development of atomic bomb and the consequences of the exposition of the human body to ionizing radiation a big boost in the research. By the 1950's scientists, on their attempts to find a treatment for patients that were exposed to lethal doses of radiation, found that spleen and bone marrow transplants could rescue lethally irradiated mice <sup>23</sup>. Moreover, these early experiments demonstrated that the survival was due to the proliferation of donor cells in the bone marrow of the transplanted

mice <sup>4</sup>. Starting in 1960, Till and McCulloch published a breakthrough series of experiments that made possible that hematopoiesis could be studied as a quantitative science: in their initial work they were able to quantify the number of transplanted cells necessary to provide radioresistance in mice <sup>5</sup>. These experiments quickly led to follow up studies where they found that transplanted bone marrow led to the formation of macroscopic hematopoietic colonies on the recipient mouse's spleen <sup>6</sup>, and that these colonies (now called spleen colony forming units, CFU-S) contained at least four blood cell types: monocytic, granulocytic, erythroid and megakaryocytic. Moreover, the number of colonies was linearly related to the number of bone marrow cells transplanted. In perhaps the most brilliant experiment of the series, they induced gross chromosomal aberrations by sublethally irradiating the donor cells, so they were detectable by cytogenetic analysis. Then they transplanted them to form CFU-S that were genetically distinct and whose chromosome marks existed in all dividing cells of the colony, proving definitively that each multilineage colony were indeed clonal and thus derived from a single cell <sup>7</sup>. One of their last important findings of this period was to show that many of these spleen colonies also contain daughter cells that generated similar macroscopically visible, multilineage colonies in the spleens of secondary irradiated recipients <sup>8</sup>, nonetheless the numbers and types of mature and primitive cells present in individual spleen colonies varied widely and independently, in other words these cells were "stochastic" in nature <sup>9</sup>. Despite the important insights afforded by these early experiments, not all their methods have stood the test of time.

Subsequent studies revealed that spleen colony formation is obtained from a biologically more heterogeneous population than was originally appreciated, and that only a very tiny part of this population was composed by long-term repopulating cells <sup>10</sup>. Altogether, it cannot be understated the lasting contribution Till and McCulloch had in the field of stem cell research: not only their findings provided the foundation for the proof of the existence of HSCs but they also served to establish the importance of clonogenic assays to detect and quantify the hematopoietic stem cells and paved the way for the foundation of modern approaches to quantify stem cell frequency. More broadly, HSCs have become a paradigmatic model for all types of adult stem cells in the body.

## **1.2 Characterization of primitive cells in the hematopoietic hierarchy.**

### 1.2.1 Prospective isolation of HSCs

Till and McCulloch found early on that CFUs are a heterogeneous population, containing cells that self-renewed and could propagate secondary colonies while others did not. A study by Worton et al. provided the first demonstration of the prospective isolation of different classes of early stem and progenitor cells, where they achieved by density centrifugation methods, the isolation of distinct fractions of cells that upon transplantation gave rise to CFU-S with varying degrees of self-renewal capacity <sup>11</sup>. Over the next ten years two important techniques were developed that revolutionized the study of HSCs and their purification from the milieu of cells in the bone marrow: the development of fluorescently labeled monoclonal

antibodies against cell surface antigens of immune cells<sup>12</sup> and that of multiparametric flow cytometry (FACS) to analyze the expression of surface markers on single cells<sup>13</sup>. These methods led to a systematic dissection of the cell-surface phenotype of hematopoietic progenitor and stem cells by Irving Weissman and colleagues, during the 1980s. The initial prospective purification of hematopoietic stem cells from mouse bone marrow was achieved by isolation of a population that was negative for lineage markers (B220, CD4, CD8, Mac-1 and Gr-1) and expressed Thy-1 and Sca-1 antigens (Lin- Thy-1low Sca-1+). Spangrude and colleagues demonstrated that these were the only cells in mouse Bone Marrow (BM) capable of transferring long-term reconstitution of the entire hematopoietic system (defined as persistence for more than 3 months) when transplanted into lethally irradiated mice<sup>10</sup>. Since these initial studies, nearly three decades have been spent searching for the cell surface marker combination that would allow the purification of HSCs to near homogeneity through the process of FACS purification and transplantation<sup>14–19</sup>. Comparison of the engraftment capabilities of different FACS purified populations resulted into the dissection of multiple classes of HSCs and their progenitors that resulted in a widely accepted hierarchical model of hematopoiesis, where progenitor cells progressively differentiate in a stepwise manner while they undergo a loss of self-renewal potential (Figure 3A). At the apex of the hierarchy are the multipotent long term HSCs (LT-HSCs), which are able to repopulate recipients for at least 16 weeks after transplantation. Through a process of asymmetric cell division LT-HSCs can self-renew to sustain the stem cell pool and differentiate

into short-term HSCs (ST-HSCs) and lineage-restricted progenitors. ST-HSCs or multipotent progenitors (MPPs) are able to produce various types of mature blood cells upon transplantation, but detectability of ST-HSC derived cells in the peripheral blood and bone marrow declines after 12 weeks and from MPPs in less than 6 weeks. (Figure 2)

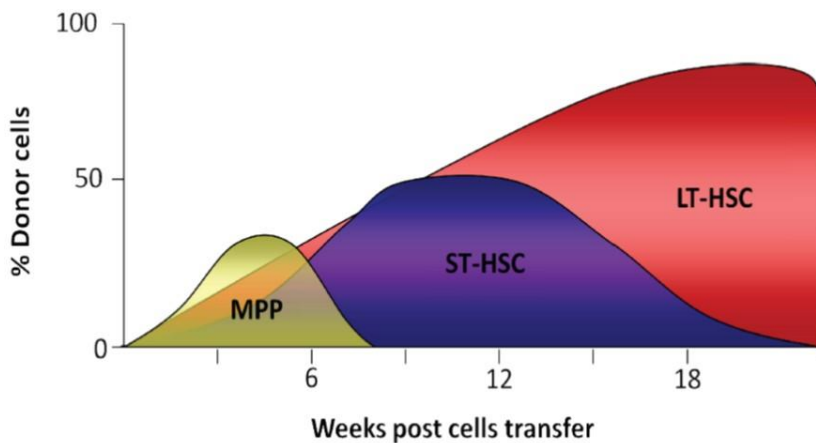


**Figure 2.** Transplantation kinetics of mouse hematopoietic stem and progenitor cells (HSPCs). Cartoon shows schematics of general engraftment and survival kinetics of three subsets of mouse HSPCs. Adapted from Stefan Rentas with permission.

MPPs undergo extensive proliferation and differentiation to produce common myeloid and common lymphoid progenitor populations (CMP and CLP), that eventually will give rise to more differentiated cells (granulopoietic, megakaryocytes and erythroid cells on one hand, and lymphoid cells on the other) <sup>20,21</sup>. This simple myeloid/lymphoid bifurcation model, although conceptually attractive, has subsequently come under question with more recently acquired experimental data. Studies combining single cell gene

expression analysis with clonal functional assays have revealed that significant numbers of multipotent hematopoietic cells coexpress genes associated with multiple different lineages, a phenomenon termed multilineage priming, increasing the heterogeneity within both HSC and MPP populations. Adolfson et al found that, although HSCs generate all hematopoietic lineages, they specifically express myeloid- and MegE-associated genes but not lymphoid genes; moreover they identified a population of lymphomyeloid-restricted progenitors in the MPP compartment, termed lymphoid primed multipotent progenitors (LMPPs), that represented the most primitive cells to express common lymphoid genes<sup>22</sup> (Figure 3B). Both the original and the revised model of hematopoiesis assume that self-renewal and commitment are separated such that multipotency is lost only upon exit from the self-renewing stem cell compartment, the only difference between the two models is the level at which lymphoid versus myeloid restriction occurs. However, single cell transplantation studies have shown that individual HSCs exhibit different stable myeloid or lymphoid biases, revealing functional heterogeneity in the most-purified HSC compartment<sup>23,24</sup>. In a recent elegant work Yamamoto et al<sup>25</sup> demonstrated that a large number of cells in the most primitive HSC compartment have undergone myeloid commitment but have long-term self-renewal and engraftment capacity, features considered as the hallmark of stem cells. These myeloid restricted progenitors (MyRPs) arise directly from HSCs upstream of the traditional committed progenitors. These findings suggest a new model of hematopoietic differentiation where

a substantial proportion of MegE and myeloid cells may be derived from this myeloid bypass pathway (Figure 3C).

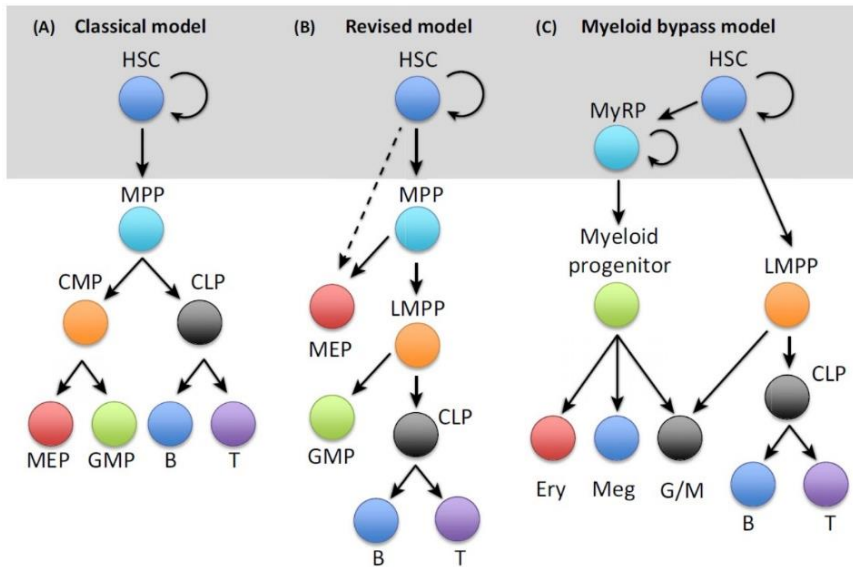


**Figure 3.** Classic and revised models of hematopoiesis. Adapted from Nimmo RA et al (2015)<sup>26</sup>

### 1.2.2 In vivo and in vitro assays to assess hematopoietic stem cell function

As described in the previous section, dissection of the hematopoietic hierarchy and characterization of the different hematopoietic progenitor populations was possible due to the development of transplantation assays that measure the functional potential of an unknown source of HSCs after transplantation into lethally irradiated mice. Nowadays transplantation experiments still serve as the gold standard for quantitative and qualitative analyses of murine HSC biology. The most common of these assays is the competitive repopulation assay<sup>27</sup>, which measures the functional potential of an



unknown source of HSCs against a known number of HSCs (usually whole bone marrow cells from congenic wild-type mice). While providing information about the function of HSCs in their capacity to repopulate compared to the competing bone marrow, this assay provides qualitative or at best semi-quantitative information about the HSCs within a given population. In order to quantify the number of actual functional LT-HSCs in a given population, the limiting dilution assay (LDA) is used. In this assay, a series of dilutions of the donor test cells are competed against a set number of competing bone marrow cells. The number of mice negative for reconstitution in each cell dose is then measured, and the frequency of HSCs is estimated using Poisson statistics<sup>28-30</sup> But the most stringent test of HSC potential is the serial transplantation assay, based on the fact that only the most immature HSCs are capable of sustaining hematopoiesis throughout serial transplantation<sup>31</sup>. In this assay, the source of HSCs is sequentially transplanted into irradiated recipients, and the ability of this population to sustain hematopoiesis by presumptive self-renewing divisions is determined. A key aspect in any transplantation assay is to ensure that engrafted test cells can be distinguished from both the competitive and recipient cells. This is most often accomplished by using donor congenic mouse strains that express different alleles for the pan leukocyte antigen CD45 (CD45.1 or CD45.2) while the recipient strain is heterozygous for both alleles (CD45.1/CD45.2)<sup>32</sup>.

It is well known that despite phenotypic uniformity, hematopoietic stem cells (HSC) possess great functional heterogeneity. From the methods described above, only the single cell transplantation

approach allows to assess the function and stemness of single HSC cells in a heterogeneous population. Unfortunately, this assay is very difficult to perform technically, time consuming and costly as it requires lots of animals. Alternative strategies emerged consisting of in vivo approaches that do not depend on HSC isolation. A classic approach of this type consists of tracking HSC clones marked with stably integrated retroviral vectors<sup>33</sup> Originally, it was assumed that these integrations are randomly distributed over the genome and do not confer a selective advantage to the cell. However, molecular analysis of hematopoiesis in mice after serial transplantation of retrovirally marked HSC revealed a surprising accumulation of vector insertions in genes known to be involved in the growth/survival regulation of HSC<sup>34</sup>. A relatively large database of those insertions confirmed that integrations into growth-regulatory genes become particularly dominant<sup>35</sup>, showing that the distribution of insertions in long-term reconstituting cells significantly differs from that in freshly transduced cells and suggesting an in vivo selection towards ‘supportive insertions’. Similarly, a non-random distribution of retroviral vector insertion sites with the MDS1/EVI1 locus, representing the most hit locus, was established in HSC clones reconstituting long-term hematopoiesis in non-human primates<sup>36</sup>. The subsequent demonstration that murine leukemia virus (MLV)–based vectors preferentially target the promoter regions of active genes<sup>37</sup>, and the recurrent activation of the LMO2 oncogene after integration of an MLV–based vector in a human gene therapy trial<sup>38</sup>, showed that insertion events can activate proto-oncogenes. These observations suggested that previous conclusions of HSC dynamics

based on gamma-retroviral gene marking should be confirmed with improved vectors that have a limited capacity to transactivate endogenous genes.

The low trans-activation activity of self-inactivating lentiviral vectors (LVs) made them the ideal candidates for tracking HSC clones *in vivo*. In fact, Guenechea et al. showed that lentivirally transduced HSCs have no competitive repopulation advantages over untransduced HSCs<sup>39</sup>. Moreover, the predicted safety of lentiviral vectors was challenged in a tumour-prone mouse model (*Cdkn2a*<sup>-/-</sup>), increasing the sensitivity to the genotoxicity caused by vector integration. In this scenario, lentiviral vector transduction, even at high integration loads, did not accelerate tumorigenesis in transplant recipients. In contrast, retroviral MLV-based vector transduction triggered a dose-dependent acceleration of tumor onset dependent on integration at known proto-oncogenes and cell cycle genes<sup>40</sup>. Lentiviral vectors have been widely used for cell tracking experiments<sup>41-44</sup>. Techniques to trace cells using distinct viral insertion sites have been improved by increasing the sensitivity and resolution of single-cell clones detection through PCR-based strategies, Sanger sequencing detection, microarray or DNA barcoding<sup>43,45,46</sup>. More recently, stem cell barcoding has gone a step further, by overcoming the drawbacks of using bone marrow transplantation to experimentally evaluate HSCs: much of what we know today about HSCs may therefore be largely influenced by transplantation and not reflective of normal homeostatic blood production. Camargo et al. have described clonal dynamics of hematopoiesis in mice engineered with doxycycline induced

Sleeping Beauty Transposase. The enzyme mediates the mobilization of a transposon that is randomly inserted into a unique position, creating a stable genomic tag, that allows to track blood production from individual clones, without the need for transplantation<sup>47</sup>.

These findings suggest that we may have to change our definition of an HSC to distinguish the cell capable of inducing repopulation from that which contributes to normal hematopoiesis. I discuss in more detail about this paradigm shift of HSC definition in the following sections.

## **2 HEMATOPOIETIC STEM CELL GENERATION AND MAINTENANCE**

### **2.1 Embryonic origin of hematopoiesis**

#### **2.1.1 Primitive and definitive hematopoiesis**

Hematopoietic stem cells emerge during early embryogenesis. During development, the embryo produces several waves of hematopoiesis (primitive and definitive) that produce specialized subsets of hematopoietic cells. (Figure 4)

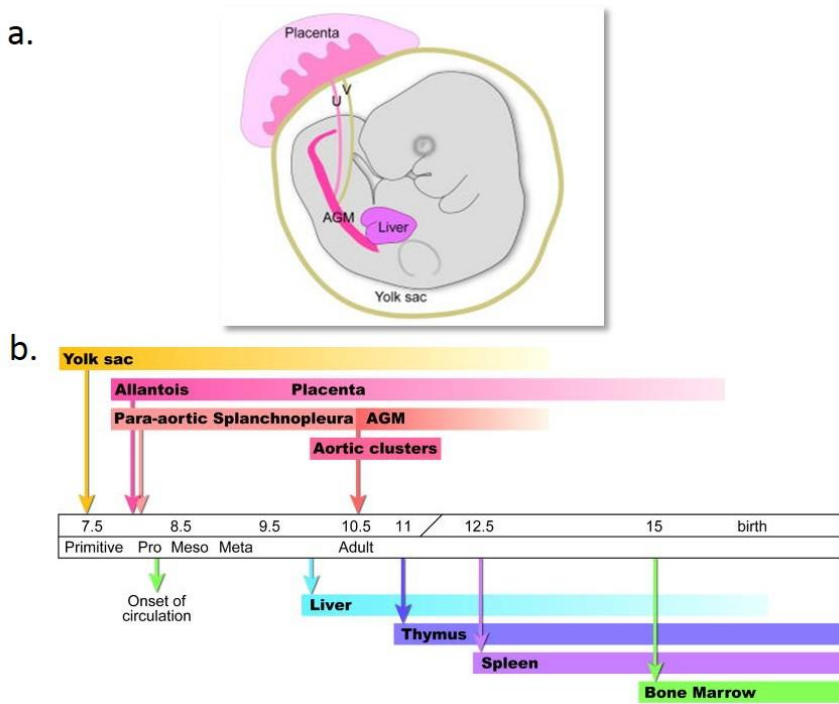


**Figure 4.** Mouse conceptus at E (embryonic day) 10.5 showing the anatomical position of the Aorta-Gonada-Mesonephros (AGM), the placenta and the liver (a) Timeline of hematopoietic events in the mouse conceptus. Arrows above indicate the onset of specific hematopoietic cell generation and/or appearance; arrows below indicate the earliest time of colonization of the secondary hematopoietic territories (b). Adapted from Dzierzak et al (2008)<sup>48</sup>

The first wave of hematopoiesis in both mice and humans occurs in the yolk sac starting at mouse embryonic day (E) 7.5, and results in the production initially of myeloid and erythroid cells that helps the developing embryo through its first growth steps<sup>49</sup>. Additional mature and more primitive hematopoietic cell types appear subsequently, including the first lymphoid cells<sup>50,51</sup> Transplantable cells that display the self-sustaining properties of HSCs arise even later in midgestation, predominantly from hemogenic cells with endothelial features in the ventral wall of the dorsal aorta, in a region

termed the aorta-gonad-mesonephros (AGM) (Figure 4a) <sup>48,52–55</sup> In the AGM region, intra-aortic hematopoietic clusters (IAHCs) are observed in the ventral wall of the dorsal aorta and are the presumptive structures that contain developing HSCs <sup>56</sup>. HSCs are generated in a process termed the endothelial-to-hematopoietic transition (EHT) that is conserved across vertebrates and that occurs in the embryonic (E) day 10-E11 <sup>53,57–59</sup>. This transition occurs in a three-step process initiated by CD31+ c-kit- CD45- endothelial-like cells, that became CD31+ c-kit+ CD45- pre-HSCs and then generates CD31+ c-kit+ CD45+ cells (Figure 5).

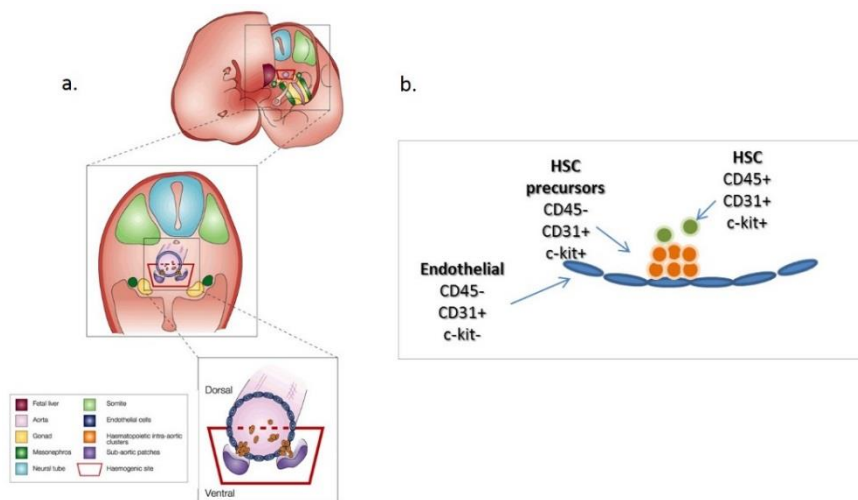


**Figure 5.** General structure of an ED10.5–11 mouse embryo, showing the location of the aorta, gonads and mesonephros, as well as the area that has haemogenic activity (red outline). On the bottom, an enlargement of the aortic region, schematically showing the intra-aortic clusters, which are restricted to the ventral part (floor) of the vessel. The area that has haemogenic activity is shown in a red box. AGM, aorta–gonad–mesonephros; ED, embryonic day; HSC, haematopoietic stem cell (a). Schematic representation of the endothelial/hematopoietic populations present in the AGM region during the endothelial-to-hematopoietic (EHT) transition (b). Adapted from Godin et al. 2002<sup>56</sup>

More recently, the placenta has been defined as another anatomical site that participates in HSC development<sup>60,61</sup> In fact, the placenta is a major hematopoietic organ contributing to both generation and expansion of multipotent hematopoietic stem and progenitor cells. The first HSCs in the placenta appear at E10.5-11.0, concurrently with the AGM, and HSC activity increases rapidly by E12.5-13.5. HSCs in the placenta display the classical surface phenotype of actively cycling fetal HSCs, expressing CD34 and c-kit, and they are considered a more immature population when compared with the HSCs seeding the fetal liver (see next section)

Despite the multiple sites of origin of different types of blood cell precursors during development, including the final generation of HSCs, lineage tracing experiments have suggested that, at least in mice, all of the HSCs detectable throughout adulthood are derived from cells that acquire hematopoietic potential before birth <sup>62,63</sup>

### 2.1.2 Secondary hematopoietic territories in the embryo

The newly generated HSCs then enter the circulation and colonize the fetal liver, starting from late E9 onward (Figure 4b). Later the spleen and thymus are seeded either directly from circulating cells or from the fetal liver <sup>64,65</sup>. In the fetal liver, HSCs undergo multiple rounds of symmetrical self-renewing cell divisions to give rise to the pool of stem cells required for the lifetime of the organism. Just before birth HSCs migrate to developing niches in the bone marrow where they remain concentrated throughout adult life, although some may also recirculate.

## 2.2 The adult HSC

### 2.2.1 Fate options

HSCs are responsible for maintaining steady state hematopoiesis and for responding rapidly to potential crises including acute blood loss, injury and infection, facilitating the recovery of normal blood levels. To accomplish this, a complex balance of different cell fate decisions is taking place in the natural microenvironment of HSCs. These fate options are controlled by fine-tuned interactions of intrinsic (cell-autonomous) and extrinsic (cell non-autonomous) signals.<sup>66-68</sup> (described in more detail in the next sections) and include the possibility of quiescence, self-renewal, differentiation or apoptosis (Figure 6)<sup>69</sup>. Still, relatively little is known about how (and if) these different intrinsic and extrinsic cues interact in networks<sup>70</sup>.

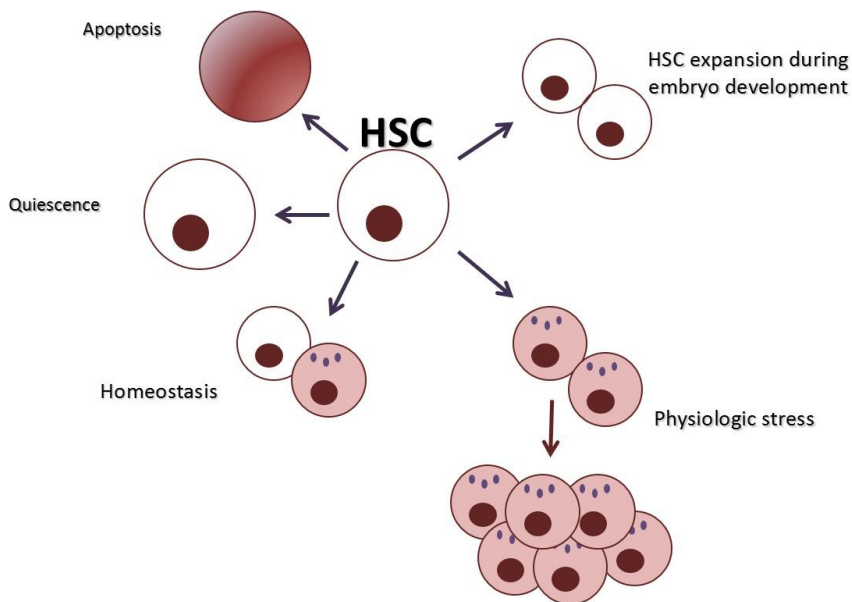


**Figure 6.** The biological properties of HSCs vary to meet the demands of the organism.



### 2.2.2 HSC quiescence, homeostasis and self-renewal

Around three weeks after birth mouse development undergoes a major switch from fetal to adult hematopoiesis, completely changing the cycling rate of HSCs from highly active to a hibernation state known as quiescence<sup>71,72</sup>. It is believed that quiescence is a protective mechanism intended to prevent DNA damage and premature exhaustion of HSCs, thereby ensuring long-term performance of the otherwise stress sensitive HSC<sup>73</sup>. If the body is exposed to hematopoietic stress and urgently needs more blood cells, HSCs can be (reversibly) activated and enter the cell cycle, facilitating fast reestablishment of hematopoietic homeostasis<sup>74,75</sup>. As they divide, somatic cells go through the different phases of the cell cycle, G1 (interphase), S (DNA synthesis phase) G2 (interphase) and M (mitosis phase)<sup>76</sup>. Fluctuations in cyclin-dependent kinases (CDKs) and cyclins control progression through these phases<sup>77</sup>. Inhibitory effects on CDK-cyclin complexes may lead to cell cycle arrest, differentiation, quiescence, or even apoptosis<sup>77</sup>. Important negative regulators of CDKs are the CDK inhibitors (CKIs), divided into two families, the Ink4 and the Cip/Kip family. The Ink4 members (p15, p16, p18 and p19) cause G1 arrest through competition with cyclin D. At low levels, the Cip/Kip family members p21, p27 and p57 bind to cyclin-CDK complexes and promote their assembly, whereas at high levels they abrogate CDK activity, thus negatively regulating cell cycle progression<sup>78</sup>. The DNA-labeling thymidine analog 5-bromo-2-deoxyuridine (BrdU) has been used to study the phenomenon of quiescent HSCs. In vivo BrdU experiments demonstrated that although 75% of the HSCs are quiescent at any

given moment, they are all regularly recruited into the cell cycle, dividing on average every 57 days<sup>79</sup>. However, more recent label retaining studies, using drug-inducible histone 2B-GFP (green fluorescent protein) expression, discovered that a subpopulation of the HSC population divided only every 145 days, equivalent to five times per lifetime. This suggested the presence of two populations of HSCs, where the more dormant one is thought to be triggered upon hematopoietic stress<sup>74,80</sup>. These findings suggest that LT-HSC do not in fact contribute very much to steady-state hematopoiesis, but instead are only activated during stress (e.g. immune activation and blood loss)<sup>81</sup>.

Two important studies further support this view<sup>47,82</sup> by demonstrating through different lineage tracing experimental designs, that during homeostatic maintenance of hematopoiesis, MPPs and committed progenitors, typically understood to be non-self-renewing, persist for long periods of time and are responsible for the bulk of blood cell production. In the study by Busch et al. the investigators found after labeling HSCs with YFP, that there was a moderate percentage (30%) of predicted LT-HSCs contributing to the production of mature cells, however, the actual total output of cells from these LT- HSCs across lineages was exceedingly small at <1%, a value that did not change over any period of time measured. Similarly in the study by Sun et al., fewer than 5% of LT-HSC clones were found in mature cell populations nearly one year after inducing genetic tagging (a laboratory mouse's lifespan is typically 2 years), whereas half of the MPP and myeloid progenitor clones contributed mature hematopoietic cells. Additionally Sun et al. found that 4

months after genetically marking cells (a time point they predicted should allow activation of HSCs) large and diverse changes were observed in the clonal contribution of hematopoietic populations, providing evidence that steady-state hematopoiesis is maintained by successive recruitment and proliferation (or waves) of many progenitors that are longer-lived than previously thought.

Thus, the best evidence to date suggests that only during hematopoietic stress do HSCs provide meaningful support to re-establish equilibrium in hematopoiesis<sup>74,82–84</sup>, as well as other highly proliferative events like aiding the initial development and establishment of the growing hematopoietic system during post-natal growth<sup>82</sup> (Figure 7).

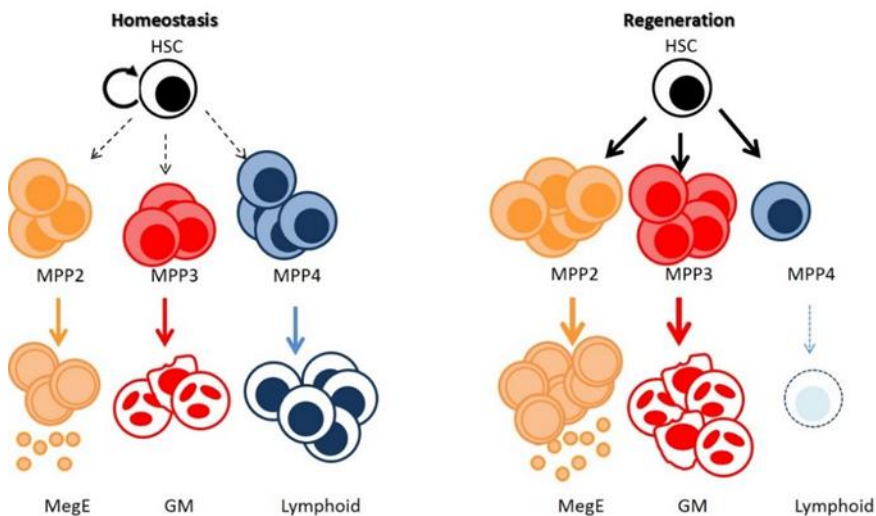


**Figure 7.** Unequal distributions of distinct subsets of lineage-biased multipotent progenitors control blood production in normal and regenerative conditions.

The process of self-renewal is a defining feature of HSCs essential to prevent depletion of the HSC pool. When a cell divides, the outcome can be either self-renewal, where at least one daughter cell preserves the stem cell properties, or differentiation, generating committed

cells. A symmetric division will generate two identical daughter cells, either with HSC characteristics and thus expanding the HSC pool, or it will give rise to two progenitor cells destined for differentiation<sup>85</sup>. While expansion is important during development and in situations of hematopoietic stress, self-renewal has to be tightly controlled to avoid a premature exhaustion of HSCs or improper differentiation. Asymmetrical division of HSCs, resulting in one stem cell and one committed progenitor cell, ensures enough production of all short-lived mature blood cells while maintaining the HSC pool<sup>85</sup>. Mechanisms for asymmetric cell division have been well studied in model systems such as *Drosophila* neural stem cells (neuroblasts) and *C. elegans* embryos<sup>86</sup>. These models generally show an intrinsic axis of polarity that directs unequal partitioning of fate determinants (typically proteins or mRNA) during mitosis which influence downstream signaling pathways and gene expression programs to elicit fate changes in the recipient cell<sup>87</sup>. Neurogenesis in *Drosophila* proceeds through apical-basal neuroblast cell divisions, where the cell dividing away from the neuroepithelium undergoes differentiation to a mature neuron<sup>88</sup>. Null mutants for proteins that segregate into the neuronal precursor cell and direct differentiation, such as Numb, result in unchecked cell division and tumor growth<sup>88</sup>. Thus, modulating the activity of genes that function in asymmetric cell division has a direct effect on stem cell numbers.

There are very few examples of HSCs undergoing asymmetric division *in vitro* in the manner described above (unequal partitioning of fate determinants at mitosis) and no direct evidence of it occurring *in vivo*, although mathematical modelling of lineage tracing data

from fluorescently tagged HSCs does favor its occurrence <sup>82</sup>. Evidence for in vitro asymmetric division in mouse HSPCs was provided by time-lapse imaging and a GFP reporter that indicates active Notch signaling. By tracking single cell divisions the Reya group found that some of the HSPCs gave rise to one sister cell that remained GFP+ and the other one that was GFP-. This asymmetric activity in Notch signaling was attributed to unequal partitioning of Numb protein since its presence is known to suppress Notch<sup>86</sup>. Several additional studies determined whether knockdown/knockout or overexpression of a particular gene of interest impacts symmetric renewal (none of the daughters express Numb), symmetric differentiation (both daughters inherit Numb) and asymmetric division (one daughter gets Numb) in HSCs <sup>89-91</sup>. That the segregation pattern of Numb is significant for the downstream function of HSPCs appears unlikely since conditional deletion of Numb shows normal hematopoiesis at steady-state and during transplantation <sup>92</sup>. However, Wu et al. observed that overexpression of Numb promotes a loss of primitive cells during in vitro culture <sup>93</sup>. To show that Numb, or indeed any other protein that potentially segregates asymmetrically during HSC cell division, would require creation of a lineage tracing mouse such as the one identifying histone-label retaining dormant LT-HSCs in a pulse chase protocol developed for this purpose <sup>74</sup>. Besides from Numb, other proteins that have been shown to segregate asymmetrically in mouse HSPCs include Ap2a2 <sup>94</sup> and in humans the HSC markers CD133 and CD34 <sup>95-97</sup>.

### 2.2.3 The HSC niche and cell-extrinsic pathways

**HSC niche cells and regulators.** HSC self-renewal and hematopoietic differentiation are tightly controlled by multiple positive and negative regulatory elements. Both intrinsic as well as extrinsic mechanisms are likely to be involved in the regulation of these processes. Extrinsic pathways include cues that are dictated by the stem cell microenvironment. Adult HSCs reside in a specialized three-dimensional microenvironment in the BM known as the HSC niche, which comprises different cell types, signaling cascades and gradients as well as physical factors<sup>98</sup>. Two distinct anatomical niches have been proposed, the endosteal and the vascular niche<sup>18,99–102</sup>. Although for some time the endosteal niche was proposed to mediate maintenance of HSC quiescence, while the vascular niche to provide an environment for active HSCs<sup>103,104</sup>, recent studies suggest that the distinction between these two regions is not so clear. It has been proposed that the sinusoidal vessels reside in close proximity to the endosteum<sup>100,102</sup>, insinuating that these candidate niches may actually be connected and both play important roles in the regulation of HSCs. Moreover, recent studies suggest that cells that form the endosteal niche (mainly osteoblasts) could regulate HSCs indirectly, through their effect on lymphoid progenitors, while HSCs mainly reside in the perivascular (endothelial) niche<sup>105,106</sup>. Probably, HSCs are not static, but instead dynamically change their niche location in response to injury or to feedback signals<sup>81</sup>. Moreover it is highly likely that the niche undergoes a dynamic remodeling process during regeneration and may not be identical to the homeostatic HSC niche (Figure 8). The current lack of methods that combine *in vivo* imaging

with functional analysis of HCSs limits the definitive determination of where in the BM the HSCs are housed.

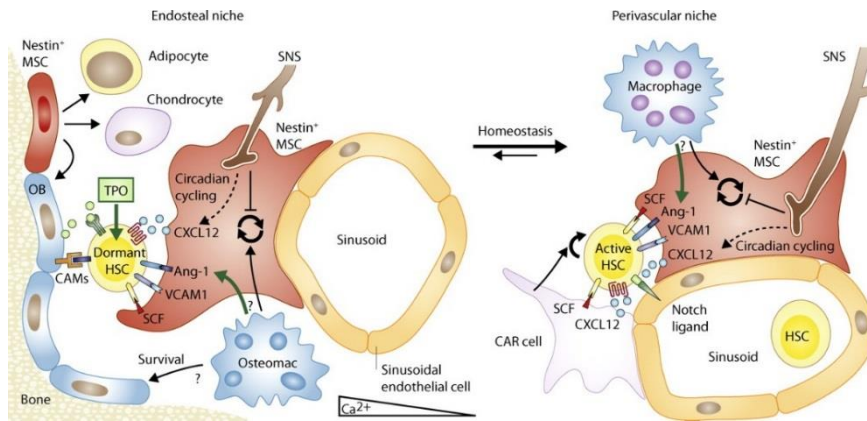


**Figure 8.** Model illustrating the quiescent endosteal (left) and the active perivascular HSC niche (right) during BM homeostasis. Deeply quiescent (dormant) HSCs in the endosteal niche are likely to be in close contact with osteoblasts and nestin<sup>+</sup> mesenchymal stromal cells (MSCs), both of which supply HSC maintenance and quiescence factors and cooperate to retain HSCs in their niche. The perivascular niche includes perivascular chemokine CXCL12-expressing MSCs (CAR) cells. Self-renewal is also stimulated by sinusoidal endothelial cells. Adapted from Trumpp et al. (2011)<sup>81</sup>

The major functional component of the endosteal niche is the bone-synthesizing osteoblasts<sup>107</sup>, which provide factors that are important to maintain HSCs, such as thrombopoietin (TPO), osteopontin (OPN) and angiopoietin-1 (Ang-1)<sup>103,108–110</sup>. They also express high levels of the chemotactic agent C-X-C motif ligand 12 (CXCL12) that interacts with C-X-C chemokine receptor 4 (CXCR4) on the surface of HSCs and other hematopoietic cells<sup>111</sup> mediating not only chemotaxis and homing but also HSC proliferation and survival<sup>112</sup>. HSCs is also regulated by gradients of Ca<sup>2+</sup> and oxygen<sup>107,113–116</sup>. Additionally, the bone-resorbing osteoclasts have been shown to be important for HSC mobilization into circulation, by cleavage of the stromal derived factor 1 (SDF-1 or CXCL12)<sup>117</sup>. The developmental

cue Cripto, a cytoplasmic membrane signaling protein, was identified as a HSC regulator since HSCs responsive to Cripto signaling were shown to be located in the endosteal region, largely quiescent cells with high glycolytic activity<sup>118</sup>. On the other hand, the vascular niche is composed of sinusoidal endothelial cells, perivascular stromal cells and cells of the peripheral nervous system<sup>18,112,119</sup>. Both perivascular and endothelial cells produce stem cell factor (SCF) and Mesenchymal stromal cells (MSCs) express the chemokine CXCL12 (CAR cells), all of which which are essential for HSC maintenance.<sup>112,120,121</sup> Nestin+ MSCs, expressing several soluble factors, are also important for HSC maintenance<sup>120</sup>. Finally, adrenergic fibers of the sympathetic nervous system have been shown to regulate circulating HSCs, by releasing circadian signals controlling mobilization of HSCs<sup>103,122</sup>

**The Notch pathway.** This ligand defines a highly conserved pathway responsible for cell lineage-specific differentiation and stem cell self-renewal in many tissues, including the hematopoietic system<sup>123,124</sup>. All Notch receptor paralogs (Notch 1-4) and their ligands (Delta and Jagged family) have been implicated in the regulation of diverse functions in the hematopoietic system. The best-described functions of Notch are in the emergence of fetal HSCs and T cell commitment. Although the role of Notch in T lymphocyte commitment and differentiation has been well established<sup>125</sup>, data regarding Notch involvement in adult HSC function are often controversial. Notch1 and Notch2 receptors, which bind ligands from the Notch and Jagged families, have been found to promote the expansion of LT-HSCs while preserving self-renewal ability<sup>126,127</sup>.



These results were supported by the finding that Jagged-1 regulates LT-HSC number and function during homeostasis and regeneration<sup>128</sup>, while Jagged-2 supports the expansion of ST-HSCs. Although these findings suggest that canonical Notch signaling promotes HSC self-renewal and maintenance, other studies have suggested that it may be dispensable<sup>129,130</sup>. These apparent contradictions might be explained by the innate complexity of the Notch signaling pathway and the methodologies used to evaluate its function in HSC regulation.

**The Wnt pathway.** Just like for Notch, the Wnt pathway has been demonstrated to regulate the development of various tissues, including hematopoietic cells<sup>131</sup>. The Wnt signaling pathway is subdivided into canonical ( $\beta$ -catenin dependent) and non-canonical ( $\beta$ -catenin independent) pathways. Wnt signaling begins when one of the Wnt proteins binds the N-terminal extra-cellular cysteine-rich domain of a Frizzled (Fz) family receptor. These receptors span the plasma membrane seven times and constitute a distinct family of G-protein coupled receptors. However, to facilitate Wnt signaling, co-receptors (LRP-5/6, Ryk and ROR2) may also be required alongside the interaction between the Wnt protein and Fz receptor. Binding of different Wnt proteins to frizzled (Fzd) receptors can trigger different Wnt pathways. Wnt proteins function as proliferation-inducing growth factors but may also affect cell-fate decisions, apoptosis and quiescence<sup>132</sup>. In the canonical Wnt pathway, Wnt proteins bind to their receptors, thereby preventing proteosomal degradation of the Wnt-mediator  $\beta$ -catenin. Subsequently,  $\beta$ -catenin translocates to the nucleus where it will form an active transcription complex with Tcf

(T-cell Factor) transcription factors or the related factor Lef1 (lymphocyte-enhancer-binding factor). Upon transcriptional activation, several target genes will be activated including Axin2, c-fos, c-myc and many others, which are important for proliferation and/or cell-fate decisions. In the absence of Wnt signaling, free cytoplasmic  $\beta$ -catenin is rapidly targeted for degradation by a multiprotein complex containing the scaffold proteins axin and adenomatous polyposis coli (APC), and the serine/threonine kinases casein kinase 1  $\alpha$  (CK1 $\alpha$ ) and glycogen synthase kinase 3 $\beta$  (GSK3 $\beta$ ). After binding axin and APC,  $\beta$ -catenin is initially phosphorylated by CK1 $\alpha$ , which primes  $\beta$ -catenin for subsequent GSK3 $\beta$ -dependent phosphorylation. Phosphorylated  $\beta$ -catenin is then recognized by an E3 ubiquitin ligase complex which marks  $\beta$ -catenin for proteasomal mediated degradation<sup>133</sup> (Figure 9).

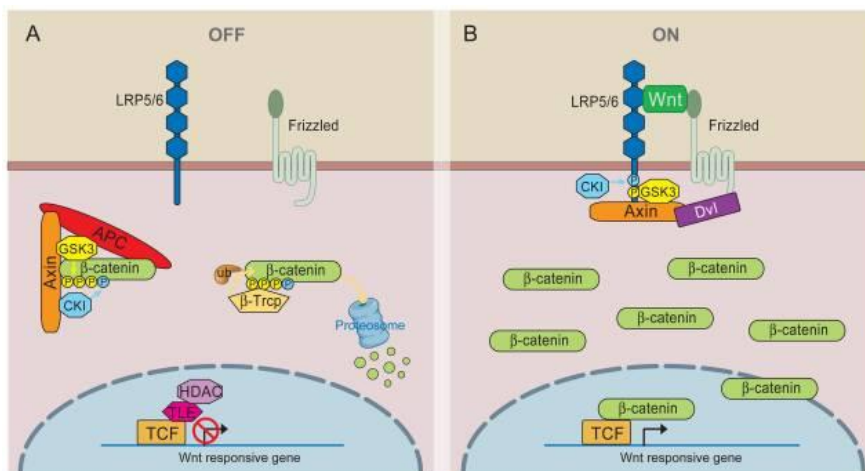


**Figure 9** The canonical Wnt pathway. A) In the absence of Wnt, cytoplasmic  $\beta$ -catenin forms a complex with Axin, APC, GSK3 and CK1, and is phosphorylated by CK1 (blue) and subsequently by GSK3 (yellow). Phosphorylated  $\beta$ -catenin is

recognized by the E3 ubiquitin ligase  $\beta$ -Trcp, which targets  $\beta$ -catenin for proteasomal degradation. Wnt target genes are repressed by TCF-TLE/Groucho and histone deacetylases (HDAC). B) In the presence of Wnt ligand, a receptor complex forms between Fz and LRP5/6. Dvl recruitment by Fz leads to LRP5/6 phosphorylation, and Axin recruitment. This disrupts Axin-mediated phosphorylation/degradation of  $\beta$ -catenin, allowing  $\beta$ -catenin to accumulate in the nucleus where it serves as a co-activator for TCF to activate Wnt responsive genes. Adapted from MacDonald et al. (2009)<sup>133</sup>

Non-canonical Wnt signaling involves recognition of distinct Wnt ligands by a Frz-LRP receptor complex, heterotrimeric G protein activation of phospholipase C, as well as the release of intracellular  $\text{Ca}^{2+}$  ions. Non-canonical Wnt signaling regulates cellular polarization and migration (the so-called planar-cell-polarity pathway).

The role of the canonical Wnt signaling cascade in hematopoiesis is controversial, mostly because of the complexity of the signaling pathway itself. Wnt3a treatment of bone marrow cells in vitro leads to HSC expansion while maintaining their function<sup>134</sup>. Retroviral expression of a constitutively active form of  $\beta$ -catenin in Bcl2-transgenic LSK cells resulted in augmented multilineage repopulation capacity<sup>135</sup>. Similarly, increased proliferation and maintenance of a functional precursor was observed in human and mouse HSC induced to express  $\beta$ -catenin by the inhibition of GSK3 $\beta$ <sup>136</sup>. In agreement, ectopic expression of the Wnt-signaling inhibitor Axin yielded opposite results<sup>135</sup>. However, subsequent gain- and loss-of-function approaches to further elucidate the role of Wnt signaling in HSCs yielded contradictory results. Two independent studies using a conditional mouse model to express a stabilized form of  $\beta$ -catenin showed impaired multilineage differentiation and a transient increase in stem cell numbers, followed by exhaustion of

the HSC pool<sup>137,138</sup>. In another set of experiments it was found that deleting the canonical Wnt ligand Wnt3a led to lower HSC and progenitor cell numbers in the fetal liver, decreased self-renewal and reduced long-term repopulation ability<sup>139</sup>, supporting a role for canonical Wnt in regulating HSC self-renewal. Moreover, conditional deletion of  $\beta$ -catenin using Vav-Cre or specific overexpression of a negative regulator of canonical Wnt, Dkk1, in osteoblastic cells in vivo also resulted in decreased hematopoietic reconstitution after transplantation and further confirmed the role of Wnt in HSC self renewal<sup>139–141</sup>. However, conditional deletion of both  $\beta$ -catenin and  $\gamma$ -catenin in Mx1-Cre mice did not affect self-renewal or hematopoiesis after transplantation, suggesting that a compensatory  $\beta$ -catenin homolog may exist<sup>142,143</sup>. Although the majority of the studies published have investigated canonical Wnt, the noncanonical Wnt pathway has also been suggested to affect HSC behavior. The noncanonical Wnt ligand Wnt5a has been found to inhibit canonical Wnt signaling as well as cell proliferation in vitro and increase the repopulating ability of HSCs in a mouse model<sup>144</sup> by acting through the receptor-like tyrosine kinase (Ryk) receptor<sup>145</sup>. Recently a study by Sugimura and colleagues has demonstrated the importance of the cooperation between canonical and noncanonical Wnt pathway in HSCs function. LT-HSCs have been reported to express two receptors of noncanonical Wnt signaling: flamingo (Fmi, also called Celsr) and frizzled 8 (Fzd8), which promote quiescence during homeostasis by preventing nuclear localization of nuclear factor of activated T cell (NFAT), suppressing interferon- $\gamma$  (IFN- $\gamma$ ) expression and antagonizing canonical Wnt signaling. Stress-

mediated activation of HSCs in mice may result in the repression of noncanonical Wnt signaling and enhanced canonical Wnt signaling, leading to HSC activation<sup>146</sup>(Figure 10).

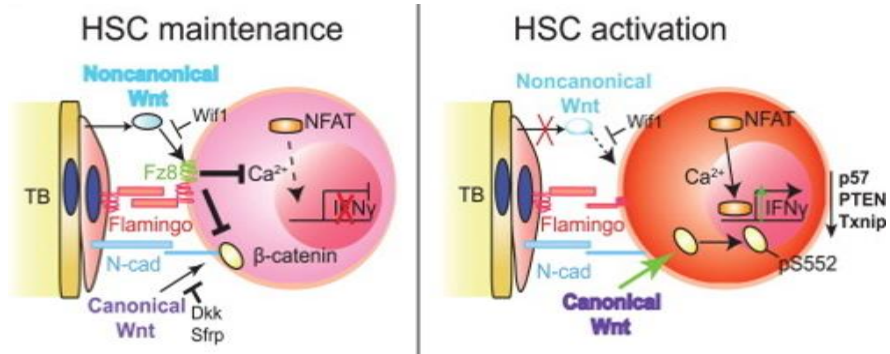


**Figure 10.** Switch from non-canonical to canonical Wnt signaling in HSC activation. The endosteal-localized N-cad<sup>+</sup>osteoblasts in the Trabecular bone (TB) region form a quiescent niche. Noncanonical Wnt signaling, mediated by Fmi-Fz8, restricts NFAT nuclear translocation through controlling intracellular Ca<sup>2+</sup> level and maintains quiescence, partially through downregulation of IFN $\gamma$  expression, and partially via antagonizing canonical Wnt signaling. Adapted from Sugimura et al. (2012)<sup>146</sup>

Generation of a gradient of canonical Wnt signaling levels confirmed the previously noted differences in HSC behavior, where the maintenance of an immature phenotype and enhanced long-term repopulation capacity of HSCs were favored by low levels of canonical Wnt signaling, as opposed to higher levels of Wnt signaling, which impaired the ability of HSCs to repopulate<sup>147</sup>. Whereas complete loss of Wnt signaling resulted in impaired self-renewal, low levels of Wnt signaling led to HSC maintenance, demonstrating a high sensitivity to dosage.

**The PI3K/Akt/mTORC1 pathway.** There are several cytokines secreted by the BM niche components that signal through the PI3K/Akt/mTORC1 pathway and that also regulate the cycling state

of HSCs. The PI3K family consists of 3 distinct subclasses of which, to date, only the class I isoforms have been implicated in regulation of hematopoiesis. Activation and recruitment of the PI3K by stimulation of several cytokines receptor leads to the conversion of phosphatidylinositol-4,5-bisphosphate (PIP2) to phosphatidylinositol-3,4,5-trisphosphate (PIP3). The activity of PI3K can be inhibited by phosphatase and tensin homologue (PTEN), a ubiquitously expressed tumor suppressor protein that can dephosphorylate PIP3, resulting in the formation of PI(4,5)P2. PIP3 recruits AKT/PKB and phosphoinositide-dependent kinase 1 (PDK1) to the plasma membrane, resulting in AKT/PKB phosphorylation by PDK1 at Thr308. For full activation, AKT/PKB is also phosphorylated by mTORC2 at Ser473. The choices from this point onwards are numerous, as more than 100 AKT/PKB substrates have been uncovered. Among them, GSK3, FOXO and mTOR signaling pathways have been shown to play an important role in the regulation of not only cell survival and proliferation of HSCs but also of cell fate decisions during hematopoietic lineage development<sup>148</sup> (Figure 11).

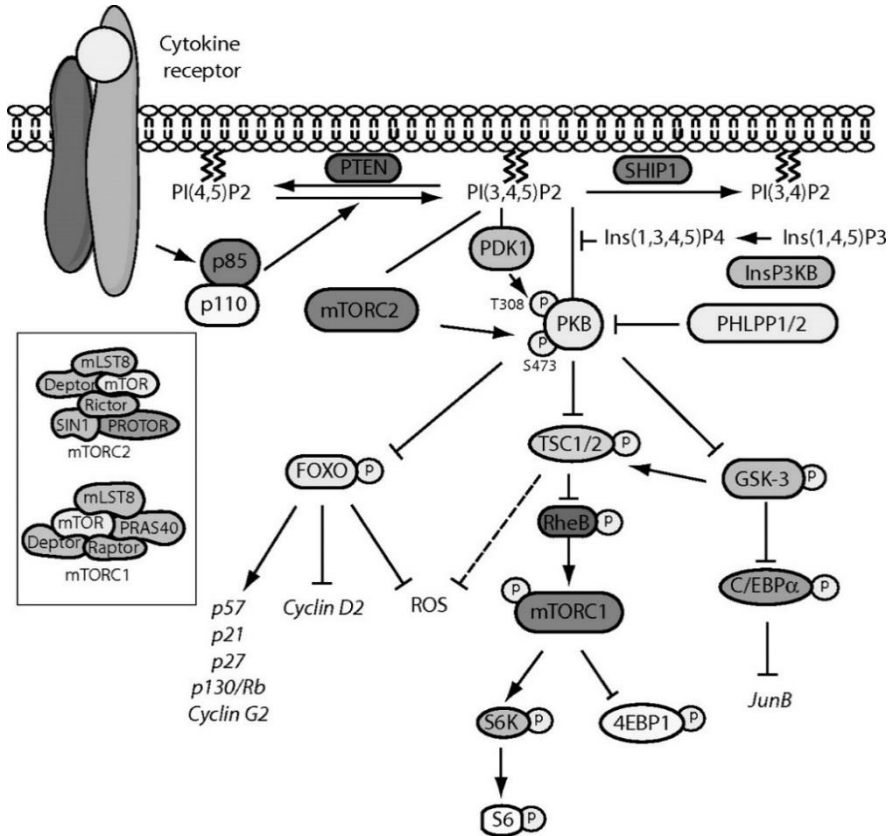


**Figure 11.** Schematic representation of the PI3K/PKB signaling module. Activation of PI3K by receptor stimulation results in the production of PtdIns(3,4,5)P<sub>3</sub> at the plasma membrane. PKB subsequently translocates to the plasma membrane where it is phosphorylated by PDK1 and the mTORC2 complex. On phosphorylation, PKB is released into the cytoplasm where it can both inhibitory phosphorylate multiple substrates, including FoxO transcription factors and GSK-3, and induce the activity of other substrates, such as mTOR as part of the mTORC1 complex. Negative regulators of the PI3K/PKB signaling module include PTEN, SHIP1, Ins (1,3,4,5)P<sub>4</sub>, and PHLPP1/2. Adapted from Polak et al (2012)<sup>148</sup>

Several studies have demonstrated a role of PKB in HSC function. PKB deficient HSCs were found to persist in the G<sub>0</sub> phase of the cell cycle, suggesting that the functional defects observed in these mice with regard to long-term hematopoiesis were caused by enhanced quiescence<sup>149</sup>. In addition, ectopic expression of constitutively active

PKB in mouse HSCs conversely resulted in transient expansion and increased cycling of HSCs, followed by apoptosis and expansion of immature progenitors in BM and spleen, which was also associated with impaired engraftment<sup>150</sup>.

Loss of PTEN, the negative regulator of the PI3K/AKT signaling, leads to promotion of cell survival, proliferation and angiogenesis, as well as activation of the mTOR and S6 kinases, resulting in enhanced protein translation commonly observed in cancers<sup>218</sup>. Therefore PTEN induced deficiency in postnatal mice exhausted normal HSCs and promoted excessive proliferation of leukemogenic stem cells, resulting in the development of myeloproliferative disorders (MPD) and eventually leukemia<sup>219, 220</sup>. The latter study further showed that the mTOR inhibitor rapamycin effectively suppressed growth of the leukemogenic stem cells and prevented exhaustion of normal HSCs. FoxO transcription factors, which are inhibitory phosphorylated by PKB/AKT, are known to play an important role in HSC maintenance. Conditional deletion of FoxO1, FoxO3 and FoxO4 in the adult hematopoietic system led to an initial expansion of HSCs, which correlated with abnormal cell cycle regulation, followed by a reduction in HSC numbers and defective long-term repopulating capacity<sup>151</sup>. Similarly, competitive repopulation experiments revealed that deletion of FoxO3 alone is also sufficient to impair HSC function<sup>152</sup>. Modulation of the activity of either PKB/Akt or FoxO transcription factors has been observed to alter the level of reactive oxygen species (ROS). It has been found that PKB deficient mice contain reduced ROS levels<sup>149</sup>, while mice deficient for FoxO exhibit



increased levels<sup>152</sup>, demonstrating that correct regulation of ROS by FoxO transcription factors is essential for normal hematopoiesis. Recent findings have demonstrated that correct regulation of the activity of GSK-3, which is inhibited through phosphorylation by PKB<sup>153</sup>, is also essential for HSC maintenance. For example, a reduction in long-term, but not short-term, repopulating HSCs has been observed in GSK3-deficient mice<sup>154</sup>. In addition, disruption of GSK-3 activity in mice with a pharmacologic inhibitor or with shRNAs has been shown to transiently induce expansion of both HSCs and progenitor cells followed by exhaustion of long-term repopulating HSCs<sup>136,154</sup>. A third, important mediator of PI3K/PKB signaling is mTOR. In contrast to GSK-3 and FoxO transcription factors, which are inhibited through phosphorylation by PKB, the activity of mTOR is positively regulated by PKB. Inhibition of the GTPase activating protein Tuberous sclerosis protein 2 (TSC2)/TSC1 complex by PKB results in accumulation of GTP-bound Rheb and subsequent activation of mTOR<sup>155</sup>. In addition, because rapamycin, an mTOR inhibitor, was sufficient to revert the HSC phenotype of mice in which GSK-3 was depleted, it is probable that mTOR is an important effector of GSK-3<sup>154</sup>. Conditional deletion of TSC1 in mice, resulting in activation of mTOR, has been demonstrated to enhance the percentage of cycling HSCs and to reduce the self-renewal capacity of HSCs in serial transplantation assays<sup>156</sup>. Moreover, treatment of PTEN-deficient mice with rapamycin, appears to be sufficient to revert the HSC phenotype in those mice, indicating that mTORC1 is an important mediator of PI3K in regulation of HSC proliferation.

## 2.2.4 Cell-intrinsic pathways

In addition to all cell non-autonomous signals affecting HSC fate there are also several intrinsic players involved in HSC regulation, including transcription factors, transcriptional suppressors, cell cycle regulators and apoptotic signals<sup>157-160</sup>.

The homeobox (Hox) genes are well-studied transcription factors that have been implicated in HSC regulation. For example, overexpression of HoxB4, HoxA9 and HoxA10 has been shown to lead to expansion of HSCs<sup>161-164</sup>. In the absence of HoxA9 HSCs display a severely compromised reconstitution capacity<sup>165</sup>. Surprisingly, HoxB4-deficient mice do not dramatically affect HSC function, which could be explained by redundancy with other Hox proteins<sup>166-168</sup>.

Several cell cycle regulators, including CDKIs, have been proven to have a role in HSC biology. The G1 checkpoint regulator p21, belonging to the Cip/Kip family, is important for HSCs to be able to re-enter quiescence after cell cycle activation, as well as for maintaining the cells in dormancy<sup>169</sup>. This was concluded from studies in a knockout mouse model, where deletion of p21 led to increased proliferation, resulting in HSC exhaustion and hematopoietic failure<sup>169</sup>. However, deletion of p21 in another mouse strain did not result in any substantial differences in either cell cycle status or HSC number<sup>170</sup>), demonstrating that the mouse background has to be taken into consideration when drawing conclusions. When analyzing the mRNA expression of different Cip/Kip family members in LSKCD34- cells, Yamazaki et al. observed low levels of both p21 and p27, while a third member, p57 was highly expressed

<sup>171</sup>. p57 has been suggested to play a role in HSC quiescence <sup>172–174</sup>. Mice overexpressing the apoptotic-suppressing gene Bcl-2 showed an increased HSC population and these reconstituted better than WT HSCs <sup>157,175,176</sup>. This indicates the importance of apoptosis in the modulation of HSC numbers.

Epigenetic control, including DNA methylation, chromatin remodeling, histone modifications and non-coding RNAs, are also key players in HSC regulation. These modifications affect the overall chromatin or DNA structure and thereby determine the transcription factor accessibility to target genes. The polycomb group members are examples of transcriptional repressors exerting such epigenetic regulation. One of them, B lymphoma Mo-MLV insertion region 1 (Bmi-1), is needed to generate self-renewing adult HSCs and loss of this protein led to impaired repopulation capacity of fetal liver HSCs <sup>177</sup>. Furthermore, enforced expression of Bmi-1 resulted in increased self-renewal in vitro and expansion of the stem cell pool both in vitro and in vivo <sup>178</sup>, confirming an important role of Bmi-1 for functional HSCs. Finally, microRNAs (small non-coding RNAs) offer another way of controlling HSC fate determination by affecting gene expression at the translational and post-transcriptional level <sup>158,179,180</sup>.

### 3 THE ROLE OF MUSASHI 2 IN MURINE HEMATOPOIESIS

#### 3.1 The identification of Msi2 in mouse HSCs

The Musashi (Msi) gene was initially discovered in *Drosophila*, in which it was found to mediate asymmetrical cell division during bristle development<sup>181</sup>. Since its discovery, orthologues of Msi protein have been identified in other eukaryotic species including frogs, mice and humans<sup>182–185</sup>. Interestingly, the structure and expression pattern of Musashi is largely conserved among these highly varied species<sup>186</sup>. Two Msi gene homologues have been identified in mammals, Msi1 and Msi2<sup>183,187</sup>. The two genes have a high degree of sequence similarity, exhibiting a 75% overall amino acid identity<sup>187</sup>(Figure 12).

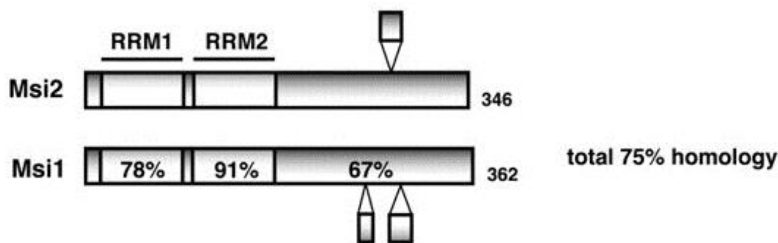


**Figure 12.** Domain structures of the mouse Msi2 and Msi1 proteins. The percentages of amino acid identity between Msi1 and Msi2 within each RRM and in the C-terminal half are shown. Bulged small boxes represent the regions arising from alternative splicing. Adapted from Sakakibara et al. 2001<sup>187</sup>

Msi1, the Msi family member most widely studied, is expressed in a wide variety of mouse tissues including intestine, brain, breast, hair follicle and pancreas, preferentially marking primitive cell populations<sup>183,188,189</sup>. Moreover, Msi1 has been demonstrated to have a maintenance role for neural stem and mammary progenitor cell populations where it promotes self-renewal by maintaining Notch signaling through translational repression of Numb<sup>190–193</sup>. Msi2 has also been found to be expressed in neural progenitor cells, including stem cells<sup>187</sup> as well as in the bulge region of the hair follicle<sup>194</sup> and in immature pancreatic  $\beta$ -cells<sup>189</sup>. However, in the last years, several studies, among them the one included in this thesis<sup>195</sup>, have shown that it also functions in normal and leukaemic blood cells<sup>195–199</sup>(Figure 13)

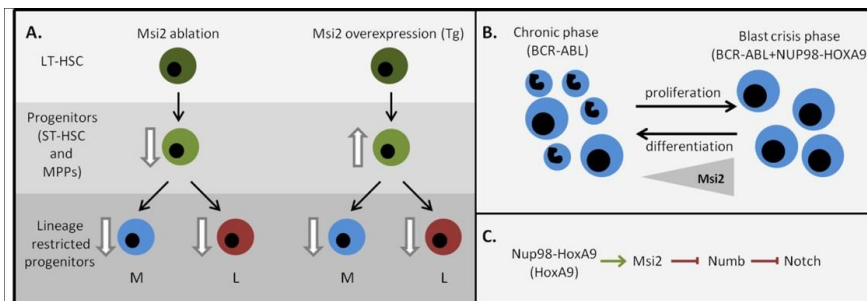


**Figure 13.** Role of Msi2 in normal and malignant haematopoiesis. (a) Msi2 ablation leads to a depletion of progenitor cells (ST-HSC and MPPs) which eventually translates into a decrease of both myeloid (M) and lymphoid (L) progenitors and mature cells. Msi2 overexpression in transgenic (Tg) mice leads to an expansion of ST-HSC and MPPs and also inhibits the differentiation of mature populations. (b) In a CML mouse model, overexpression of BCR-ABL induces chronic myeloid leukaemia, whereas overexpression of BCR-ABL together with Nup98-HoxA9 generates a myeloproliferative disorder resembling blast crisis phase of CML. In addition, Msi2 is upregulated as chronic phase CML progresses to blast crisis. In contrast, inactivation of Msi2 in this model gives rise to more differentiated leukaemic cells. (c) Nup98-HoxA9 (in malignant hematopoiesis) or HoxA9 (in normal hematopoiesis) activates the transcription of Msi2. Msi2 inhibits the translation of Numb which in turn inhibits Notch signalling. BCR-ABL, breakpoint

cluster region-Abselon; CML, chronic myelogenous leukemia; MPPs, multipotent progenitors; ST-HSC, short-term hematopoietic stem cells. From de Andrés-Aguayo et al. (2011)

Msi2 is expressed in the hematopoietic system, a tissue in which Msi1 is almost completely absent<sup>195-197</sup>. Mouse expression profiling and reporter gene analysis have shown that within the hematopoietic system, Msi2 is preferentially expressed in the most primitive cells, that is, in the lineage negative, Sca-1+ kit+ (LSK) population. Upon differentiation into the different hematopoietic lineages, its expression is downregulated<sup>195-197</sup>. Moreover, Msi2 has been identified as a crucial gene in HSC homeostasis and long-term engraftment. Hope et al.<sup>197</sup> used RNA interference in mouse HSCs to inhibit genes known to be implicated in polarity and asymmetric cell division in other stem cell systems. They identified three genes that function as positive regulators, including Msi2, and one gene as a negative regulator (Prox1) of HSC function<sup>197,199</sup>. They found that *Msi2* downregulation impairs the competitive repopulation potential of HSCs in a dose-dependent manner, without affecting their cell cycle profile, rate of apoptosis or homing capacity. Using a very similar approach, Kharas et al.<sup>196</sup> knocked down Msi2 in LSK cells and found that upon transplantation the competitive repopulation ability of these cells was dramatically impaired. As in the Hope et al. study, the effect on LSK cells was not due to increased apoptosis, impairment of homing capacity or a defect in committed progenitors, but rather to a decrease in the number of more primitive progenitors. These findings were further supported and extended with the work included in this thesis as part of the results. Gene expression arrays showed alterations in the expression level of several key cell cycle

regulators in Msi2 deficient LSK cells <sup>196,197</sup>, these alterations could explain the reduction in progenitor numbers. Msi2 overexpression also causes significant alterations of normal hematopoiesis. Using a doxycycline- inducible Msi2 transgenic mouse, Kharas et al. <sup>196</sup> observed an increase in the number of LSK cells, and this increase could be attributed to ST-HSCs and MPPs, whereas the LT-HSC proportion decreased. Changes in MPP/ST-HSC numbers were attributed to cell cycle kinetics alterations. On the contrary, Msi2 overexpression also increased LT-HSC numbers in transplanted animals, suggesting that it can also affect LT-HSC self-renewal under conditions of stress-induced hematopoiesis. However, the same animals showed a reduced contribution of Msi2 overexpressing cells in peripheral blood after short-term and long-term reconstitution, pointing to a partial block in differentiation mediated by Msi2 overexpression. In contrast to these observations, Hope et al. <sup>197</sup> found that Msi2 overexpression by means of retroviral transduction in primitive bone marrow cells followed by transplantation enhanced long term engraftment when compared with wild-type cells. This latter finding is also supported by results from our original retroviral insertion screen aimed at identifying novel regulators of mouse hematopoiesis, described in more detail in the Results section. The discrepancy between the findings in the work by Kharas et al. <sup>196</sup> and those of both Hope et al. <sup>197</sup> and ours could be due to differences in the methods used for Msi2 overexpression, which may influence the extent and duration of Msi2 overexpression. Importantly, regardless of the method of Msi2 overexpression-induction, in no case was leukemia observed as a result <sup>197</sup>.

After the initial publications describing the role of Msi2 in the hematopoietic system, more studies have followed trying to understand the role of this protein in the hematopoietic system.

### **3.2 Msi2 in mouse models of leukemia**

Aside from the burgeoning role in maintaining normal murine HSC function, there are several studies that have implicated Msi2 in both primary human and mouse models of leukemia. MSI2 was originally found in a novel chromosomal translocation with HOXA9 in a cohort of acute myeloid leukemia (AML) patients<sup>200</sup>. MSI2 was found to be highly expressed in human AML and blast crisis (BC)-CML patient samples and correlated with decreased patient survival<sup>196,198</sup>. This spurred studies into exploring its role in mouse models of chronic myeloid leukemia (CML) where it was found to have a positive role in the progression from the chronic to the acute and lethal blast crisis phase of the disease<sup>196,198</sup>. Mouse survival was significantly increased by Msi2 knockdown in BC cells compared to control BC leukemia cells<sup>198</sup>. Msi2 has further been shown to maintain a preleukemic state in a mouse model of myeloid dysplastic syndrome (MDS)<sup>201</sup>, since knocking out Msi2 eliminates MDS HSPCs while overexpression accelerates the disease. Additional clinical findings support this conclusion, as elevated MSI2 levels and in particular rare cells with high amounts of nuclear protein in AML blast cells are negative prognostic indicators of disease outcome<sup>202</sup>. These studies collectively show MSI2 as a central player in disease progression among several types of myeloid leukemias.



### 3.3 Mechanisms of Musashi action

#### Musashi domain structure and function

Musashi family proteins are RNA-binding proteins that form a subgroup within the heterogeneous nuclear ribonucleoprotein (hnRNP) A/B class of proteins. Like other proteins of this class, Musashi proteins have two RNA recognition motifs (RRMs) separated by a short linker region<sup>163</sup>. The RRM domains, located in the N-terminal half of the protein, are highly conserved across diverse species. Each Musashi RRM has the characteristic structure of RNP-type RNA-binding domains and a four-stranded<sup>203,204</sup>, antiparallel  $\beta$ -sheet backed by two  $\alpha$ -helices, with each RRM containing hallmark RNP1 octamer and RNP2 hexamer sequences (Figure 14).

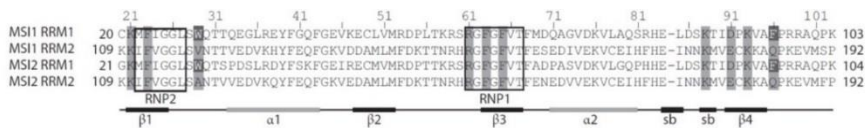


**Figure 14.** Amino acid sequence alignment of the RNA-binding domains, RNA recognition motifs (RRMs), of MSI1 and MSI2. Residues of MSI1 thought to interact with the r(GUAGU) target sequence are highlighted in gray. These residues are highly conserved between RRM1 and RRM2 within and between MSI1 and MSI2. In addition, residues that may confer RRM1 binding specificity are shown in white against a gray background (W29 and F96). RNP sequences are boxed, and secondary structure element positions are shown below ( $\beta$ ,  $\beta$ -strand;  $\alpha$ ,  $\alpha$ -helix; sb, short  $\beta$ -strands that form a  $\beta$ -turn)

Studies of the domain structure of the mammalian Musashi proteins have shed light on the mechanisms by which these proteins regulate gene expression. Musashi RNA-binding affinity and specificity appear to be largely determined by the N-terminal RNA-binding domain, RRM1. Although the more C-terminal RRM2 can bind RNA weakly in isolation, its primary role is likely to enhance binding

affinity in combination with RRM1: RNA binding increases ~100-fold in the presence of RRM2 compared with RRM1 alone<sup>204,205</sup>. In support of this idea, putative target sequences for the respective RRM1s are often found near one another in 3'-UTRs of known Musashi target transcripts. The weaker binding strength of RRM2 is likely a result of its less favorable surface electrostatic potential and less flexible  $\beta$ -sheet compared with RRM1<sup>203</sup>. RRM1 and RRM2 in mouse MSI1 bind the consensus sequences r(GUAG) and r(UAG), respectively<sup>206</sup>. RRM1 has unique stacking interactions that confer binding specificity. These interactions involve aromatic residues (F96 and W29) that are conserved between the MSI1 and MSI2 RRM1s but are absent in other known hnRNP RRM1s, including MSI RRM2<sup>206</sup> (Figure 14). Accordingly, RRM2 does not appear to contribute to binding specificity.

Although these studies have provided important insights into the binding specificity of the Musashi RRM domains, the short nature of these binding determinants suggests that protein-RNA affinity alone may be insufficient to determine Musashi target specificity. Musashi proteins are usually found in the cytoplasm and are enriched in polysome fractions, consistent with their function in translational regulation<sup>207,208</sup>. By contrast, other hnRNPs are primarily localized to the nucleoplasm, and in certain contexts Musashi proteins have also been observed in the nucleus<sup>181,207,209,210</sup>. It is not clear how Musashi subcellular localization is determined in these contexts, but the RNA-binding domain may play an important role. Putative nuclear localization signal (NLS) sequences are present in both RRM1 and RRM2: a classical NLS in RRM1 and a peptide-like NLS

in RRM2<sup>211</sup>. These NLSs may regulate nuclear import of MSI via interaction with the importin- $\alpha$  protein. It has been postulated that when MSI1 binds mRNA in the cytoplasm, the NLSs are effectively blocked, owing to their location within the RRM.

The MSI1 and MSI2 RRMs show high sequence homology, with complete conservation of residues important for RNA-binding specificity, making it likely that the RRMs of MSI1 and MSI2 bind similar if not identical RNA target sequences<sup>187,206</sup>. However, additional domains, outside of the RRMs, also impinge on the mechanisms by which Musashi regulates gene expression. Thus, the C-terminal halves of the two mammalian Musashi proteins differ significantly in length and amino acid sequence, with only 56% identity. In addition, two key protein interaction domains in the C-terminal half of MSI1 have been identified, a polyA-binding protein (PABP) domain and a LIN28-binding domain<sup>211,212</sup>. These domains are not found in the MSI2 protein, maybe indicating that the mechanism by which MSI2 is regulating its targets is different from MSI1.

### 3.3.1 Post transcriptional regulation by Musashi family proteins

To elucidate the molecular underpinning responsible for the function of Msi2, recent work has utilized genomic tools to identify Msi2 targets globally and characterize the regulatory network governed by Msi2<sup>89,213</sup>. Transcriptome-wide binding assays, such as High-Throughput Sequencing of RNA isolated by CrossLinking ImmunoPrecipitation (HITS-CLIP), were used to identify a number of Msi2 targets, such as involved in cell cycle control in human

leukemia cell lines and murine intestinal progenitor cells. The primary sequence motif recognized by Msi2 in these studies is unclear as numerous divergent sequence motifs were identified<sup>213</sup>. In contrast, biochemical and structural analyses of Msi binding sites in experimentally identified targets, Numb and Jag1, and in vitro target selection experiments identified a tripartite nucleotide sequence, UAG, as the most prominent recognition motif for both Msi1 and Msi2<sup>205,206,214</sup>. More recently, ribosome profiling (Ribo-Seq) was used to analyze changes in mRNA expression in neural stem cells with genetic overexpression or depletion of Msi1 and Msi2<sup>214</sup>. Little change in mRNA expression was observed after 48 h of Msi1 or Msi2 overexpression, consistent with the primary function of these proteins being the regulation of translation rather than transcription. However as expected, changes in the translation efficiency of many genes were observed after overexpression of either Msi1 or Msi2.

### 3.3.2 Msi2 mechanism of action in normal and malignant hematopoiesis

One of the best-studied Musashi targets is Numb, an inhibitor of the Notch intracellular signaling pathway, and binding to the Numb 3'-UTR was confirmed both in vitro and in vivo<sup>193</sup>. MSI1 binding downregulates Numb expression at the translational but not transcriptional level in neural stem cells, and this downregulation potentiates Notch signaling activity<sup>193</sup>. In leukemia, the regulation of NUMB levels by Msi2 was shown to play a key role in the progression of CML to blast crisis<sup>198</sup>. In a mouse model of CML, loss of Msi2 restored Numb expression and impaired the development and progression of blast crisis CML through increased differentiation<sup>198</sup>.

Interestingly, this corresponds to the MSI2 and NUMB expression level changes observed during CML progression, where upregulation of MSI2 and down-regulation of NUMB was found in patients who have progressed to blast crisis. In this context, transcriptional levels of NUMB are clearly affected by MSI2 modulation, raising the possibility that MSI2 may influence RNA stability or act indirectly through another Msi2 target<sup>198</sup>. In fact, no change in NUMB levels was detected in the HSCs/progenitor cells of Msi2 conditional knockout mice<sup>89</sup>.

Gene expression profiling in mouse HSPC populations after Msi2 knockdown/out or overexpression showed transcriptional changes in cell cycle regulators such as p21 and Cyclin D1 as well as Notch, Sonic Hedgehog, and Myc signaling pathways<sup>195–197</sup>. Additional experiments with conditionally deleted Msi2 in a hematopoietic cell line by high-throughput sequencing of RNA and crosslinking immunoprecipitation (HITS-CLIP) revealed perturbed TGF- $\beta$  signaling. In line with this finding knockout cells became nonresponsive to TGF- $\beta$  mediated expansion. Although *smad3* and *tgfbrii* mRNAs were co-immunoprecipitated with MSI2, it was not demonstrated that these proteins are responsible for mediating the phenotype<sup>89</sup>. In the context of MLL-AF9 driven leukemia, Msi2 was found to stabilize and promote translation of various oncogenes including *Hoxa9*, *Myc*, and *Ikzf2* mRNAs<sup>215</sup>. A similar Msi2-driven activating effect was seen with *Tspan3* mRNA in mouse models of leukemia, highlighting a novel post-transcriptionally driven leukemia promoting pathway<sup>216</sup>.

Aside from regulating mRNA translation there is also evidence pointing to a role of Msi2 in controlling microRNA (miRNA) biogenesis, specifically at the stage when primary miRNA (pri-miRNA) is cleaved by Drosha to precursor miRNA (pre-miRNA)<sup>217</sup>. Msi2 was found to interact with HuR protein and bind and stabilize pri-miRNA stemloops, leading to repression of the mature form of mir-7 (Figure 4B). Consequently, mir-7 was found to be upregulated in various tissues of our Msi2 deficient mouse<sup>195</sup>. These studies, and previous work with Msi1, demonstrate that Musashi proteins modulate translation and affects miRNA maturation by interacting with various protein partners.

**PART II RESULTS**

## **Chapter 1**

de Andres-Aguayo L, Varas F, Kallin EM, Infante JF, Wurst W, Floss T, et al. [Musashi 2 is a regulator of the HSC compartment identified by a retroviral insertion screen and knockout mice.](#) *Blood*. 2011 Jul 21;118(3):554–64. DOI: 10.1182/blood-2010-12-322081



**Chapter 2**

**Characterization of the hematopoietic system during embryo development in Msi2 deficient mice**



We previously have shown that Msi2 has an important role in the maintenance of the most primitive hematopoietic cells in adult mice. Nonetheless, hematopoietic stem cells are generated already during embryonic development, a process occurring sequentially in several niches. The results obtained in the characterization of the adult hematopoietic system in Msi2 deficient mice encouraged us to study if Msi2 could have a role in the generation and/or expansion of hematopoietic progenitor cells that happens during embryo and fetal development.

### **HSCs generated from the ventral part of the dorsal aorta in the AGM express Msi2**

Msi2 is expressed in the most primitive hematopoietic cells in the adult BM and its expression decreases as they differentiate into progenitors and mature cells. In order to examine whether Msi2 was also expressed in the emergent HSCs generated in the AGM during embryo development, 10.5 dpc embryos were fixed and stained with antibody against Msi2. CD41 was also included as it has been demonstrated to be a marker for the earliest emerging aortic HSCs as they are transiting from endothelial to hematopoietic fate, and then is considered as a bona fide HSC marker<sup>1,2</sup>. As shown in figure 1, Msi2 is expressed mainly in the neural tube, in the mesonephros and, more importantly, in a very specific group of cells corresponding to intra-aortic hematopoietic clusters (IAHCs).

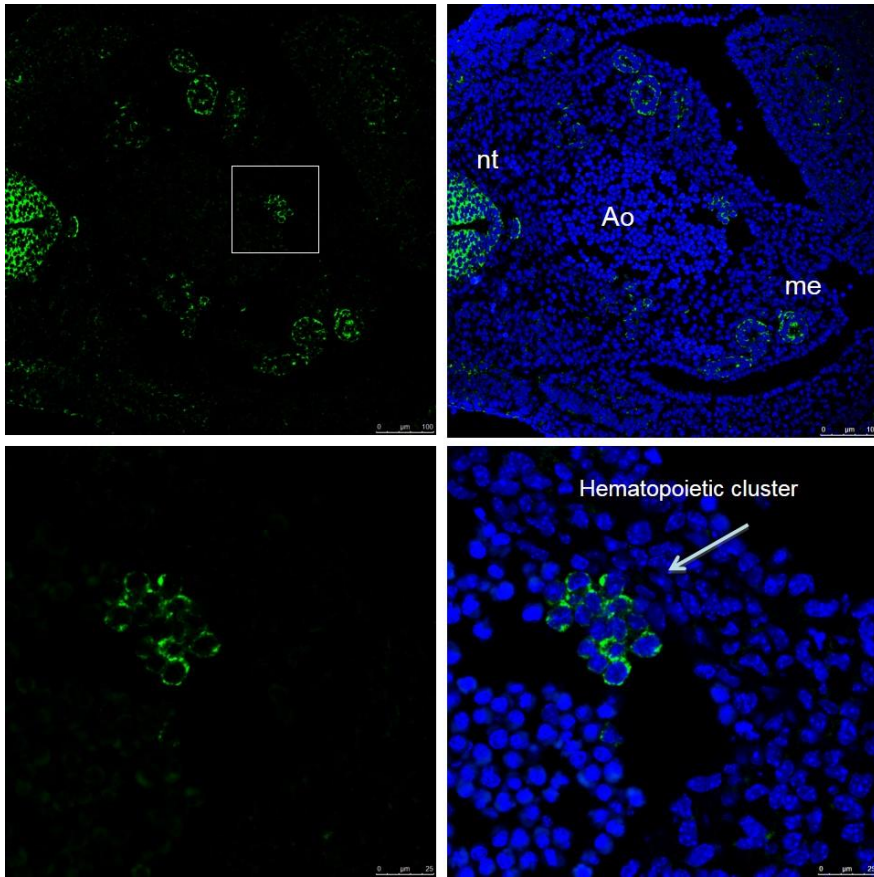


**Figure 1.** Msi2 immunostaining of E10.5 wild-type embryo section showing (top panel) the neural tube (nt), mesonephros (me) and Aorta (Ao) and (bottom panel) a magnified image of the ventral wall of the aorta, with a hematopoietic cluster. Msi2 expression is shown in green and DAPI in blue.

These data were confirmed by the co-expression of Msi2 and CD41 in the hematopoietic cluster as shown in Figure 2.

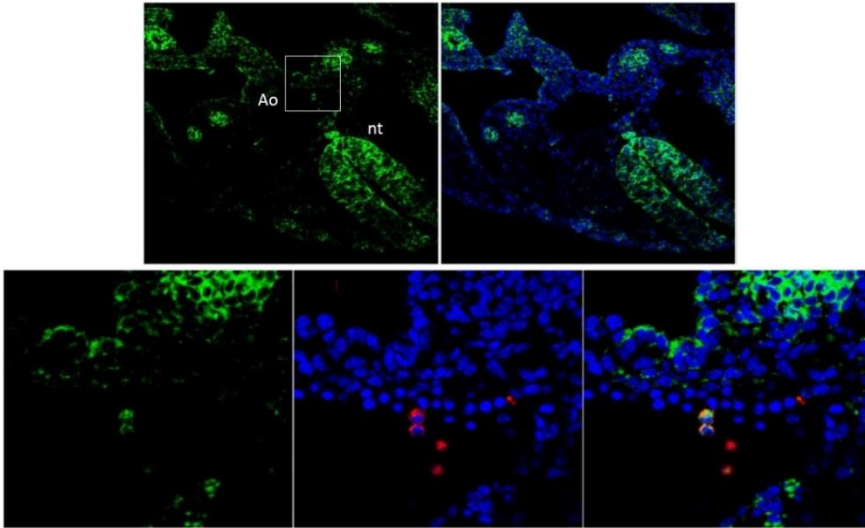


**Figure 2.** Immunostaining of E10.5 wild-type embryo section showing (top panel) the neural tube (nt), and Aorta (Ao) and (bottom panel) a magnified image of the ventral wall of the aorta. Msi2 expression is shown in green (left), CD41 expression is shown in red (center) and merged image (right) where yellow represent overlap of Msi2 and CD41.

As described in the introduction, HSCs are generated from endothelial-like cells (identified as CD31<sup>+</sup> CD45<sup>-</sup> c-Kit<sup>-</sup>) through a process that is called endothelial-to-hematopoietic transition (ETH), giving rise to the precursors of HSCs (pre-HSCs; CD31<sup>+</sup> CD45<sup>-</sup> c-kit<sup>+</sup>) that eventually will generate HSCs (defined as CD31<sup>+</sup> CD45<sup>+</sup> c-kit<sup>+</sup>) (Figure 3a). qRT-PCR to detect Msi2 expression was performed from RNA extracted from sorted cells of the three populations mentioned from wild-type E10.5 AGMs. As shown in Figure 3, Msi2 mRNA levels slightly decrease in the transition from endothelial (CD31<sup>+</sup> c-Kit<sup>-</sup> CD45<sup>-</sup>) to HSC precursors (CD31<sup>+</sup> c-Kit<sup>-</sup> CD45<sup>-</sup>), and upon HSC generation Msi2 levels increase again (Figure 3b). In an independent experiment, Msi mRNA levels were also measured in CD31<sup>+</sup> c-kit<sup>-</sup> endothelial-like cells and CD31<sup>+</sup> c-kit<sup>+</sup> (which includes pre-HSCs and HSCs) cells from the AGM, and

compared to adult LSK cells (HSC-enriched population that includes LT-HSC, ST-HSC and LMPP). As shown in Figure 3c, *Msi2* mRNA is downregulated upon transition from endothelial-like cells to hematopoietic stem and progenitor cells, confirming the results shown in Figure 3b. Moreover, *Msi2* in adult HSC-enriched populations (LSKs) is slightly upregulated compared to their fetal counterparts (Figure 3c)

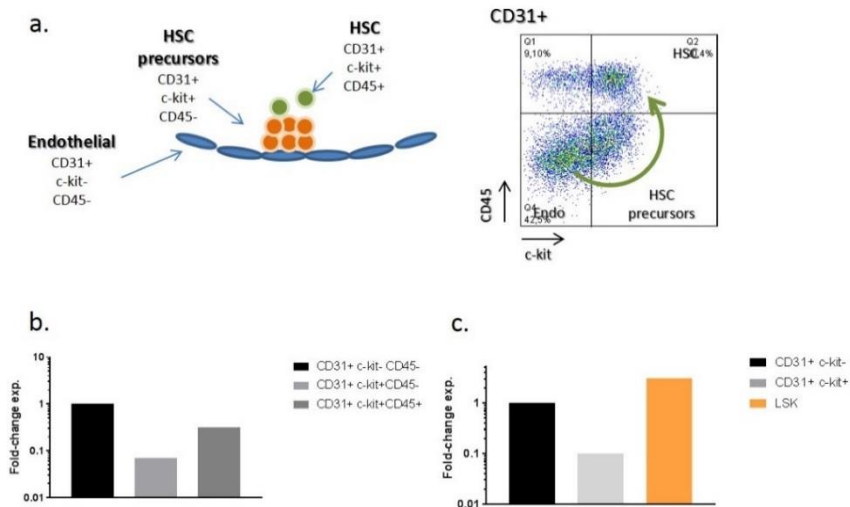


**Figure 3.** Schematic representation of the endothelial/hematopoietic populations present in the AGM region and the surface markers expressed (a) *Msi2* expression as determined by qRT-PCR on sorted cells from (b) endothelial (CD31+ c-kit- CD45-), pre-HSCs (CD31+ c-kit+ CD45-) and HSCs (CD31+ c-kit+ CD45+) and (c) endothelial (CD31+ c-kit-), pre-HSC and HSC (CD31+ c-kit+) from WT AGM.

In short, *Msi2* mRNA levels transiently decrease in pre-HSCs during endothelial to hematopoietic transition, and although *Msi2* mRNA is expressed in the emergent HSCs, its expression is lower compared to the LSK population in adult mice. On the other hand *Msi2* protein expression in the AGM is specific for hematopoietic clusters and colocalize with CD41 protein, indicating that *Msi2* may be a marker of emerging HSCs.

**The number of emerging aortic HSCs is slightly decreased in Msi2 deficient embryos.**

We next assessed whether Msi2 loss of function could affect the formation of intra-aortic clusters of cells, which are considered to be the first sign of HSC emergence in the dorsal aorta. Single cell suspensions of the AGMs dissected from Msi2 <sup>+/+</sup>, Msi2 <sup>+/<sup>Gt</sup></sup>, Msi2 <sup>Gt/Gt</sup> embryos at 10.5 dpc and 11.5 dpc were analysed by FACS. Endothelial-like cells, pre-HSCs and HSCs were stained using CD31, c-kit and CD45 antibodies. As can be seen in Figure 4, the numbers of endothelial, HSC precursors and HSCs are quite similar, indicating that a deficiency in Msi2 doesn't affect the generation of any of these populations.

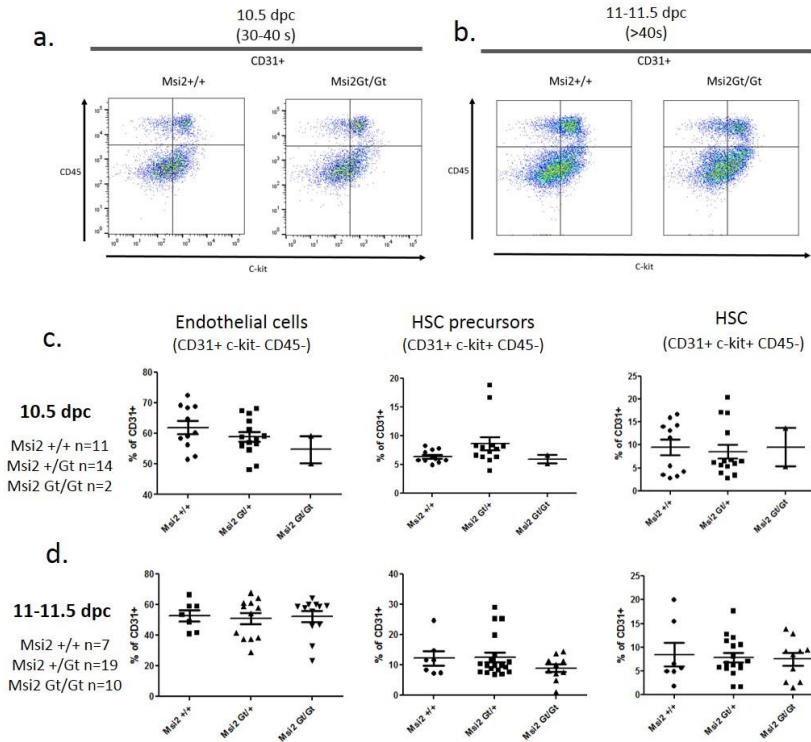


**Figure 4** Flow cytometric analysis of (a,c) E10.5 and (b,d) E11-11.5 AGM. Representative FACS plots of CD31+ cells (a,b) are shown with the distribution of endothelial cells (c-kit- CD45-), pre-HSCc (c-kit+ CD45-) and HSCs (c-kit+ CD45+) from Msi2<sup>+/+</sup> and Msi2<sup>Gt/Gt</sup> mice. Quantification of the three populations based on the percentage of endothelial cells, pre-HSCs and HSCs in the CD31+ population in 10.5 AGMs (c) and 11-11.5 AGMs (d). The number of embryos of each phenotype used in the analysis is shown.

To analyse in more detail the formation of HSCs in the AGMs, some of the samples were also stained with an antibody against CD41, considered as a marker of the earliest emerging aortic HSCs. As shown in figure 5, although in the 10.5 AGMs the number of CD41 positive cells in the endothelial population doesn't show any difference between the three phenotypes, the 11-11.5 AGMs from Msi2 deficient mice show a slightly decrease in the CD41 positive



endothelial cells. Reduced numbers of this population may be reflecting a defect in the Msi2 Gt/Gt emerging HSCs.

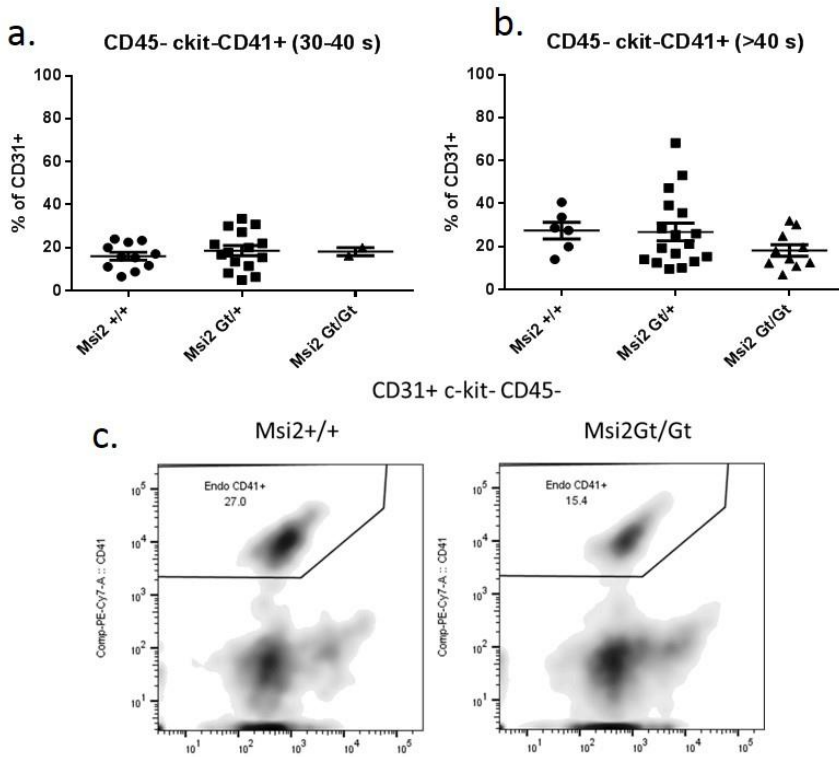


**Figure 5** Flow cytometric analysis of CD41+ cells in (a) E10.5 and (b,c) E11-11.5 AGM. Quantification of CD41+ CD31+ CD45- c-kit- cells in AGMs of Msi2 WT, heterozygous and deficient Msi2 mice (a,b). Numbers expressed the % CD41+ cells in the CD31+ population.

### LSK and HSC expansion in the fetal liver is defective in Msi2 Gt/Gt mice

After HSCs originate in the AGM at around E11 day, they migrate into the fetal liver (FL), where they expand through multiple rounds of divisions. Due to the fact that Msi2 deficient LSKs have a defect in cell cycle progression, we wanted to test if FL LSKs were also affected. We analysed FL from Msi2<sup>+/+</sup>, Msi2<sup>+/Gt</sup> and Msi2<sup>Gt/Gt</sup> E14

embryos by FACS (Figure 6a). The number of  $Msi2^{+/Gt}$  LSK cells was reduced to approximately 72% of that of  $Msi2^{+/+}$ , and the difference was even more striking when we compared  $Msi2^{Gt/Gt}$  and  $Msi2^{+/+}$ , being the reduction of almost 50%. (Figure 6b)

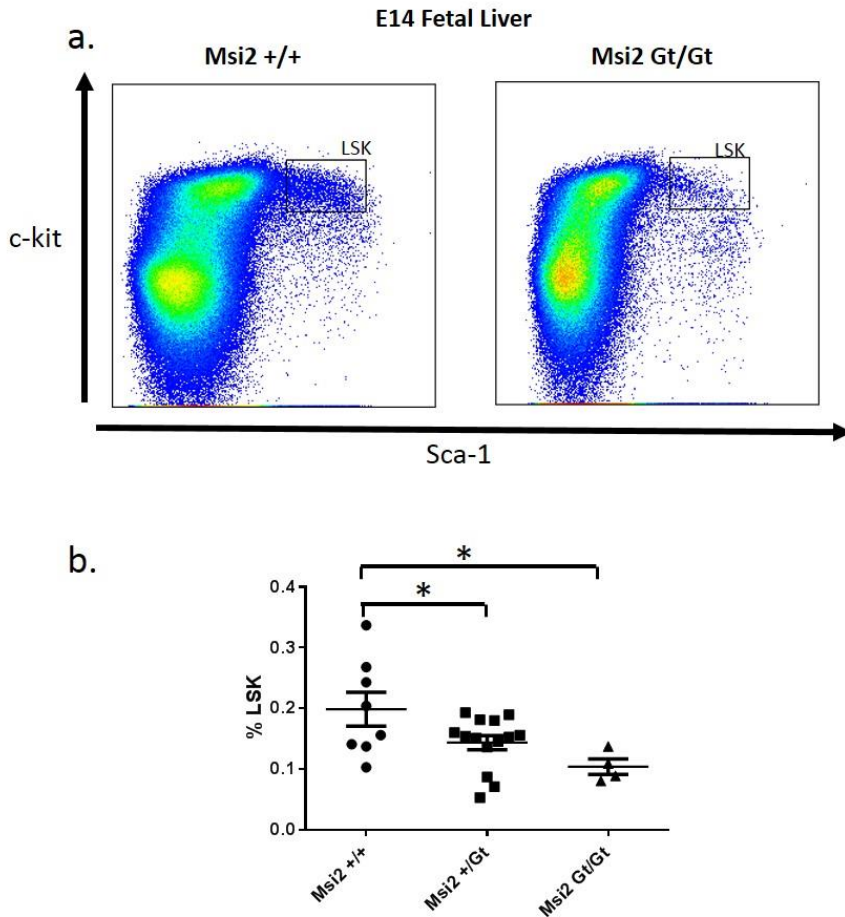


**Figure 6.** Flow cytometric analysis of LSK cells in fetal liver of  $Msi2^{+/+}$  and  $Msi2^{Gt/Gt}$  mice. Representative FACS plots of LSK (gated on Lineage negative cells) (a). Quantification of LSK cells as a percentage of the total analysed cells (b). Means plus S.D. are shown (\*,  $P < 0.05$ ).

These results indicate that  $Msi2$  deficiency significantly affects the number of hematopoietic stem cells in fetal liver. An impaired HSC

pool could be one of the main causes leading to the reduced number of hematopoietic progenitors in *Msi2* defective adult mice (as described in the first chapter).

### ***Msi2* deficient embryos show a decrease in the myelo-erythroid progenitors in the placenta**

More recently, the placenta has been defined as another anatomical site that participates in HSC development<sup>3,4</sup>. HSCs at the placenta display the classical surface phenotype of actively cycling fetal HSCs, expressing CD34 and c-Kit<sup>5</sup>. Moreover, these cells have been found to have a more immature phenotype than the HSCs in the fetal liver, as they lack CD150 and CD48 expression. So we wondered if the number of placental HSCs could be influenced by the expression of *Msi2*. Although the number of CD34<sup>+</sup> c-kit<sup>+</sup> cells (phenotypically defined as HSCs and progenitors) was similar in the placenta from *Msi2*<sup>+/+</sup>, *Msi2*<sup>+/Gt</sup> and *Msi2*<sup>Gt/Gt</sup> embryos analysed, we found that *Msi2* deficient embryos had a significant decrease on more differentiated progenitors (CD34<sup>-</sup> c-kit<sup>+</sup> cells), that include erythroid and megakaryocyte precursors. This decrease was also evident in heterozygous mice (Figure 7).

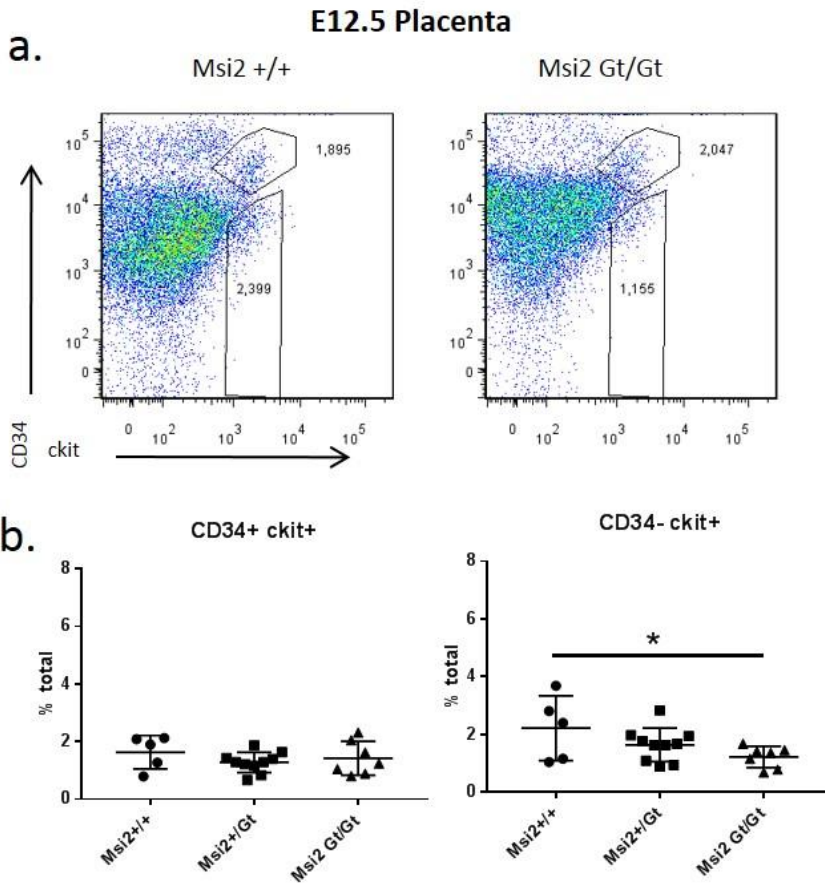


**Figure 7.** Flow cytometric analysis of CD34+ c-kit+ and CD34- c-kit+ populations in placenta of Msi2<sup>+/+</sup>, Msi2<sup>+/-</sup> and Msi2<sup>Gt/Gt</sup>. Representative FACS plots of Msi2<sup>+/+</sup> and Msi2<sup>Gt/Gt</sup> placenta cells (gated on live cells) (a.). Quantification of the percentage of CD34+ c-kit+ and CD34- c-kit+ cells (b). Means and S.D. are shown (\*,  $P < 0.05$ ).

These results indicate that, in contrast with what we see in the fetal liver where the number of actively proliferating LSKs is significantly lower in the Msi2 deficient embryos, the frequency of placental HSC and progenitors is not affected. Maybe the phenotypical differences mentioned between placental HSCs and fetal liver HSCs could explain that the frequency in placenta is not affected in a Msi2 deficiency scenario. However, we cannot discard a functional defect

in these cells and transplantation experiments using the different HSCs populations found along the different embryonic development stages would be required to clarify the role of Msi2 in fetal HSC function.

## **MATERIAL AND METHODS**

### **Genotyping**

Genotyping was performed as described in the supplemental methods section in chapter 1.

### **Animals and embryo harvest**

For embryo generation, male and female mice were housed together late in the evening, and vaginal plugs were examined on the following morning. Discovery of a vaginal plug was scored as E 0.5. Whenever was possible embryos were staged by somite counting: embryos with 32-40 somite pairs, 42-48 somite pairs, 48-51 somites were staged as E10.5, E11.5, and E12.5 respectively. E14.5 embryos were obtained counting 14 days after vaginal plug was observed. To generate  $Msi2^{+/+}$  and  $Msi2^{Gt/Gt}$  embryos,  $Msi2^{+/Gt}$  mice were crossed. Pregnant females were sacrificed and embryos were isolated into room temperature (RT) PBS, supplemented with 10% (vol/vol) FCS, and 1% (vol/vol) penicillin and streptomycin (PenStrep). Embryos were kept at 4°C until ready for dissociation. Portion of the limb bud from staged embryos were used for genotyping analyses. AGM and fetal liver was dissociated by incubation in PBS supplemented with FBS and 2.5mg/ml collagenase type I (Sigma-Aldrich) for 20 minutes at 37°C, and then passed through a syringe with a 28G needle (BD). The placenta, separated from the decidua was dissected, washed in PBS, dissociated mechanically through a 16G needle, and treated with 0.12% collagenase in PBS with 10% FCS for 1.5 hr in 37°C, followed by passages through 18–25G needles. Single cell suspensions were filtered through 50 µm filters (BD) and subjected to cell-counting (Turk solution). Animals were kept under pathogen-

free conditions and experimental procedures were approved by the Parc de Recerca Biomèdica de Barcelona (PRBB) Animal Care Committee and Government of Catalonia.

### **Immunofluorescence**

For tissue-section immunostainings, embryos were fixed overnight in 4% paraformaldehyde (Sigma-Aldrich) at 4 °C, included in paraffin or Optimal Cutting Temperature (OCT) (Tissue-Tek, Sakura) and sectioned at 8 µm. Primary antigen retrieval of paraffin-embedded embryos was performed in 10 mM sodium citrate pH 6, 20 min in autoclave. On peroxidase exhaustion (3% H<sub>2</sub>O<sub>2</sub>), slides were incubated in blocking solution (3% BSA, 20 mM MgCl<sub>2</sub>, 0.3% Tween20 and 5% FBS in PBS). Primary antibodies were used at the following concentrations: anti-Msi2 1:100 (ab76148, Abcam), anti-CD41 1:50 (BD) and developed using AF488-goat-anti-rabbit and AF546-goat-anti-mouse (Invitrogen).

### **RNA extraction and RT-qPCR**

Total RNA from sorted population was extracted using RNeasy Midi C-kit (QIAGEN). RNA quality was assessed on agarose gels and quantified by Nano-Drop1000 (Thermo Fisher Scientific). cDNA was obtained with RT First Strand cDNA Synthesis (GE Healthcare) according to the manufacturer's instructions. Real-time PCR was performed in triplicate on the ViiA7 RealTime (Applied Biosystems) and with SYBR Green (Applied Biosystems). The primers used for SYBR Green detection are:

Msi2-for	GTATTAGGTCAGCCCCACCA;
Msi2-rev	CTCGACGAGGAAATGCAACT;
Tfrc-for	CCCATGACGTTGAATTGAACC;
Tfrc-rev	

GTAGTCTCCACGAGCGGAATA. Ct values were calculated and normalized to Tffc, and the relative expression ratio was calculated using the Pfaffl method<sup>6</sup>

### **FACS analysis**

Cells were stained for 30 min with different antibodies. Antibodies used were CD31, CD45, CD117 (c-kit), CD41 (BD), lineage positive cell staining was performed with the following mix of biotinylated antibodies: CD3e, CD4, CD5, CD8a, CD19, CD45R, Gr-1, Ter119. DAPI staining (Molecular Probes) was used to exclude dead cells. Flow cytometry analysis was performed on a LSRII or Fortessa (BD). Cell sorting was performed on a FACSVantage (BD). All data were analyzed with FlowJo software (Tree Star).

### **Statistical analysis**

For bar graphs, the unpaired two-tailed Student's t test was used to compute p-values. Error bars reflect the SD. All statistical analyses were performed using Prism 4.0 (GraphPad Software)



## REFERENCES

1. Boisset, J.-C. *et al.* In vivo imaging of haematopoietic cells emerging from the mouse aortic endothelium. *Nature* **464**, 116–20 (2010).
2. Robin, C., Ottersbach, K., Boisset, J.-C., Oziemlak, A. & Dzierzak, E. CD41 is developmentally regulated and differentially expressed on mouse hematopoietic stem cells. *Blood* **117**, 5088–5091 (2011).
3. Gekas, C., Dieterlen-Lièvre, F., Orkin, S. H. & Mikkola, H. K. A. The placenta is a niche for hematopoietic stem cells. *Dev. Cell* **8**, 365–375 (2005).
4. Ottersbach, K. & Dzierzak, E. The murine placenta contains hematopoietic stem cells within the vascular labyrinth region. *Dev. Cell* **8**, 377–387 (2005).
5. Gekas, C. *et al.* Hematopoietic stem cell development in the placenta. *Int. J. Dev. Biol.* **54**, 1089–98 (2010).
6. Pfaffl, M. W. A new mathematical model for relative quantification in real-time RT-PCR. *Nucleic Acids Res.* **29**, e45–e45 (2001).
7. Busch, K. & Rodewald, H.-R. Unperturbed vs. post-transplantation hematopoiesis. *Curr. Opin. Hematol.* **23**, 295–303 (2016).
8. Park, S.-M. *et al.* Musashi-2 controls cell fate, lineage bias, and TGF- $\beta$  signaling in HSCs. *J. Exp. Med.* **211**, 71–87 (2014).
9. Huang, J. *et al.* Pivotal role for glycogen synthase kinase-3 in hematopoietic stem cell homeostasis in mice. *J. Clin. Invest.* **119**, 3519–29 (2009).
10. Kligun, E. & Mandel-Gutfreund, Y. The role of RNA conformation in RNA-protein recognition. *RNA Biol.* **6286**, 00–00 (2015).
11. Perry, J. M. *et al.* Cooperation between both Wnt/{beta}-catenin and PTEN/PI3K/Akt signaling promotes primitive hematopoietic stem cell self-renewal and expansion. *Genes Dev.* **25**,

1928–1942 (2011).

12. Zhang, C. C. & Lodish, H. F. Murine hematopoietic stem cells change their surface phenotype during ex vivo expansion. *Blood* **105**, 4314–4320 (2005).
13. He, J., Kang, X., Yin, Y., Chao, K. S. C. & Shen, W. H. PTEN regulates DNA replication progression and stalled fork recovery. *Nat. Commun.* **6**, 7620 (2015).
14. Emerling, B. M., Weinberg, F., Liu, J. L., Mak, T. W. & Chandel, N. S. PTEN regulates p300-dependent hypoxia-inducible factor 1 transcriptional activity through Forkhead transcription factor 3a (FOXO3a). *Proc Natl Acad Sci U S A* **105**, 2622–2627 (2008).
15. Schmid, A. C., Byrne, R. D., Vilar, R. & Woscholski, R. Bisperoxovanadium compounds are potent PTEN inhibitors. *FEBS Lett.* **566**, 35–38 (2004).
16. Wang, S. *et al.* Transformation of the intestinal epithelium by the MSI2 RNA-binding protein. *Nat. Commun.* **6**, 6517 (2015).
17. Pinto do O, P., Kolterud, A. & Carlsson, L. Expression of the LIM-homeobox gene LH2 generates immortalized steel factor-dependent multipotent hematopoietic precursors. *EMBO J.* **17**, 5744–5756 (1998).
18. Kawahara, H. *et al.* Neural RNA-binding protein Musashi1 inhibits translation initiation by competing with eIF4G for PABP. *J Cell Biol* **181**, 639–653 (2008).

**Chapter 3**

**Msi2 targets and their role in the regenerating hematopoietic system**

As described in the first chapter of this section, adult *Msi2* defective mice have in homeostasis, e.g. in normal and unperturbed conditions, a significant reduction of primitive hematopoietic progenitors but only modestly reduced proportions of LT-HSCs. It has been described that some phenotypes only become evident when HSCs are challenged by diverse sources of stress. In fact, recent findings suggest that LT-HSC are rarely contributing to normal hematopoiesis and mostly become active upon injury or stress<sup>7</sup>.

### ***Msi2* deficiency impairs the regeneration ability of HSCs after 5-FU treatment**

To evaluate the influence of *Msi2* deficiency on the regenerative capacity of HSCs under hematopoietic stress, we challenged mice with a single injection of 5-fluoruracil (5-FU), a cytotoxic agent that kills cells that are actively dividing, causing a transient leukopenia in blood. HSCs were analysed at different time points following 5-FU treatment in *Msi2* Gt and WT mice (Figure 1a). After treatment with 5-FU, LSK cells were drastically depleted in both the *Msi2*<sup>Gt/Gt</sup> and *Msi2*<sup>+/+</sup> at day 4, but slightly recovered on day 7. At day 11, the number of LSK cells in wild-type mice increased substantially as a response to regeneration of the hematopoietic system. In contrast, LSK cells from *Msi2* deficient mice were not able to repopulate the bone marrow, most probably caused by either an inability to proliferate or an increase in apoptosis (Figure 1b and c). Moreover, a detailed analysis of the LSK compartment showed that in *Msi2* deficient mice not only ST-HSCs and MPPs were not able to

regenerate themselves (Figure 1d), but also LT-HSCs failed to proliferate (Figure 1e)

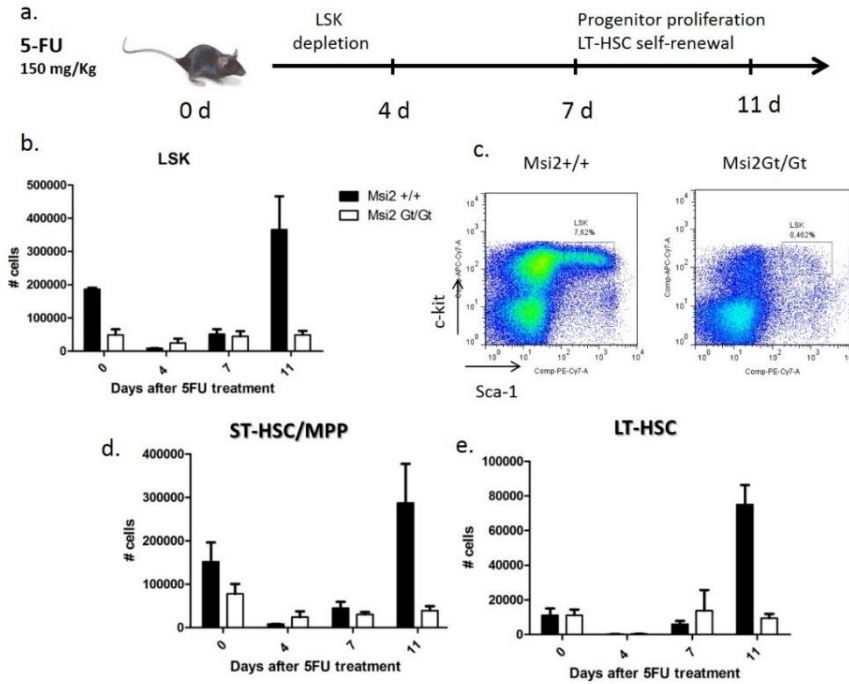


**Figure 1.** Effects of 5FU treatment. a, Experimental outline. b, Histogram showing the mean of absolute LSK cells number in bone marrow of Msi2<sup>+/+</sup> and Msi2<sup>Gt/Gt</sup> mice at the indicated days after 5-FU injection. c, FACS profiles of WT and Msi2<sup>Gt/Gt</sup> LSK subsets at day 11 after treatment. d, e Frequency of ST-HSC/MPPs (LSK CD34+) and LT-HSCs (LSK CD34-) of Msi2<sup>+/+</sup> and Msi2<sup>Gt/Gt</sup> mice on the indicated days after 5-FU injection. Black bars show cells derived from WT, white bars from Msi2<sup>Gt/Gt</sup> mice.

### Msi2 deficient mice LT-HSCs are not able to repopulate secondary transplanted animals

We further studied the function in LT-HSCs by serial transplantation.  $10^7$  total BM cells from mutant and control mice were transplanted into lethally irradiated recipients in the absence of competitor cells. Analysis of the peripheral blood for cells of donor origin up to 5

months after transplantation showed efficient engraftment by  $Msi2^{Gt/Gt}$  BM cells in the absence of competition at all time points analysed (results shown in the first chapter). Subsequently, 4000 sorted LSK cells from primary recipients were transplanted into lethally irradiated mice. Survival of secondary recipients was monitored up to 150 days after transplantation. As shown in Figure 2, mice transplanted with  $Msi2$  deficient LSK cells succumbed to the transplantation and didn't survive longer than 120 days, whereas WT animals were still all alive, moreover 50% of the mice already died before day 80 after transplantation.

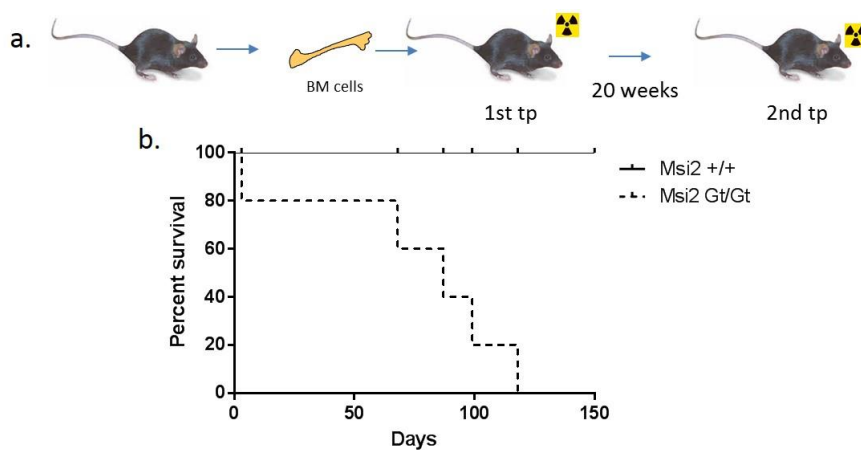


**Figure 2.** Secondary transplantation a, Experimental outline of the primary transplantation (1st tp) and secondary transplantation (2nd tp) experiments. b, Kaplan-Meier survival curve for secondary recipients after transplantation with LSKs derived from primary transplanted mice with  $Msi2^{+/+}$  and  $Msi2^{Gt/Gt}$  total BM.

Thus, the inability of  $Msi2$  deficient HSC population (both long-term and more differentiated progenitors) to respond to hematopoietic stress and the defective regeneration after injury, indicate that  $Msi2$  could have an important role not only in steady-state hematopoiesis but also in stress-induced regeneration of the hematopoietic system.

In light of these results and to understand the molecular basis of the defects observed in Msi2 deficient cells, we decided to search for Msi2 targets.

### **Protein-RNA binding propensity estimation identifies Msi2 target candidates**

By using the web server CatRapid, which estimates the binding propensity of protein-RNA pairs by evaluating the interaction propensities of polypeptide and nucleotide chains using their physicochemical properties (secondary structures, hydrogen bonding and van der Waals contributions), we analysed a list of potential candidates. Microarray data performed with Msi2 deficient and wild-type LSK population (see chapter 1) as well as the gene sets resulting from the Gene Set Enrichment Analysis (GSEA) were used as the source of putative candidates. The criteria to select these candidates, and taking into account that the mechanism of action of Msi2 is not well-known, was based on two different possibilities, (i) Msi2 regulates the stability of mRNA (so changes in Msi2 protein levels lead to changes in its targets mRNA levels) and/or (ii) Msi2 regulates the translation efficiency in which case the mRNA of putative targets doesn't change upon Msi2 protein expression changes. In the first scenario, we would expect to find Msi2 targets among the differentially regulated genes uncovered in the microarray analysis; in the second we would assume that Msi2 targets are not among the regulated mRNAs but may be included in the list of significantly enriched gene sets. In this case, the changes of mRNA levels in Msi2 deficient cells are a consequence of the regulation of Msi2 putative targets at the level of protein expression. Therefore for the analysis

we used FASTA sequences from differentially regulated genes in the microarray analysis (see chapter 1) as well as from the significant gene sets resulting from the Gene Set Enrichment Analysis (GSEA). Interaction propensity of Msi2 with 621 down-regulated genes (corresponding to 2521 transcripts) and 552 up-regulated genes (corresponding to 2367 transcripts) was computed. The top 1% interacting fragments were selected and ranked by average binding propensity (mean score) of the different fragments as well as by highest binding propensity (maximum score). The genes whose mRNAs ranked among the ones who had higher mean score as well as maximum score were: *sos1*, *ccdc88a*, *gsk3b*, *tnxb*, *pten*, *papa*, *lamc1*, *maf*, *irs1* and *gabbr2* (Figure 3)

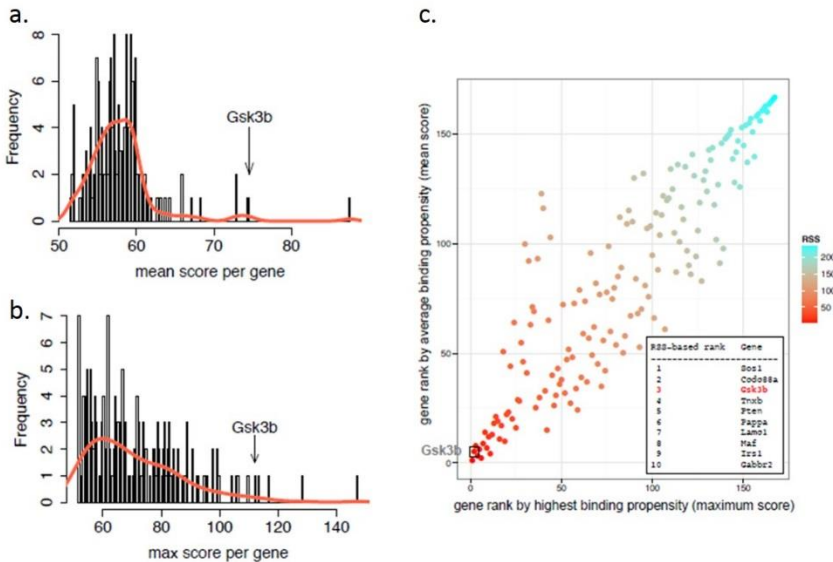


**Figure 3.** CatRapid prediction analyses. Plots showing the mean scores (a) and maximum scores (b) for the genes that had a higher interaction score calculated by using the CatRapid web server. Ranked genes based on the mean score and the maximum score (c)



**Most of the candidates predicted in the CatRapid analysis could be confirmed by RNA-binding immunoprecipitation (RIP)-qPCR analysis**

To further support that Msi2 binds to the predicted downstream targets, we performed RNA immunoprecipitation (IP)-qPCR experiments in the murine HPC-7 cell line, a hematopoietic cell line derived from LHX2-overexpressing embryonic stem cells. HPC-7 requires stem cell factor for growth and exhibits multilineage differentiation upon stimulation with the proper cytokines. Moreover, HPC-7 expresses Msi2 while maintained in SCF media (Figure 4a). RIP-qPCR analysis confirmed 5 out of the 10 predicted genes: *sos1*, *gsk3b*, *tnxb*, *pten* and *lamc1* (Figure 4b). For the other 5 (*ccdc88a*, *papa*, *maf*, *irs1* and *gabbr2*) mRNAs, RIP analysis could not be performed as they are not expressed in HPC-7 cells. *Tgfbrii*, already described as a Msi2 target<sup>8</sup>, was included as a positive control, and c-Myc and Msi-2 were analyzed as negative controls. Moreover, binding of Msi2 to Gsk3b mRNA was further confirmed by the overexpression of the Flag tagged wild-type Msi2 (figure 4c). Moreover the overexpression of two forms of Msi2 mutated in its RNA binding domains (RRM1 and RRM2) abrogated the binding, confirming that the binding of Msi2 to Gsk3b mRNA occurs through its RNA binding domains (Figure 4d and 4e).

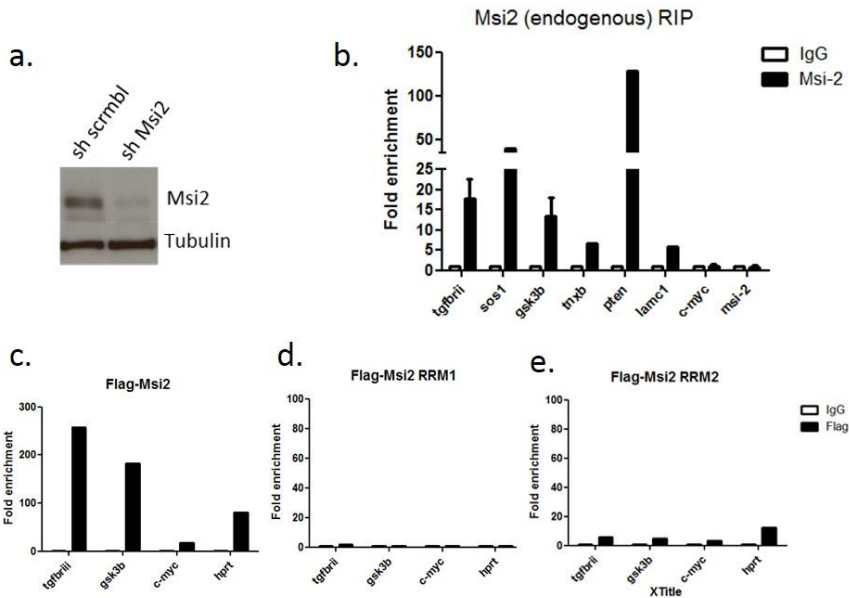


**Figure 4.** RIP-qPCR analyses in HPC-7 cells. Msi2 expression measured in HPC-7 cells by Western-blot (a); RIP-qPCR analysis of endogenous Msi2 (b), overexpressed Flag-tagged Msi2 (c) and Flag-tagged RRM1 (d) and RRM2 (e) Msi2 mutants. Ct values for either Msi2 or flag and IgG immunoprecipitated samples obtained from the qPCR were normalized to the Input sample Cts and represented as fold enrichment expression over input sample.

### Msi2 binds the 5'UTR of the Gsk3b mRNA and regulates its expression in the HPC-7 cell line

Among the 5 candidates that were confirmed by RIP analysis we decided to focus first on Gsk3b. Gsk3b has been found to be an important regulator of hematopoiesis, both in the adult as well as in the embryo. Previous studies have demonstrated that Gsk3b is able to regulate both the Wnt and the mTOR signalling pathways, playing pivotal roles in self-renewal and lineage commitment of the murine HSCs<sup>9</sup>.

A modified version of the RIP-qPCR assay was used with HPC-7 cells expressing Flag-Msi2. Briefly, an additional step of UV radiation was added in order to cross-link RNA binding proteins to the RNA that they are bound to. During cell extract preparation, a partial RNA digestion was performed so after Flag IP only the regions that were bound by Flag-Msi2 would be recovered. RNA was retrotranscribed and analysed by qPCR. A set of primers spanning 100-150 bp regions over 5' untranslated region (UTR), coding DNA sequence (CDS) and 3'UTR of the Gsk3b mRNA were designed and used in the qPCR. As shown in Figure 5a, two primer pairs corresponding to the region from 25 to 96 bp and 1037-1116 bp, both in the 5'UTR of the Gsk3b mRNA, were amplified, indicating that most likely Msi2 regulates Gsk3b expression through its binding to the 5'UTR of the mRNA. Moreover, binding motif analysis of the mRNA Gsk3b revealed that the 5'UTR is enriched for Msi binding motifs, more specifically in the regions that span from nucleotides 412 to 512 and from nucleotides 1612 to 1712 (figure 5b). Although the regions don't match exactly with what we found in the modified RIP-qPCR analysis, they are very close. Differences can be attributed to conformational changes that occur in the RNA when RNA-protein complexes are formed, suggesting that the RNA binding proteins not only interact with the recognition motifs but also with adjacent regions<sup>10</sup>.

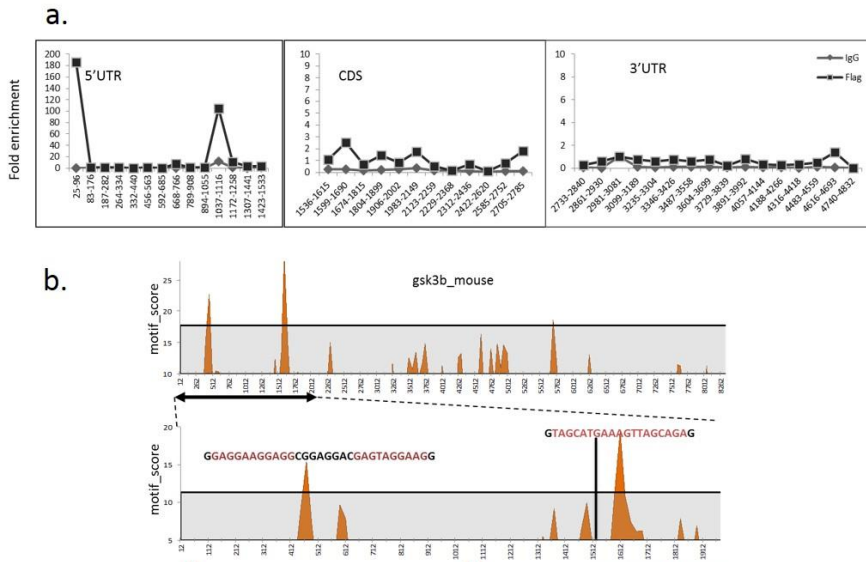


**Figure 5.** Modified RIP-qPCR assays. Plots show the fold enrichment values for IgG (grey) and Flag IP (black) (a). Ct values for flag and IgG immunoprecipitated samples obtained from the qPCR, were normalized to the Input sample Cts and represented as fold enrichment expression over input sample. Motif analysis graphs for *msi2* on *gsk3b* mRNA (b) show the motif scores calculated for 250bp-regions across the whole mRNA (top) and 100 bp-regions of a zoomed fragment of 2kb (bottom) in the 5'UTR region. Shaded grey area and black line marks the region of 2.5 standard deviations above the mean. The sequences that correspond to the regions with highest motif score values are shown.

To test whether *Gsk3b* expression levels are regulated upon downregulation of *Msi2* expression, we knocked down *Msi2* in HPC-7 cells and analysed the levels of *Gsk3b* protein expression by immunofluorescence. *Msi2* knockdown led to a slight increase of *Gsk3b* expression compared to scramble shRNA overexpressing cells (Figure 6).

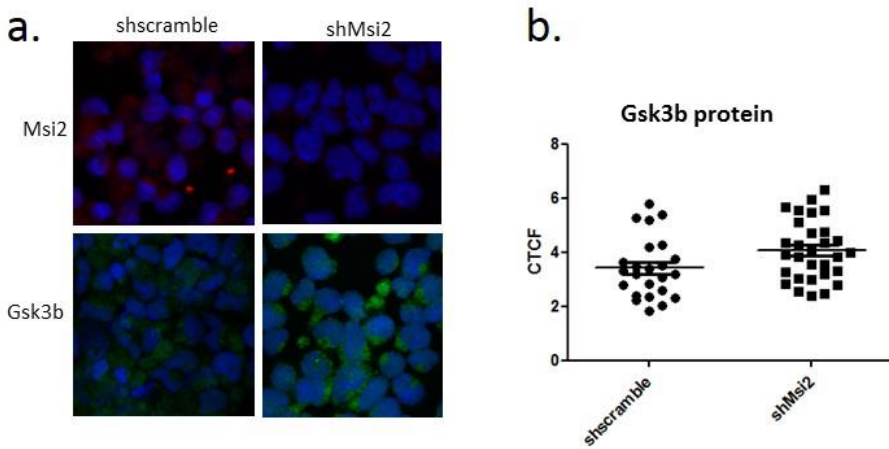


**Figure 6.** Immunofluorescence analysis for Gsk3b in HPC-7(a) Representative images of HPC-7 cells overexpressing the shRNA for Msi2 and a scrambled shRNA as a control, stained with a specific antibody against Msi2 (top row, in red) and Gsk3b (bottom row, in green). (b) Plot showing the corrected total cell fluorescence (CTCF) values for Gsk3b expression in shScramble and shMsi2 overexpressing HPC-7 cells. CTCF was calculated as indicated in the Methods.

From these results we conclude that in the HPC-7 cell line Msi2 regulates Gsk3b protein expression through the interaction of the Msi2 RRM binding domains with the 5'-UTR of the Gsk3b mRNA.

### **Canonical Wnt pathway activation is diminished in cultured Msi2 deficient LSK**

The results with HPC-7 cells prompted us to further examine the link between Msi2 and Gsk3b in murine primary hematopoietic progenitors. Gsk3b, as mentioned in the introduction (Section 2.2.2.3), is part of a complex that tags  $\beta$ -catenin for ubiquitination and degradation, thus inhibiting the canonical Wnt pathway. It's already known that the optimal base medium for expanding phenotypic HSCs (StemSpan SFEM) contains a high concentration of insulin, a major stimulator of the PI3K/Akt pathway, forcing the

cells to proliferate<sup>11</sup>. Moreover, we have seen that Wnt pathway is activated (measured as an increase in the Wnt target Axin2) upon culturing LSK cells in the aforementioned media supplemented with cytokines (Lodish conditions) (see Material and Methods)<sup>12</sup> (Figure 7a). So we thought that the analysis of the Gsk3b protein levels and Wnt pathway in WT and *Msi2*<sup>Gt/Gt</sup> cultured in vitro could be a good model to study the link between *Msi2*, Gsk3b and Wnt pathway. We analysed Gsk3b and activated  $\beta$ -catenin, as well as total  $\beta$ -catenin protein levels in sorted LSK cells grown in vitro. Surprisingly, immunofluorescence analysis showed that levels of Gsk3b protein didn't differ when we compared LSKs from wild-type and *Msi2* deficient mice (Figure 7b). In contrast, we found reduced levels of activated  $\beta$ -catenin in *Msi2* deficient LSKs (Figure 7c) and also a decrease in the total protein (Figure 7d). These findings indicate that there is a deficiency in the activation of the canonical Wnt pathway in cells that lack *Msi2*.

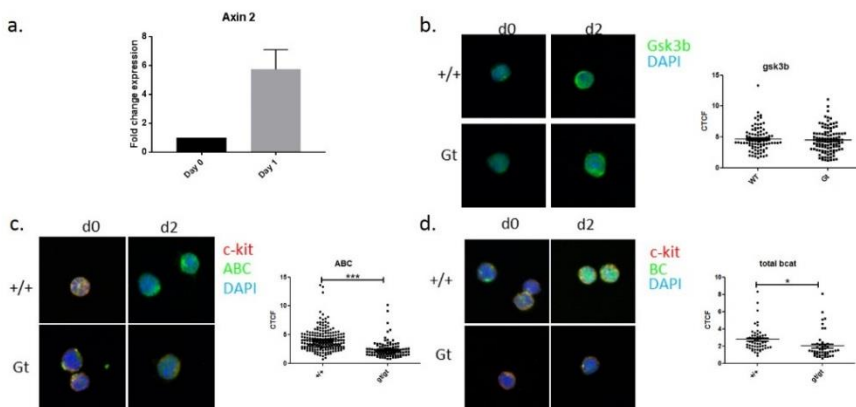


**Figure 7.** Gsk3b and  $\beta$ -catenin immunofluorescence analysis (a) qRT-PCR of Axin2 expression in wild-type LSKs cultured in Lodish conditions for 24 hours. WT and *Msi2*<sup>Gt/Gt</sup> sorted LSKs were stained with antibodies against gsk3b (b) activated  $\beta$ -catenin (ABC) (c) and total  $\beta$ -cat (d) before (d0) and after (d2) growing them in vitro. Fluorescence intensity was measured at d2 and the corrected total

cell fluorescence was calculated (as described in Material and Methods) for individual cells and plotted. Means are shown (\*,  $P < 0.05$ ; \*\*,  $P < 0.01$ ; \*\*\*,  $P < 0.001$ )

In order to test if the phenotype that we observed could be rescued upon pathway activation, we incubated the cells with Wnt3a, a canonical Wnt ligand, and measured the activation of the  $\beta$ -catenin (Figure 8a). Although the defect in Msi2<sup>Gt/Gt</sup> HSCs and progenitors was partially rescued (Figure 8b) there were still differences in the levels of activation, indicating that the defect is due to a direct effect of Msi2 on one or more components of the signalling pathway.

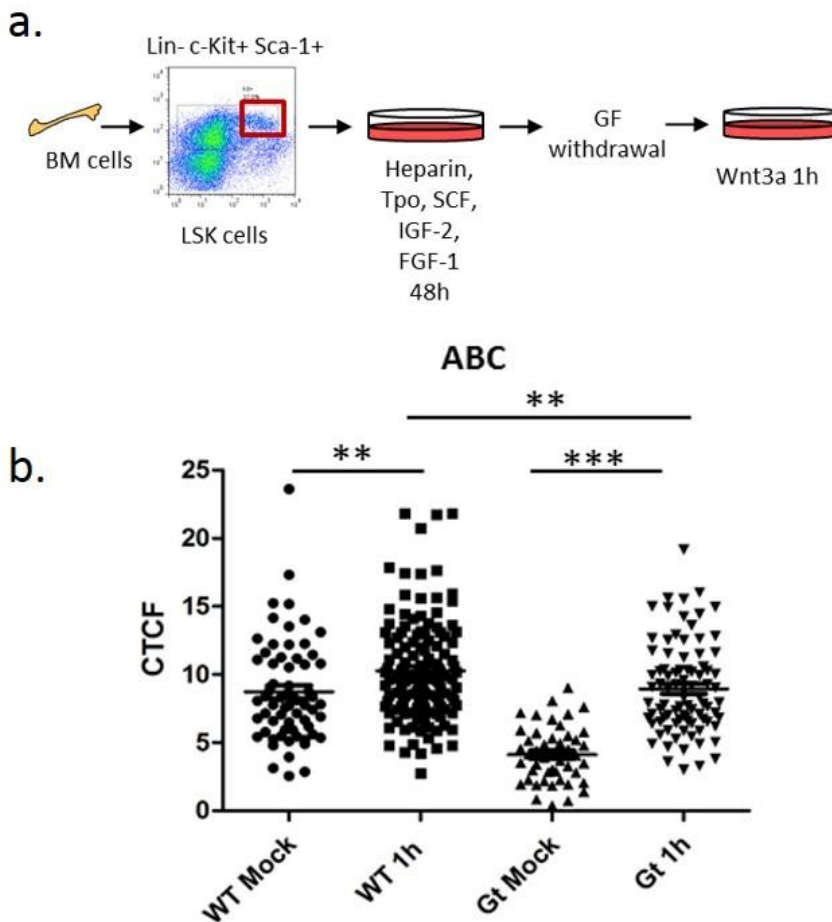


**Figure 8.** Wnt3a rescue experiment. Experimental outline of the rescue experiment with Wnt3a (d), cells were incubated for 48h and the growth factors were withdrawn for 4 hours, Wnt3a was added to the cell culture and incubated for 1 hour. Then cells were harvested and stained with activated  $\beta$ -catenin and the fluorescence was quantified as specified above. Means and S.D. are shown (\*,  $P < 0.05$ ; \*\*,  $P < 0.01$ ; \*\*\*,  $P < 0.001$ )

These results suggest a defect in the output of the Wnt signalling pathway when the cells are forced to enter the cell cycle. Although we found that Gsk3b protein is regulated by Msi2 in the HPC-7 cell line, in primary cells it does not seem so as it is expressed at the same levels both in wild-type and Msi2 deficient cells. We therefore



conclude that the differences in Wnt pathway activation are not primarily due to a different expression of Gsk3b protein.

As described in the introduction, different signalling pathways can influence the behaviour of HSCs. In fact a wide variety of factors critical for HSC regulation have been identified that establish a complex molecular cross-talk. Therefore, we could not discard that changes in other signalling pathways due to the Msi2 deficiency may be influencing the Wnt pathway output. In fact, CatRapid analysis and RIP-qPCR assay pointed to another interesting candidate that has been already described as an important regulator of HSC function, the PTEN protein. Moreover, PTEN has also been found to regulate the Wnt pathway through the PI3K-Akt signalling pathway. So to further understand how Msi2 loss could negatively control Wnt pathway, we focus on PTEN function.

### **Msi2 deficient LSK cells express higher levels of Pten but with a different subcellular localization**

We first wanted to check if Pten protein levels are regulated in Msi2<sup>Gt/G</sup> LSK cells. In order to do that we analysed the expression of Pten protein in LSKs sorted from wild-type and Msi2 deficient mice, after culturing them for 48 hours in Lodish conditions (as described in the experiments for Gsk3b). In this case we observed an increase of PTEN expression in Msi2<sup>Gt/Gt</sup> LSKs compared to their wild-type counterparts (Figure 9b). Moreover, not only Pten protein levels were increased but also the subcellular localization was different when we compared with the wild-type LSK cells. Thus, upon activation of proliferation in WT LSK cells, Pten protein localizes rapidly to the

nucleus, forming prominent nuclear speckles. In contrast, Pten in Msi2 deficient LSKs remained at the cytoplasm (Figure 9a, c).

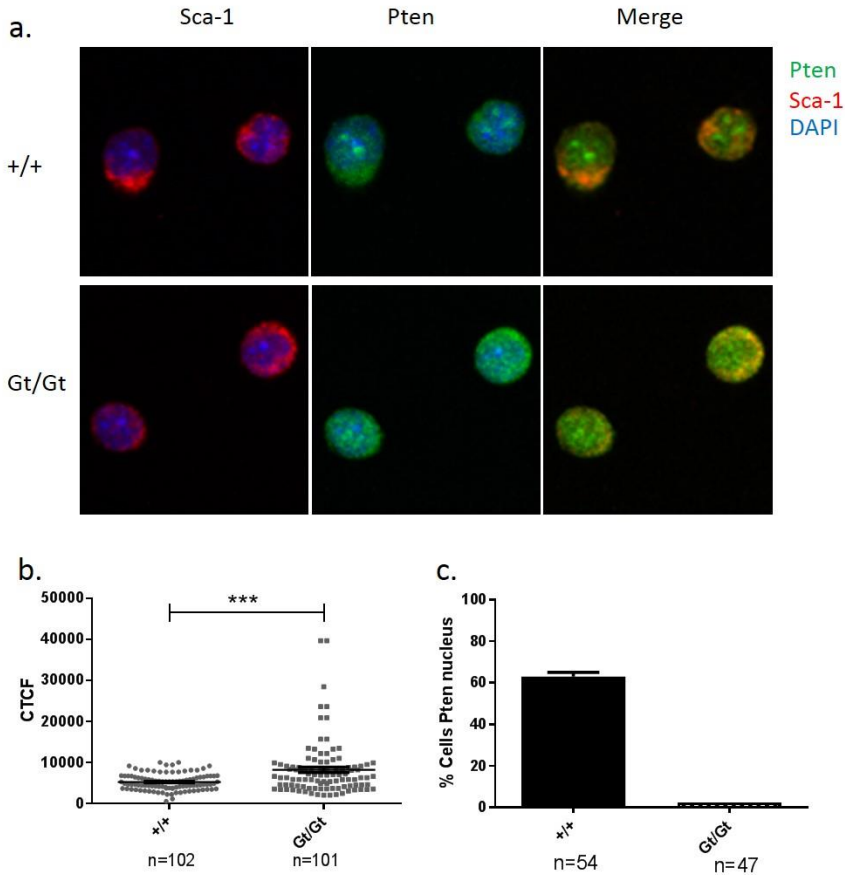


**Figure 9. Immunofluorescence analysis** WT and Msi2<sup>Gt/Gt</sup> sorted LSKs were stained with antibodies against Pten (green) and Sca-1 (red) (a) after growing them in vitro for 2 days. Fluorescence intensity was measured and the corrected total cell fluorescence was calculated (as described in Material and Methods) for every cell and plotted (b). Means plus S.D. are shown (\*\*\*, P<0.001)

### Cytoplasmic localization of PTEN in Msi2<sup>Gt/Gt</sup> may indicate a cell cycle progression and DNA damage repair malfunction.

For a long time it was thought that PTEN localized exclusively to the cytoplasm. However, recent publications shows that it can also be

found in the nucleus, playing crucial functions as DNA repair, cell cycle progression<sup>13</sup> and expression of hypoxia regulated genes<sup>14</sup>. Although this has been shown in different cell types, there is no report of nuclear PTEN in hematopoietic cells. To further study the link between nuclear PTEN and DNA repair, we analysed how DNA damage could modulate PTEN subcellular localization in the hematopoietic progenitor cell line HPC-7. Our preliminary experiments show that upon DNA damage induction with hydrogen peroxide, PTEN accumulates in the nucleus of HPC-7 cells (Figure 10a). Moreover, inhibition of PTEN activity by bpV(HOpic), an inhibitor of protein tyrosine phosphatases that at nanomolar concentrations is specific for PTEN<sup>15</sup>, sensitized HPC-7 cells to DNA-damage induced apoptosis (Figure 10b). Increase in apoptosis may be due to an inhibition of the phosphatase activity without a change of PTEN localization, as the protein remained in the nucleus after bpV(HOpic) treatment (Figure 10c).

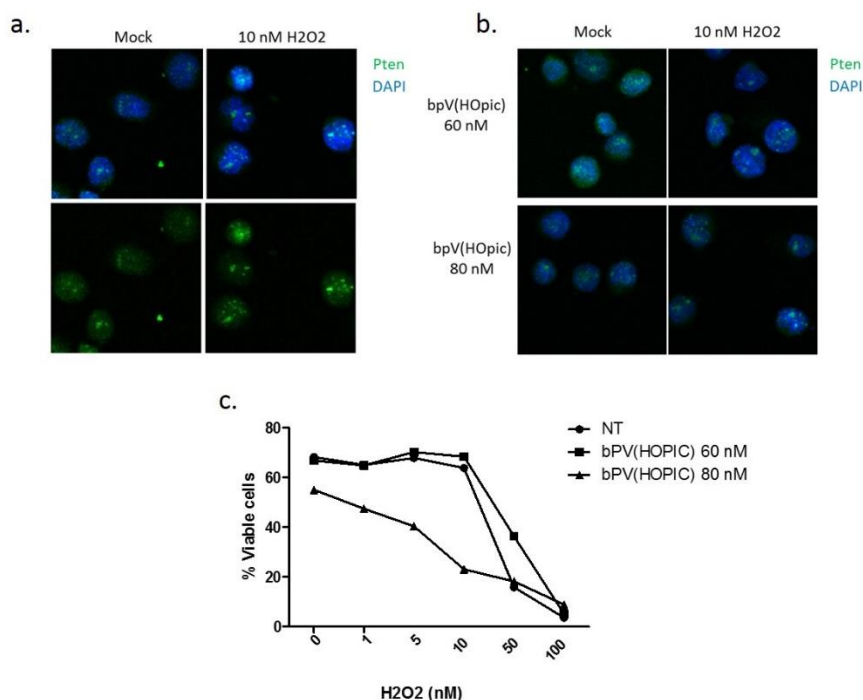


**Figure 10.** Inhibition of Pten activity and DNA damage. HPC-7 cells were treated with different concentrations of H<sub>2</sub>O<sub>2</sub> (1, 5, 10, 50 and 100 nM) for 24h and stained with Pten antibody. For Pten inhibition experiments, cells were pre-treated with 60 nM and 80 nM bpV(HOPIC) for 1 hour. Immunofluorescence images (Pten in green) are shown for not treated cells and cells treated with 10 nM H<sub>2</sub>O<sub>2</sub> (a) and for bpV (HOPIC) pre-treated cells and treated with 10 nM H<sub>2</sub>O<sub>2</sub> (b). Plot shows percentage of viable cells as calculated performing an apoptosis assay. Means from two independent experiments are shown.

In conclusion, our preliminary results suggest that nuclear PTEN protects cells from DNA-damage induced apoptosis. Further experiments need to be done to confirm this hypothesis.

### **Msi2 binds to the 3'UTR of the Pten mRNA and regulates its expression**

When we started to study the link between Pten and Msi2, RNA crosslinking, immunoprecipitation and massively parallel sequencing (CLIP-Seq) data for Msi2 in the intestinal epithelium was

published<sup>16</sup>. In fact, the same authors demonstrated that Msi2 is a potent oncogene, as it was able to inhibit the mTORC1 pathway, possibly through the regulation of PTEN protein. Taking advantage of this we could perform Msi2 binding motif analysis in the *PTEN* mRNA that revealed the existence of two adjacent recognition motifs in the 3'UTR, spanning from nucleotides 7913 to 7937 and from nucleotides 7957 to 7968 (Figure 11a). To assess whether Msi2 directly can alter the expression of PTEN, either the pGL4-PTEN 3'UTR, containing the firefly luciferase reporter construct under the control of the 3'UTR of *PTEN* mRNA, or the empty pGL4 vector were cotransfected with a control Renilla reporter construct into 293T, 293T overexpressing Msi2 (293T-Msi2) and 293T overexpressing either RRM1 (293T-Msi2RRM1) or RRM2 (293T-Msi2RRM2) mutant Msi2 (Figure 11b). A decrease in relative luciferase activity was noted upon overexpression of Msi2, indicating that Msi2 can modulate *PTEN* gene expression through its 3'UTR (Figure 11c). Surprisingly, although the expression of luciferase in the RRM mutants increased significantly when we compared to the wild-type Msi2-overexpressing 293T cells, it didn't completely rescue the phenotype. In order to discard any issues with the mutants' functionality, we performed a RIP assay in these cell lines. As shown in figure 9d, the binding of *TGFBR2* (used as a positive control) and *PTEN* mRNAs decreased upon overexpression of the Msi2-RRM2, nevertheless there was still a significant amount of mRNA that was bound to the mutated Msi2. These findings may explain the partial rescue of luciferase expression in the Msi2 RRM2 compared to the wild-type 293T cells. To further understand how Msi2 regulates

PTEN expression, we measured the luciferase mRNA levels in the different cell lines. As shown in Figure 9e, luciferase mRNA levels decreased upon overexpression of Msi2, indicating that at least one of the mechanism by which Msi2 regulates PTEN expression is by regulating the stability of *PTEN* mRNA.

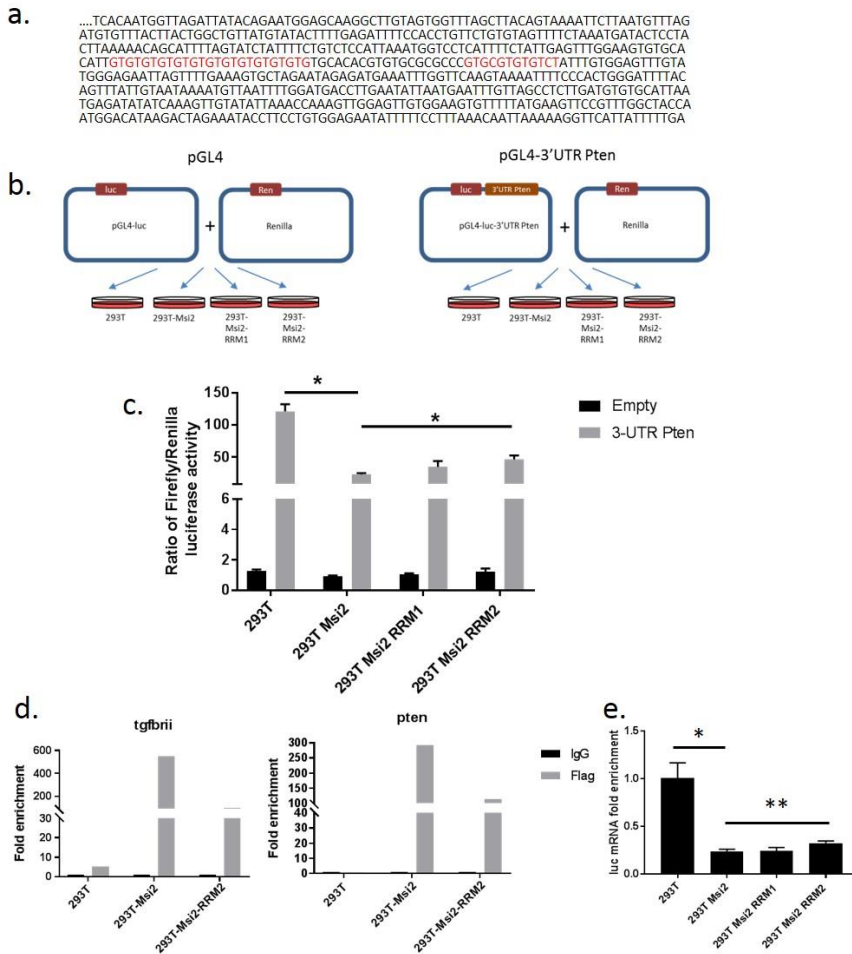


**Figure 11.** Luciferase assay on 3'UTR *PTEN*. Fragment of *Pten* 3'UTR showing putative Msi2 recognition motifs in red (a). Experimental outline of the luciferase assay (b). Plot showing normalized values of Firefly luciferase activity assay in 293T, 293T-Msi2 and 293T overexpressing RRM Msi2 mutants (c). qRT-PCR of *TGFBRII* and *PTEN* mRNAs targets with RIP performed as in figure 4 (d) and qRT-PCR of luciferase mRNA in the different cell lines. Means are shown (\*,  $P < 0.05$ ; \*\*,  $P < 0.01$ )

Altogether, these results indicate that Msi2 may regulate PTEN expression by binding to its 3'UTR and decreasing the stability of the mRNA. Further experiments would be necessary to clarify if it also regulates translation efficiency.

## **MATERIAL AND METHODS**

### **Bone Marrow transplantation**

Bone marrow transplantation was performed as described in the Material and methods section in Chapter 1

### **Reagents**

Recombinant mouse Wnt-3A was purchased from Peprotech LTD. bpV(HOpic) was purchased from Sigma-Aldrich.

### **5-FU treatment**

5-FU (150 mg/kg) was injected in mice. Mice were euthanatized 4, 7 and 11 days after and BM was extracted and analysed by FACS.

### **RIP-qPCR**

33 million HPC-7 control vector cells and cells overexpressing Flag-MSI2 were used for RIP using the Magna RIP RNA binding protein immuno-precipitation kit (EMD Millipore). In brief, cells were washed with cold PBS and lysed with RIP lysis buffer provided from the kit. 5 µg anti-Flag M2 Ab (Sigma-Aldrich), anti-rabbit Ab, or anti-Msi2 Ab (EMD Millipore), which were incubated with magnetic beads, were used to immunoprecipitate Flag-MSI2-RNA complexes. Immunoprecipitated complexes were washed and treated with proteinase K. RNA was extracted using the phenol/chloroform method, and the resulting RNA was converted to cDNA using the High Capacity RNA-to-cDNA kit (Thermo Fisher Scientific). cDNA was then used for qRT-PCR validating candidates.



### **RNA extraction and qRT-PCR**

Total RNA was extracted using RNeasy Mini kit (QIAGEN). RNA quality was assessed on agarose gels and quantified by Nano-Drop1000 (Thermo Fisher Scientific). cDNA was obtained with High Capacity RNA-to-cDNA Master Mix (Applied Biosystems). Real-time PCR was performed in triplicate on the ViiA7 RealTime (Applied Biosystems) and with SYBR Green (Applied Biosystems). Ct values were calculated and normalized to Tfr<sub>c</sub>, and the relative expression ratio was calculated using the Pfaffl method<sup>6</sup>

### **Cell lines**

Hematopoietic precursor cell-7 (HPC-7) cells were grown in stem cell factor as previously described<sup>17</sup>.

### **Vectors, virus production and infection**

cDNAs encoding full length mouse Msi2 was generated by RT-PCR from RNAs extracted from murine total bone marrow. Msi2 cDNA was first fused to the tag Flag2A by cloning in the pCCALL-Flag2A. Afterwards Msi2-Flag2A was cloned into CSIE<sub>m</sub> vector (gift from Dr. R. Gupta) to obtain the CSIE<sub>m</sub>-Msi2-Flag2A. For the RRM mutant's generation, mutations were introduced by site-directed mutagenesis using the QuickChange Kit (Stratagene). The mutations introduced were based on the ones previously published for Msi1<sup>18</sup>. For virus production HEK293T cells were co-transfected with vector plasmid, VSV.G and delta 8.9 and the supernatant harvested after 48 hours. Supernatant was concentrated by ultracentrifugation. HPC-7 cells were infected by spin infection.

### **Immunofluorescence**

LSK cells were sorted from primary mice and cultured with STIF media (Stemspan media [STEMCELL Technologies] containing 10 ng/ml heparin, 10 ng/ml SCF, 20 ng/ml TPO, 20 ng/ml IGFII, and 10 ng/ml FGF) in 96 round-bottom wells for 24 hours. Afterwards cells were harvested and centrifuged on poly-L-Lysine treated round covers in 24-well plates. Cells were fixed with 4% PFA and permeabilized with 0.1% Triton X-100. Cells were stained with the following antibodies: activated  $\beta$ -catenin 1:500 (BD),  $\beta$ -catenin 1:1000 (BD), GSK3b 1:400 (Santa Cruz Biotechnologies), Pten 1:200 (Santa Cruz Biotechnologies), Sca-1 1:100 (BD), c-kit 1:200 (BD) and developed using AF488-goat-anti-rabbit or goat-anti-rat, AF546-goat-anti-mouse or goat-anti-rat (Invitrogen). Nuclei were counterstained with DAPI (Sigma-Aldrich). Image acquisition was performed either with a Leica Inverted DMI6000B or Confocal TCS SPE (Leica). Signal intensity was measured using ImageJ (<http://imagej.nih.gov/ij/>). Corrected total cell fluorescence (CTCF) was calculated by dividing the integrated density by surface area and normalized for background staining.

### **Apoptosis assay**

Apoptosis assay was performed using the Violet Annexin V/Dead Cell Apoptosis kit (Invitrogen), following manufacturer's instructions.

### **FACS analysis and sorting**

FACS analysis were performed as described in the Material and Methods section in Chapter 1. For sorting of LSK cells, bone marrow cells were first depleted of lineage-positive cells using Lineage Cell Depletion Kit, mouse (Miltenyi Biotec), according to the manufacturer's instructions. Lineage-depleted cells were then stained with the following fluorochrome-conjugated Abs: CD117 (c-kit) and Sca-1 (BD) and sorted using FACS Aria I running the Diva software (BD Biosciences). Dead cells were excluded using DAPI staining.

### **Luciferase Reporter Assay**

The pGL3-PTEN-3'-UTR construct, which contains the putative binding site for mir-21 downstream of the stop codon in the pGL3 Firefly luciferase reporter, was constructed as reported.<sup>10</sup> SK-HEP-1 and SNU-182 cells were plated ( $2 \times 10^6$  cells/well) in 6-well plates. One microgram of pGL3-PTEN-3'-UTR construct was cotransfected with 1  $\mu$ g of a Renilla luciferase expression construct pRL-TK (Promega), using Trans-It (Mirus, Madison, WI). Luciferase assays were performed 48 hours after transfection using the dual-luciferase reporter assay system (Promega). Firefly luciferase activity was normalized to Renilla luciferase expression for each sample.

### **Statistical analysis**

For bar graphs, the unpaired two-tailed Student's t test was used to compute p-values. Error bars reflect the SD. All statistical analyses were performed using Prism 4.0 (GraphPad Software)

## REFERENCES

1. Boisset, J.-C. *et al.* In vivo imaging of haematopoietic cells emerging from the mouse aortic endothelium. *Nature* **464**, 116–20 (2010).
2. Robin, C., Ottersbach, K., Boisset, J.-C., Oziemlak, A. & Dzierzak, E. CD41 is developmentally regulated and differentially expressed on mouse hematopoietic stem cells. *Blood* **117**, 5088–5091 (2011).
3. Gekas, C., Dieterlen-Lièvre, F., Orkin, S. H. & Mikkola, H. K. A. The placenta is a niche for hematopoietic stem cells. *Dev. Cell* **8**, 365–375 (2005).
4. Ottersbach, K. & Dzierzak, E. The murine placenta contains hematopoietic stem cells within the vascular labyrinth region. *Dev. Cell* **8**, 377–387 (2005).
5. Gekas, C. *et al.* Hematopoietic stem cell development in the placenta. *Int. J. Dev. Biol.* **54**, 1089–98 (2010).
6. Pfaffl, M. W. A new mathematical model for relative quantification in real-time RT-PCR. *Nucleic Acids Res.* **29**, e45–e45 (2001).
7. Busch, K. & Rodewald, H.-R. Unperturbed vs. post-transplantation hematopoiesis. *Curr. Opin. Hematol.* **23**, 295–303 (2016).
8. Park, S.-M. *et al.* Musashi-2 controls cell fate, lineage bias, and TGF- $\beta$  signaling in HSCs. *J. Exp. Med.* **211**, 71–87 (2014).
9. Huang, J. *et al.* Pivotal role for glycogen synthase kinase-3 in hematopoietic stem cell homeostasis in mice. *J. Clin. Invest.* **119**, 3519–29 (2009).
10. Kligun, E. & Mandel-Gutfreund, Y. The role of RNA conformation in RNA-protein recognition. *RNA Biol.* **6286**, 00–00 (2015).
11. Perry, J. M. *et al.* Cooperation between both Wnt/{beta}-catenin and PTEN/PI3K/Akt signaling promotes primitive hematopoietic stem cell self-renewal and expansion. *Genes Dev.* **25**,

1928–1942 (2011).

12. Zhang, C. C. & Lodish, H. F. Murine hematopoietic stem cells change their surface phenotype during ex vivo expansion. *Blood* **105**, 4314–4320 (2005).
13. He, J., Kang, X., Yin, Y., Chao, K. S. C. & Shen, W. H. PTEN regulates DNA replication progression and stalled fork recovery. *Nat. Commun.* **6**, 7620 (2015).
14. Emerling, B. M., Weinberg, F., Liu, J. L., Mak, T. W. & Chandel, N. S. PTEN regulates p300-dependent hypoxia-inducible factor 1 transcriptional activity through Forkhead transcription factor 3a (FOXO3a). *Proc Natl Acad Sci U S A* **105**, 2622–2627 (2008).
15. Schmid, A. C., Byrne, R. D., Vilar, R. & Woscholski, R. Bisperoxovanadium compounds are potent PTEN inhibitors. *FEBS Lett.* **566**, 35–38 (2004).
16. Wang, S. *et al.* Transformation of the intestinal epithelium by the MSI2 RNA-binding protein. *Nat. Commun.* **6**, 6517 (2015).
17. Pinto do O, P., Kolterud, A. & Carlsson, L. Expression of the LIM-homeobox gene LH2 generates immortalized steel factor-dependent multipotent hematopoietic precursors. *EMBO J.* **17**, 5744–5756 (1998).
18. Kawahara, H. *et al.* Neural RNA-binding protein Musashi1 inhibits translation initiation by competing with eIF4G for PABP. *J Cell Biol* **181**, 639–653 (2008).

## PART III DISCUSSION

The identification of numerous genetic regulators of HSC activity and niche signaling interactions has led to an increasingly comprehensive understanding of how these factors work in concert to control HSC functions<sup>221-225</sup>. Nevertheless, the same studies suggest that HSC regulation depends on complex processes where still unknown proteins can have important roles. With this in mind we designed a strategy that allowed us to discover novel genes involved in HSC function. Taking advantage of the retroviral insertion approach originally developed for the identification of oncogenes that cooperate in leukemia formation<sup>226-227</sup>, we identified the RNA-binding protein Msi2 as a novel regulator of HSC function. Further characterization of Msi2 showed that it is specifically expressed in the most primitive progenitors, including LT-HSCs, ST-HSCs and LMPPs, and that its expression decreased in committed and mature cell types. To study the role of Msi2 we decided to generate a mouse where the gene was disrupted by a gene-trap (Gt) vector, expressing a truncated Msi2 protein that lacks the C-terminal domain. The phenotypic characterization of Msi2<sup>Gt/Gt</sup> mice showed that the hematopoietic system is severely compromised in these mice, and that ST-HSCs and LMPPs (but not LT-HSCs) are the most affected populations. Moreover, Msi-2 defective LSK cells (which include LT-HSCs, ST-HSCs and LMPPs) showed a partial block in cell cycle progression and proliferation, without a significant increase in apoptosis. Gene expression arrays supported these findings showing alterations in the expression levels of several key cell cycle regulators in Msi2<sup>Gt/Gt</sup> LSK cells. In contrast to what we found under steady-state conditions, in which the LT-HSC

population was not affected, the analysis of bone marrow transplanted from Msi2<sup>Gt/Gt</sup> animals showed a decrease in the LT-HSC fraction when compared with wild-type cells, suggesting a role of Msi2 specifically during stress hematopoiesis. Consistent with these findings, treatment of Msi2<sup>Gt/Gt</sup> with 5-fluorouracil showed an impairment of stress-induced LT-HSC self-renewal.

In agreement with our results, other groups have also identified Msi2 as a crucial gene in HSC function using different approaches. Hope et al<sup>197</sup>, using RNA interference in mouse HSCs, identified Msi2 as a positive regulator of HSC function; moreover Msi2 downregulation impaired the repopulation potential of the HSCs. However, in contrast to what we found, a decrease in Msi2 expression did not affect the cell cycle profile. The discrepancy between the findings of Hope et al and our work could be due to differences in the methods used for Msi2 ablation, which may influence the extent and the duration of Msi2 downregulation. Using a doxycycline-inducible transgenic mouse over-expressing Msi2, Kharas et al<sup>196</sup> observed an increase in the number of LSK cells, and this increase could be attributed to ST-HSCs and MPPs, whereas the LT-HSC population decreased. This finding is in agreement with our observation that inactivation of Msi2 causes a reduction in MPPs and ST-HSCs numbers without affecting LT-HSCs. Moreover, in both scenarios, changes in these populations were attributed to cell cycle kinetics alterations. More recently, an Mx-1-Cre conditional Msi2 knockout mouse strain has been described, showing that the deletion induced a significant impairment in the repopulation ability of hematopoietic stem and progenitor cells (HSPC, essentially equivalent to LSK cells)



similar to what we found<sup>89</sup>, but with two important differences: (1) LT-HSC function in homeostatic conditions were found to be also severely impaired and (2) transplanted cells with induced Msi2 knock-out gave rise to myeloid biased progeny in the recipient animals, while we observed no such a lineage bias. Impairment of LT-HSC function in the inducible system is attributable to a loss of quiescence, e.g. to a premature exiting from the G0 phase, something which we have not examined. The apparent discrepancy about the defects of HSCs between the two mouse models could be explained by two alternatives: (1) differences between the gene trap-mediated truncation of Msi2 and the conditional deletion of another part of the gene, and (2) a compensation during embryo development of the Msi2 loss in the constitutive deletion model but not in the inducible system.

For the first alternative, the differences could be due to two main reasons. First, the truncated proteins in both models are completely different; in the conditional model both RNA-binding domains (on the N-terminal region) were deleted while in our model the truncated protein maintains the N-terminal region, including the RNA-binding domains. Although we do not know if these truncated proteins are actually produced, we cannot discard that the differences in the observed phenotypes are due to distinct side effects of the truncated proteins. In addition, it has been demonstrated that the molecule used for the induction of the Mx1 system, the polyinosinic:polycytidylic acid (poly I:C), can have side effects on LT-HSC cell function. This, Poly I:C leads to the induction of IFN $\alpha$  secretion that activates not only the Mx1 inducible promoter but also affects the cell cycle status

of HSCs<sup>228</sup>. Although poly I:C induces rapid and transient changes in HSC phenotype that are reverted in WT mice some days after treatment<sup>229</sup>, it seems possible that in a *Msi2*-deficient background, poly I:C treatment could lead to a permanent change in the phenotype. However, and in agreement with our findings, the defect caused by *Msi2* deficiency is cell-autonomous and induces a decrease in bone marrow and spleen cellularity. Moreover, although in the inducible model LT-HSCs are already affected under homeostatic conditions, their impairment is accentuated in response to perturbations including transplantation and replicative stress, similarly to what we found. Lastly, although transcriptome analyses showed coincidences between the inducible and the gene-trap model in gene expression changes (e.g. reduction in *Egr1*, *Gfi1* and *Junb*), they also exhibited striking differences, such an increase in *Myc* expression, opposite to what we observed in our model.

In conclusion, despite some differences in the phenotypes of mice with a constitutive deletion of *Msi2* (our studies) and those reported for mice with a conditional deletion, both models suggest that *Msi2* is important for the function and maintenance of HSCs under homeostatic conditions, and even more importantly during regeneration.

Among the regions where hematopoietic cells are detected early during development, the AGM together with the placenta are considered to represent the first sites of definitive hematopoiesis and HSC formation. This raises the question whether *Msi2* is also required for the endothelial to hematopoietic transition. Detectable levels of *Msi2* mRNA can be found already in the endothelium of the

AGM, as well as during the endothelial to hematopoietic transition and further increases in adult HSCs. However, in contrast to Msi2 mRNA, Msi2 protein is exclusively expressed in CD41<sup>+</sup> cells that most probably correspond to the earliest emerging HSCs in the AGM<sup>11</sup>. The discrepancy between Msi2 expression at the mRNA and protein levels could be attributed either to posttranscriptional regulation mechanisms, or to the fact that the sorted populations used for mRNA extraction are heterogeneous. Whether it has a function there is unclear, since 10.5 dpc AGMs from Msi2 deficient mice did not show any significant differences among the populations analyzed, while 11.5 dpc AGMs showed a slight decrease of endothelial like cells expressing CD41. The situation in the placenta is again different, as Msi2<sup>Gt/Gt</sup> placentas showed a significant decrease in the CD34<sup>-</sup> c-kit<sup>+</sup> population, which includes erythroid and megakaryocytes progenitors. In contrast, we did not observe any difference in the frequency of CD34<sup>+</sup> c-kit<sup>+</sup> cells, which include HSCs and multipotent progenitors.

Based on the fact that CD41 expression marks the onset of definitive hematopoiesis<sup>229,230</sup>, the observed co-localization of Msi2 protein and CD41 in the AGM indicates that Msi2 could be used as a marker of nascent HSCs.

Although Msi2 expression has not been examined in all the anatomical sites that participate in HSC development, the observed decrease in the frequency of the LSK population in fetal liver of Msi2 deficient embryos suggests that Msi2 expression is initiated in the AGM and maintained throughout embryo development. Nevertheless, to definitively demonstrate a role of Msi2 in the

generation of functional HSCs during embryo development additional assays (e.g. transplantation experiments) would have to be performed.

The fact that Msi2 expression is first detected at the onset of hematopoiesis during embryo development and maintained in adult animals indicates that Msi2 has an important function in the proliferation of HSPCs, first for their expansion during embryo development and later for regeneration and homeostasis in adult life. Moreover, Msi2 has an important role in the rapid proliferation and expansion of HSPCs in response to stress, as seen by the failure to repopulate the hematopoietic system when Msi2<sup>Gt/Gt</sup> HSPCs are forced to proliferate upon transplantation or 5FU treatment. It is important to note that irradiated mice that received a secondary transplantation of Msi2<sup>Gt/Gt</sup> HSPCs did not survive, indicating that Msi2 deficient LT-HSCs, in contrast to what we found in homeostatic conditions, are not able to perform their function, probably due to their inability to proliferate.

To shed light on putative Msi2 targets we used the CatRapid analysis software that predicts an interaction between RNA-binding proteins and messenger RNAs. Of 10 genes that showed the highest score in binding propensity we focused on Gsk3b and Pten, two genes with well known roles in hematopoiesis. To validate their biological role downstream of Msi2 we decided to do our experiments in cultured HSPCs, which mimic stress-induced hematopoiesis, as well as in the HPC-7 cell line. Although Msi2 was able to bind Gsk3b and regulate its expression in HPC-7 cells, we couldn't see any change in protein levels when we compared its expression in cultured WT and Msi2<sup>Gt/Gt</sup>

HSPCs. These conflicting results may be explained by a cell-type specific interaction between *Msi2* and *Gsk3b*. HPC-7 cells are derived from ES-cells overexpressing the transcription factor *Lhx2*, representing an early fetal multipotent hematopoietic progenitor<sup>231</sup>. Therefore, intrinsic differences between HPC-7 cells and HSPCs may explain differences in the targets regulated by *Msi2*. Importantly, although *Gsk3b* was not affected in *Msi2* deficient HSPC we observed a defect in the *Gsk3b*-regulated canonical Wnt pathway and a decrease in the activation of its downstream effector  $\beta$ -catenin. As described in the Introduction, it is well known that the Wnt pathway plays an important role in hematopoiesis; a recent publication has shown that non-canonical and canonical Wnt signaling have distinct roles for the maintenance of quiescence and activation of HSCs, respectively<sup>146</sup>. The ability of HSCs to exit the quiescent state when challenged depends on the switch from non-canonical pathway (that maintains HSCs in quiescence) to canonical Wnt pathway and therefore on the proper activation of the latter. Hence, our observations support the hypothesis that the inability of *Msi2*<sup>Gt/Gt</sup> LSKs to respond to stress (as shown in secondary transplantation and 5FU treatment experiments) may be due to a defect in the activation of the Wnt signaling pathway. In addition, gene expression profiling performed with *Msi2*<sup>Gt/Gt</sup> and WT LSKs showed that there is a significant correlation between genes upregulated in *Msi2*<sup>Gt/Gt</sup> LSKs with Wnt target genes that were downregulated by overexpression of APC (a negative regulator of canonical Wnt pathway).

This hypothesis is further supported by the evidence that indicates that Wnt signaling may be involved in hematopoietic ontogeny and expansion of HSCs in the embryo. Zhou et al. demonstrated that Wnt signaling is upregulated in E14.5 fetal liver, correlating with the proliferation potential of hematopoietic progenitors<sup>232</sup>. In addition, studies using Wnt3a deficient mice showed that both the proliferation and the ability to repopulate serially transplanted mice are decreased in fetal liver LSK cells<sup>139</sup>. Finally, Ruiz-Herguido et al.<sup>233</sup> have recently shown that Wnt/ $\beta$ -catenin activity is transiently required in the AGM to generate long-term HSCs. These findings indicate that the link between Msi2 and Wnt pathway observed in adult LSKs might be also important during HSC generation and expansion during embryo and fetal development.

Pten, the other target that we studied more in detail, also gave promising results. Pten has been described as an important factor to maintain quiescent adult hematopoietic stem cells through downregulation of the PI3K pathway and the downstream mTOR pathway<sup>234,219</sup>. Its downregulation promotes the mobilization of HSCs out of the BM niche and subsequent activation. Moreover, it has been shown that a cooperation between the Wnt/ $\beta$ -catenin and PTEN/PI3k/Akt pathways is critical to promote HSC self-renewal as these two pathways interact to induce expansion of HSCs while blocking differentiation<sup>236,237</sup>. In this regard, the observed upregulation of PTEN in cultured Msi2<sup>Giv/Gt</sup> LSK cells is relevant, indicating that Msi2 regulate the expression of Pten upon activation of HSCs. This result is supported by the finding that Msi2 is able to bind the 3'UTR of PTEN mRNA and downregulates its expression

as shown in the luciferase reporter assay. Moreover, mRNA quantification showed that Msi2 regulates PTEN expression most likely by affecting the stability of its messenger RNA, although a role in translation regulation by Msi2 cannot be discarded.

Surprisingly, we also observed a change in subcellular localization of PTEN when Msi2 was absent. It has previously been described that PTEN, apart from its cytoplasmic role in suppressing the PI3K/AKT pathway also has crucial functions in the nucleus where, through the control of the DNA repair machinery, it favors genomic stability and restrains cell cycle progression<sup>238-240</sup>. On the other hand, it has been recently shown that DNA damage is a direct consequence of inducing HSCs to exit their homeostatic quiescent state in response to conditions that model physiological stress, leading to the activation of the DNA repair pathway<sup>83</sup>. In addition, gene expression profiling of Msi2 deficient LSKs compared to their WT counterparts showed an enrichment of genes associated with DNA repair processes. Based on these results, the delocalization of PTEN in Msi2 deficient HSPCs in culture could indicate an inability of the cells to activate the DNA repair machinery, which on the long-term may result in HSC depletion. It is possible that similar mechanisms play out in other conditions of stress, such as after infection or injury. Our findings about the Msi2-mediated maintenance of PTEN in the cytoplasm of HSCs and its relocation after stress opens new ways to study how the Wnt/Pten signaling pathways regulate the activation of HSCs.

In light of the results described in this thesis and findings published by others, Msi2 seems to have a multidimensional and complex role in HSCs, probably by targeting different mRNAs and interacting with

different proteins in a cell-type specific manner. In fact, the important role of RNA binding proteins in controlling post-transcriptional mechanisms in many normal and malignant cellular contexts has led to the development of theories that RNA binding proteins regulate subsets of functionally related RNAs to govern specific cellular responses or phenotypes<sup>241</sup>. This “regulon” model could explain the variety of Msi2 targets that so far have been described, most of them that are connected in ways that we still do not understand. Moreover, aside from regulating mRNA translation there is also evidence pointing to a role of Msi2 in controlling miRNA biogenesis<sup>217</sup>. Most probably, the following years will bring further clarify the mechanisms controlled by Msi2 and its role in the hematopoietic system.

It is important to note that since the original discovery of Msi2, it has become clear that the protein is a critical element in controlling stem and progenitor cell function in many non-hematopoietic tissues including the intestine<sup>213,243,243</sup>, hair follicle<sup>244</sup> and pancreas<sup>189</sup>. Therefore elucidating the roles of Msi2 in post-transcriptional control mechanisms within the hematopoietic system will also give valuable insights about the regulation of other tissues.



## REFERENCES

1. Ramalho-Santos, M. & Willenbring, H. On the Origin of the Term 'Stem Cell'. *Cell Stem Cell* 1, 35–38 (2007).
2. Jacobson, L., Simmons, E. L., Marks, E. K. & Eldredge, J. H. *Ziechnical Papers Recovery from Radiation Injury* 1 No . e. 113, 510–511 (1945).
3. Lorenz, E., Congdon, C. & Uphoff, D. Modification of acute irradiation injury in mice and guinea-pigs by bone marrow injections. *Radiology* 58, 863–877 (1952).
4. Ford, C. E., Hamerton, J. L., Barnes, D. W. & Loutit, J. F. Cytological identification of radiation-chimaeras. *Nature* 177, 452–454 (1956).
5. McCulloch, E. & Till, J. The radiation sensitivity of normal mouse bone marrow cells, determined by quantitative marrow transplantation into irradiated mice. *Radiat. Res.* 13, 115–125 (1960).
6. Till, J. E. & McCulloch, E. A. A direct measurement of the radiation sensitivity of normal mouse bone marrow cells. *Radiat. Res.* 14, 213–222 (1961).
7. Becker, a J., McCulloch, E. and & Till, J. E. Cytological demonstration of the clonal nature of spleen colonies derived from transplanted mouse marrow cells. *Nature* 197, 452–454 (1963).
8. Siminovitch, L., Till, J. E. & McCulloch, E. A. Decline in colony-forming ability of marrow cells subjected to serial transplantation into irradiated mice. *J. Cell. Comp. Physiol.* 64, 23–31 (1964).
9. Till, J., McCulloch, E., and Siminovitch, L. A stochastic model of stem cell proliferation, based on the growth of spleen colony-forming cells. *Proc. Natl. Acad. Sci. U. S. A.* 51, 29–36 (1964).
10. Spangrude, G. J., Heimfeld, S. & Weissman, I. L. Hematopoietic Stem. *Science* (80-. ). 58–62 (1988).
11. Worton, R., Mcculloch, E. A. & Till, J. E. PHYSICAL SEPARATION OF HEMOPOIETIC STEM CELLS DIFFER- ( From the Department of Medical Biophysics , University of Toronto , and The Ontario Cancer Institute , Toronto , Ontario , Canada ). *J Exp Med* 130, 91–103 (1969).
12. Köhler, G. & Milstein, C. Continuous cultures of fused cells

- secreting antibody of predefined specificity. *Nature* 256, 495–497 (1975).
13. Hulett, A. H. R., Bonner, W. a, Barrett, J., Herzenberg, L. a & Url, S. Cell Sorting : Automated Separation of Mammalian Cells as a Function of Intracellular Fluorescence Cell Sorting : Automated Separation of Mammalian Cells as a Function of Intracellular Fluorescence. *Science* (80-. ). 166, 747–749 (1969).
  14. Ogawa, M., Matsuzaki, Y., Nishikawa, S., Hayashi, S., Kunisada, T., Sudo, T., Kina, T. & and Nakauchi, H. Expression and function of c-kit in hemopoietic progenitor cells. *J Exp Med* 174, 63–71 (1991).
  15. Osawa, M., Hanada, K., Hamada, H., and Nakauchi, H. Long-Term Lymphohematopoietic. *Science* (80-. ). 273, 242–245 (1996).
  16. Christensen, J. L. & Weissman, I. L. Flk-2 is a marker in hematopoietic stem cell differentiation: a simple method to isolate long-term stem cells. *Proc. Natl. Acad. Sci. U. S. A.* 98, 14541–14546 (2001).
  17. Yang, L. et al. Identification of Lin-Sca1+kit+CD34 +Flt3-short-term hematopoietic stem cells capable of rapidly reconstituting and rescuing myeloablated transplant recipients. *Blood* 105, 2717–2723 (2005).
  18. Kiel, M. J. et al. SLAM family receptors distinguish hematopoietic stem and progenitor cells and reveal endothelial niches for stem cells. *Cell* 121, 1109–1121 (2005).
  19. Benveniste, P. et al. Intermediate-Term Hematopoietic Stem Cells with Extended but Time-Limited Reconstitution Potential. *Cell Stem Cell* 6, 48–58 (2010).
  20. Akashi, K., Traver, D., Miyamoto, T. & Weissman, I. L. A clonogenic common myeloid progenitor that gives rise to all myeloid lineages. *Nature* 404, 193–197 (2000).
  21. Kondo, M., Weissman, I. L. & Akashi, K. Identification of clonogenic common lymphoid progenitors in mouse bone marrow. *Cell* 91, 661–672 (1997).
  22. Adolfsson, J. et al. Identification of Flt3+ lympho-myeloid stem cells lacking erythro-megakaryocytic potential: A revised road map for adult blood lineage commitment. *Cell* 121, 295–306 (2005).
  23. Dykstra, B. et al. Long-Term Propagation of Distinct Hematopoietic Differentiation Programs In Vivo. *Cell Stem*

- Cell 1, 218–229 (2007).
24. Kent, D. G. et al. Prospective isolation and molecular characterization of hematopoietic stem cells with durable self-renewal potential. *Blood* 113, 6342–6350 (2009).
  25. Yamamoto, R. et al. Clonal analysis unveils self-renewing lineage-restricted progenitors generated directly from hematopoietic stem cells. *Cell* 154, 1112–1126 (2013).
  26. Nimmo, R. A., May, G. E. & Enver, T. Primed and ready: Understanding lineage commitment through single cell analysis. *Trends in Cell Biology* 25, 459–467 (2015).
  27. Harrison, D. E. Competitive repopulation: a new assay for long-term stem cell functional capacity. *Blood* 55, 77–81 (1980).
  28. Szilvassy, S. J., Lansdorp, P. M., Humphries, R. K., Eaves, A. C. & Eaves, C. J. Isolation in a single step of a highly enriched murine hematopoietic stem cell population with competitive long-term repopulating ability. *Blood* 74, 930–939 (1989).
  29. Szilvassy, S. J., Humphries, R. K., Lansdorp, P. M., Eaves, A. C. & Eaves, C. J. Quantitative assay for totipotent reconstituting hematopoietic stem cells by a competitive repopulation strategy. *Proc. Natl. Acad. Sci. U. S. A.* 87, 8736–40 (1990).
  30. Taswell, C. Limiting dilution assays for the determination of immunocompetent cells frequencies. *J. Immunol.* 126, 1614–1619 (1981).
  31. Lemischka, I. R., Raulet, D. H. & Mulligan, R. C. Developmental potential and dynamic behavior of hematopoietic stem cells. *Cell* 45, 917–927 (1986).
  32. Challen, G. A., Boles, N., Lin, K. K. & Goodell, M. A. Mouse hematopoietic stem cell identification and analysis. *Cytom. A* 75, 14–24 (2009).
  33. Akagi, K., Suzuki, T., Stephens, R. M., Jenkins, N. A. & Copeland, N. G. RTCGD: retroviral tagged cancer gene database. *Nucleic Acids Res.* 32, D523-7 (2004).
  34. Kustikova, O. et al. Clonal dominance of hematopoietic stem cells triggered by retroviral gene marking. *Science* (80-.). 308, 1171–1174 (2005).
  35. Kustikova, O. S. et al. Retroviral vector insertion sites associated with dominant hematopoietic clones mark ‘stemness’ pathways. *Blood* 109, 1897–1907 (2007).
  36. Calmels, B. et al. Recurrent retroviral vector integration at the

- Mds1/Evi1 locus in nonhuman primate hematopoietic cells. *Blood* 106, 2530–2533 (2005).
37. Wu, X., Li, Y., Crise, B. & Burgees, Shawn, M. Transcription Start Regions in the Human Genome Are Favored Targets for MLV Integration. *Science* (80-. ). 300, 1749–1751 (2003).
  38. Hacein-Bey-Abina, S. LMO2-Associated Clonal T Cell Proliferation in Two Patients after Gene Therapy for SCID-X1. *Science* (80-. ). 302, 415–419 (2003).
  39. Gonzalez-Murillo, A., Lozano, M. L., Montini, E., Bueren, J. A. & Gueneehea, G. Unaltered repopulation properties of mouse hematopoietic stem cells transduced with lentiviral vectors. *Blood* 112, 3138–3147 (2008).
  40. Montini, E. et al. Hematopoietic stem cell gene transfer in a tumor-prone mouse model uncovers low genotoxicity of lentiviral vector integration. *Nat Biotechnol* 24, 687–696 (2006).
  41. Mazurier, F., Gan, O. I., McKenzie, J. L., Doedens, M. & Dick, J. E. Lentivector-mediated clonal tracking reveals intrinsic heterogeneity in the human hematopoietic stem cell compartment and culture-induced stem cell impairment. *Blood* 103, 545–552 (2004).
  42. McKenzie, J. L., Gan, O. I., Doedens, M., Wang, J. C. & Dick, J. E. Individual stem cells with highly variable proliferation and self-renewal properties comprise the human hematopoietic stem cell compartment. *Nat Immunol* 7, 1225–1233 (2006).
  43. Maetzig, T. et al. Polyclonal fluctuation of lentiviral vector-transduced and expanded murine hematopoietic stem cells. *Blood* 117, 3053–3064 (2011).
  44. Gerrits, A. et al. Cellular barcoding tool for clonal analysis in the hematopoietic system. *Blood* 115, 2610–2618 (2010).
  45. Schmidt, M. et al. High-resolution insertion-site analysis by linear amplification-mediated PCR (LAM-PCR). *Nat. Methods* 4, 1051–1057 (2007).
  46. Laukkanen, M. O. et al. Low-dose total body irradiation causes clonal fluctuation of primate hematopoietic stem and progenitor cells. *Blood* 105, 1010–1015 (2005).
  47. Sun, J. et al. Clonal dynamics of native haematopoiesis. *Nature* 514, 322–327 (2014).
  48. Dzierzak, E. & Speck, N. A. Of lineage and legacy: the development of mammalian hematopoietic stem cells. *Nat*

- Immunol 9, 129–136 (2008).
49. Palis, J., Robertson, S., Kennedy, M., Wall, C. & Keller, G. Development of erythroid and myeloid progenitors in the yolk sac and embryo proper of the mouse. *Development* 126, 5073–5084 (1999).
  50. Böiers, C. et al. Lymphomyeloid Contribution of an Immune-Restricted Progenitor Emerging Prior to Definitive Hematopoietic Stem Cells. *Cell Stem Cell* (2013). doi:10.1016/j.stem.2013.08.012
  51. Inlay, M. A. et al. Identification of multipotent progenitors that emerge prior to hematopoietic stem cells in embryonic development. *Stem Cell Reports* 2, 457–472 (2014).
  52. Müller, A. M., Medvinsky, A., Strouboulis, J., Grosveld, F. & Dzierzak, E. Development of hematopoietic stem cell activity in the mouse embryo. *Immunity* 1, 291–301 (1994).
  53. Medvinsky, A. & Dzierzak, E. Definitive hematopoiesis is autonomously initiated by the AGM region. *Cell* 86, 897–906 (1996).
  54. Kumaravelu, P. et al. Quantitative developmental anatomy of definitive haematopoietic stem cells/long-term repopulating units (HSC/RUs): role of the aorta-gonad-mesonephros (AGM) region and the yolk sac in colonisation of the mouse embryonic liver. *Development* 129, 4891–4899 (2002).
  55. De Bruijn, M. F. T. R. et al. Hematopoietic stem cells localize to the endothelial cell layer in the midgestation mouse aorta. *Immunity* 16, 673–683 (2002).
  56. Godin, I. & Cumano, A. The hare and the tortoise: an embryonic haematopoietic race. *Nat. Rev. Immunol.* 2, 593–604 (2002).
  57. Bertrand, J. Y. et al. Haematopoietic stem cells derive directly from aortic endothelium during development. *Nature* 464, 108–111 (2010).
  58. Kissa, K. & Herbomel, P. Blood stem cells emerge from aortic endothelium by a novel type of cell transition. *Nature* 464, 112–5 (2010).
  59. Boisset, J.-C. et al. In vivo imaging of haematopoietic cells emerging from the mouse aortic endothelium. *Nature* 464, 116–20 (2010).
  60. Ottersbach, K. & Dzierzak, E. The murine placenta contains hematopoietic stem cells within the vascular labyrinth region. *Dev. Cell* 8, 377–387 (2005).

61. Gekas, C., Dieterlen-Lièvre, F., Orkin, S. H. & Mikkola, H. K. A. The placenta is a niche for hematopoietic stem cells. *Dev. Cell* 8, 365–375 (2005).
62. Samokhvalov, I. M., Samokhvalova, N. I. & Nishikawa, S. Cell tracing shows the contribution of the yolk sac to adult haematopoiesis. *Nature* 446, 1056–1061 (2007).
63. Göthert, J. R. et al. In vivo fate-tracing studies using the Scl stem cell enhancer: Embryonic hematopoietic stem cells significantly contribute to adult hematopoiesis. *Blood* 105, 2724–2732 (2005).
64. Bertrand, J. Y. et al. Fetal spleen stroma drives macrophage commitment. *Development* 133, 3619–3628 (2006).
65. Kissa, K. et al. Live imaging of emerging hematopoietic stem cells and early thymus colonization. *Blood* 111, 1147–1156 (2008).
66. Enver, T. & Heyworth, C. Do stem cells play dice? *92*, 348–351 (1998).
67. Morrison, S. J. & Weissman, I. L. The long-term repopulating subset of hematopoietic stem cells is deterministic and isolatable by phenotype. *Immunity* 1, 661–673 (1994).
68. Ogawa, M. Stochastic model revisited. *Int. J. Hematol.* 69, 2–5 (1999).
69. Wagers, A. J. & Christensen, J. L. Cell fate determination from stem cells. *Gene Ther.* 9, 606–612 (2002).
70. Enver, T. & Jacobsen, S. E. W. Developmental biology: Instructions writ in blood. *Nature* 461, 183–184 (2009).
71. Arai, F. & Suda, T. Maintenance of quiescent hematopoietic stem cells in the osteoblastic niche. in *Annals of the New York Academy of Sciences* 1106, 41–53 (2007).
72. Bowie, M. B. et al. Hematopoietic stem cells proliferate until after birth and show a reversible phase-specific engraftment defect. *J. Clin. Invest.* 116, 2808–2816 (2006).
73. Orford, K. W. & Scadden, D. T. Deconstructing stem cell self-renewal: genetic insights into cell-cycle regulation. *Nat Rev Genet* 9, 115–128 (2008).
74. Wilson, A. et al. Hematopoietic Stem Cells Reversibly Switch from Dormancy to Self-Renewal during Homeostasis and Repair. *Cell* 135, 1118–1129 (2008).
75. Essers, M. a G. et al. IFNalpha activates dormant haematopoietic stem cells in vivo. *Nature* 458, 904–8 (2009).
76. Siskin, J. E. & Morasca, L. INTRAPOPULATION

- KINETICS OF THE MITOTIC CYCLE. *J. Cell Biol.* 25, 179–89 (1965).
77. Lundberg, A. . & Weinberg, R. A. Control of the cell cycle and apoptosis. *Eur J Cancer* 35, 1886–1894 (1999).
  78. Sherr, C. J. & Roberts, J. M. CDK inhibitors: positive and negative regulators of G1-phase progression. *Genes Dev.* 13, 1501–1512 (1999).
  79. Cheshier, S. H., Morrison, S. J., Liao, X. & Weissman, I. L. In vivo proliferation and cell cycle kinetics of long-term self-renewing hematopoietic stem cells. *Proc. Natl. Acad. Sci. U. S. A.* 96, 3120–5 (1999).
  80. Foudi, A. et al. Analysis of histone 2B-GFP retention reveals slowly cycling hematopoietic stem cells. *Nat. Biotechnol.* 27, 84–90 (2009).
  81. Trumpp, A., Essers, M. & Wilson, A. Awakening dormant haematopoietic stem cells. *Nat. Rev. Immunol.* 10, 201–209 (2010).
  82. Busch, K. et al. Fundamental properties of unperturbed haematopoiesis from stem cells in vivo. *Nature* 518, 542–546 (2015).
  83. Walter, D. et al. Exit from dormancy provokes DNA-damage-induced attrition in haematopoietic stem cells. *Nature* 520, 549–52 (2015).
  84. Zhang, H. et al. TGF- $\beta$  inhibition rescues hematopoietic stem cell defects and bone marrow failure in Fanconi anemia. *Cell Stem Cell* 18, 668–681 (2016).
  85. Morrison, S. J. & Kimble, J. Asymmetric and symmetric stem-cell divisions in development and cancer. *Nature* 441, 1068–1074 (2006).
  86. Gönczy, P. Mechanisms of asymmetric cell division: flies and worms pave the way. *Nat. Rev. Mol. Cell Biol.* 9, 355–66 (2008).
  87. Neumüller, R. A. & Knoblich, J. A. Dividing cellular asymmetry: Asymmetric cell division and its implications for stem cells and cancer. *Genes and Development* 23, 2675–2699 (2009).
  88. Knoblich, J. A. Mechanisms of Asymmetric Stem Cell Division. *Cell* 132, 583–597 (2008).
  89. Park, S.-M. et al. Musashi-2 controls cell fate, lineage bias, and TGF- $\beta$  signaling in HSCs. *J. Exp. Med.* 211, 71–87 (2014).

90. Will, B. et al. Satb1 regulates hematopoietic stem cell self-renewal by promoting quiescence and repressing differentiation commitment. *Nat. Immunol.* 14, 437–445 (2013).
91. Zimdahl, B. et al. Lis1 regulates asymmetric division in hematopoietic stem cells and in leukemia. *Nat. Genet.* 46, 245–52 (2014).
92. Wilson, A. et al. Normal hemopoiesis and lymphopoiesis in the combined absence of numb and numblake. *J. Immunol.* 178, 6746–51 (2007).
93. Wu, M. et al. Imaging Hematopoietic Precursor Division in Real Time. *Cell Stem Cell* 1, 541–554 (2007).
94. Ting, S. B., Deneault, E., Hope, K. & al, et. Asymmetrical segregation and self-renewal of hematopoietic stem and progenitor cells with endocytic Ap2a2. ... (2011).
95. Beckmann, J., Scheitza, S., Wernet, P., Fischer, J. C. & Giebel, B. Asymmetric cell division within the human hematopoietic stem and progenitor cell compartment: Identification of asymmetrically segregating proteins. *Blood* 109, 5494–5501 (2007).
96. Gorgens, A. et al. Multipotent hematopoietic progenitors divide asymmetrically to create progenitors of the lymphomyeloid and erythromyeloid lineages. *Stem Cell Reports* 3, 1058–1072 (2014).
97. Shin, J. W. et al. Contractile forces sustain and polarize hematopoiesis from stem and progenitor cells. *Cell Stem Cell* 14, 81–93 (2014).
98. Wilson, A. & Trumpp, A. Bone-marrow haematopoietic-stem-cell niches. *Nat. Rev. Immunol.* 6, 93–106 (2006).
99. Ehninger, A. & Trumpp, A. The bone marrow stem cell niche grows up: mesenchymal stem cells and macrophages move in. *J Exp Med* 208, 421–428 (2011).
100. Lo Celso, C. et al. Live-animal tracking of individual haematopoietic stem/progenitor cells in their niche. *Nature* 457, 92–6 (2009).
101. Méndez-Ferrer, S. & Frenette, P. S. Hematopoietic stem cell trafficking: Regulated adhesion and attraction to bone marrow microenvironment. in *Annals of the New York Academy of Sciences* 1116, 392–413 (2007).
102. Xie, Y. et al. Detection of functional haematopoietic stem cell niche using real-time imaging. *Nature* 457, 97–101 (2009).



103. Ehninger, A. & Trumpp, A. The bone marrow stem cell niche grows up: mesenchymal stem cells and macrophages move in. *J. Exp. Med.* 208, 421–8 (2011).
104. Wilson, A. et al. Dormant and self-renewing hematopoietic stem cells and their niches. in *Annals of the New York Academy of Sciences* 1106, 64–75 (2007).
105. Ding, L. & Morrison, S. J. Haematopoietic stem cells and early lymphoid progenitors occupy distinct bone marrow niches. *Nature* 495, 231–5 (2013).
106. Greenbaum, A. et al. CXCL12 in early mesenchymal progenitors is required for haematopoietic stem-cell maintenance. *Nature* 495, 227–30 (2013).
107. Calvi, L. M. et al. Osteoblastic cells regulate the haematopoietic stem cell niche. *Nature* 425, 841–846 (2003).
108. Arai, F. et al. Tie2/angiopoietin-1 signaling regulates hematopoietic stem cell quiescence in the bone marrow niche. *Cell* 118, 149–161 (2004).
109. Nilsson, S. K. et al. Osteopontin, a key component of the hematopoietic stem cell niche and regulator of primitive hematopoietic progenitor cells. *Blood* 106, 1232–1239 (2005).
110. Yoshihara, H. et al. Thrombopoietin/MPL Signaling Regulates Hematopoietic Stem Cell Quiescence and Interaction with the Osteoblastic Niche. *Cell Stem Cell* 1, 685–697 (2007).
111. Shahnazari, M., Chu, V., Wronski, T. J., Nissenson, R. A. & Halloran, B. P. CXCL12/CXCR4 signaling in the osteoblast regulates the mesenchymal stem cell and osteoclast lineage populations. *FASEB J.* 27, 3505–3513 (2013).
112. Sugiyama, T., Kohara, H., Noda, M. & Nagasawa, T. Maintenance of the Hematopoietic Stem Cell Pool by CXCL12-CXCR4 Chemokine Signaling in Bone Marrow Stromal Cell Niches. *Immunity* 25, 977–988 (2006).
113. Eliasson, P. & Jönsson, J.-I. The hematopoietic stem cell niche: low in oxygen but a nice place to be. *J. Cell. Physiol.* 222, 17–22 (2010).
114. Parmar, K., Mauch, P., Vergilio, J.-A., Sackstein, R. & Down, J. D. Distribution of Hematopoietic Stem Cells in the Bone Marrow According to Regional Distribution of hematopoietic stem cells in the bone marrow according to regional hypoxia. *PNAS* 104, 5431–5436 (2007).
115. Spencer, J. A. et al. Direct measurement of local oxygen

- concentration in the bone marrow of live animals. *Nature* 508, 269–73 (2014).
116. Suda, T., Takubo, K. & Semenza, G. L. Metabolic regulation of hematopoietic stem cells in the hypoxic niche. *Cell Stem Cell* 9, 298–310 (2011).
  117. Kollet, O. et al. Osteoclasts degrade endosteal components and promote mobilization of hematopoietic progenitor cells. *Nat. Med.* 12, 657–64 (2006).
  118. Miharada, K. et al. Cripto regulates hematopoietic stem cells as a hypoxic-niche-related factor through cell surface receptor GRP78. *Cell Stem Cell* 9, 330–344 (2011).
  119. Yamazaki, S. et al. Nonmyelinating schwann cells maintain hematopoietic stem cell hibernation in the bone marrow niche. *Cell* 147, 1146–1158 (2011).
  120. Méndez-Ferrer, S. et al. Mesenchymal and haematopoietic stem cells form a unique bone marrow niche. *Nature* 466, 829–34 (2010).
  121. Omatsu, Y. et al. The Essential Functions of Adipo-osteogenic Progenitors as the Hematopoietic Stem and Progenitor Cell Niche. *Immunity* 33, 387–399 (2010).
  122. Katayama, Y. et al. Signals from the sympathetic nervous system regulate hematopoietic stem cell egress from bone marrow. *Cell* 124, 407–421 (2006).
  123. Pajcini, K. V, Speck, N. a & Pear, W. S. Notch signaling in mammalian hematopoietic stem cells. *Leukemia* 25, 1525–1532 (2011).
  124. Bigas, A. & Espinosa, L. Hematopoietic stem cells: To be or Notch to be. *Blood* 119, 3226–3235 (2012).
  125. Ciofani, M. & Zúñiga-Pflücker, J. C. Notch promotes survival of pre-T cells at the  $\beta$ -selection checkpoint by regulating cellular metabolism. *Nat. Immunol.* 6, 881–888 (2005).
  126. Varnum-Finney, B. et al. Pluripotent, cytokine-dependent, hematopoietic stem cells are immortalized by constitutive Notch1 signaling. *Nat. Med.* 6, 1278–1281 (2000).
  127. Stier, S., Cheng, T., Dombkowski, D., Carlesso, N. & Scadden, D. T. Notch1 activation increases hematopoietic stem cell self-renewal in vivo and favors lymphoid over myeloid lineage outcome. *Blood* 99, 2369–2378 (2002).
  128. Poulos, M. G. et al. Endothelial Jagged-1 Is necessary for homeostatic and regenerative hematopoiesis. *Cell Rep.* 4, 1022–1034 (2013).

129. Maillard, I. et al. Canonical notch signaling is dispensable for the maintenance of adult hematopoietic stem cells. *Cell Stem Cell* 2, 356–66 (2008).
130. Mancini, S. J. C. et al. Jagged1-dependent Notch signaling is dispensable for hematopoietic stem cell self-renewal and differentiation. *Blood* 105, 2340–2342 (2005).
131. Malhotra, S. & Kincade, P. W. Wnt-Related Molecules and Signaling Pathway Equilibrium in Hematopoiesis. *Cell Stem Cell* 4, 27–36 (2009).
132. Clevers, H. & Nusse, R. Wnt/beta-catenin signaling and disease. *Cell* 149, 1192–1205 (2012).
133. MacDonald, B. T., Tamai, K. & He, X. Wnt/beta-Catenin Signaling: Components, Mechanisms, and Diseases. *Developmental Cell* 17, 9–26 (2009).
134. Willert, K. et al. Wnt proteins are lipid-modified and can act as stem cell growth factors. *Nature* 423, 448–452 (2003).
135. Reya, T. et al. A role for Wnt signalling in self-renewal of haematopoietic stem cells. *Nature* 423, 409–414 (2003).
136. Trowbridge, J. J., Xenocostas, A., Moon, R. T. & Bhatia, M. Glycogen synthase kinase-3 is an in vivo regulator of hematopoietic stem cell repopulation. *Nat. Med.* 12, 89–98 (2006).
137. Scheller, M. et al. Hematopoietic stem cell and multilineage defects generated by constitutive beta-catenin activation. *Nat. Immunol.* 7, 1037–1047 (2006).
138. Kirstetter, P., Anderson, K., Porse, B. T., Jacobsen, S. E. W. & Nerlov, C. Activation of the canonical Wnt pathway leads to loss of hematopoietic stem cell repopulation and multilineage differentiation block. *Nat. Immunol.* 7, 1048–1056 (2006).
139. Luis, T. C. et al. Wnt3a deficiency irreversibly impairs hematopoietic stem cell self-renewal and leads to defects in progenitor cell differentiation. *Blood* 113, 546–554 (2009).
140. Fleming, H. E. et al. Wnt Signaling in the Niche Enforces Hematopoietic Stem Cell Quiescence and Is Necessary to Preserve Self-Renewal In Vivo. *Cell Stem Cell* 2, 274–283 (2008).
141. Zhao, C. et al. Loss of beta-Catenin Impairs the Renewal of Normal and CML Stem Cells In Vivo. *Cancer Cell* 12, 528–541 (2007).
142. Koch, U. et al. Simultaneous loss of beta- and gamma-catenin

- does not perturb hematopoiesis or lymphopoiesis. *Blood* 111, 160–164 (2008).
143. Jeannot, G. et al. Long-term, multilineage hematopoiesis occurs in the combined absence of  $\beta$ -catenin and  $\gamma$ -catenin. *Blood* 111, 142–149 (2008).
  144. Nemeth, M. J., Topol, L., Anderson, S. M., Yang, Y. & Bodine, D. M. Wnt5a inhibits canonical Wnt signaling in hematopoietic stem cells and enhances repopulation. *Proc. Natl. Acad. Sci. U. S. A.* 104, 15436–41 (2007).
  145. Povinelli, B. J. & Nemeth, M. J. Wnt5a regulates hematopoietic stem cell proliferation and repopulation through the ryk receptor. *Stem Cells* 32, 105–115 (2014).
  146. Sugimura, R. et al. Noncanonical Wnt signaling maintains hematopoietic stem cells in the niche. *Cell* 150, 351–365 (2012).
  147. Luis, T. C. et al. Canonical wnt signaling regulates hematopoiesis in a dosage-dependent fashion. *Cell Stem Cell* 9, 345–356 (2011).
  148. Polak, R., Buitenhuis, M., De, W., Polak, R. & Buitenhuis, M. The PI3K / PKB signaling module as key regulator of hematopoiesis: implications for therapeutic strategies in leukemia. *Blood* 119, 911–923 (2012).
  149. Juntilla, M. M. et al. AKT1 and AKT2 maintain hematopoietic stem cell function by regulating reactive oxygen species. *Blood* 115, 4030–4038 (2010).
  150. Kharas, M. G. et al. Constitutively active AKT depletes hematopoietic stem cells and induces leukemia in mice. *Blood* 115, 1406–1415 (2010).
  151. Tothova, Z. et al. FoxOs Are Critical Mediators of Hematopoietic Stem Cell Resistance to Physiologic Oxidative Stress. *Cell* 128, 325–339 (2007).
  152. Miyamoto, K. et al. Foxo3a Is Essential for Maintenance of the Hematopoietic Stem Cell Pool. *Cell Stem Cell* 1, 101–112 (2007).
  153. Manning, B. D. & Cantley, L. C. AKT/PKB Signaling: Navigating Downstream. *Cell* 129, 1261–1274 (2007).
  154. Huang, J. et al. Pivotal role for glycogen synthase kinase-3 in hematopoietic stem cell homeostasis in mice. *J. Clin. Invest.* 119, 3519–29 (2009).

155. Sengupta, S., Peterson, T. R. & Sabatini, D. M. Regulation of the mTOR Complex 1 Pathway by Nutrients, Growth Factors, and Stress. *Molecular Cell* 40, 310–322 (2010).
156. Chen, C. et al. TSC-mTOR maintains quiescence and function of hematopoietic stem cells by repressing mitochondrial biogenesis and reactive oxygen species. *J. Exp. Med.* 205, 2397–408 (2008).
157. Domen, J., Cheshier, S. H. & Weissman, I. L. The role of apoptosis in the regulation of hematopoietic stem cells: Overexpression of Bcl-2 increases both their number and repopulation potential. *J. Exp. Med.* 191, 253–264 (2000).
158. Ooi, A. G. L. et al. MicroRNA-125b expands hematopoietic stem cells and enriches for the lymphoid-balanced and lymphoid-biased subsets. *Proc. Natl. Acad. Sci. U. S. A.* 107, 21505–21510 (2010).
159. Pietras, E. M., Warr, M. R. & Passegue, E. Cell cycle regulation in hematopoietic stem cells. *J. Cell Biol.* 195, 709–720 (2011).
160. Sauvageau, G., Iscove, N. N. & Humphries, R. K. In vitro and in vivo expansion of hematopoietic stem cells. *Oncogene* 23, 7223–7232 (2004).
161. Antonchuk, J., Sauvageau, G. & Humphries, R. K. HOXB4-induced expansion of adult hematopoietic stem cells ex vivo. *Cell* 109, 39–45 (2002).
162. Magnusson, M., Brun, A. C. M., Lawrence, H. J. & Karlsson, S. *Hoxa9/hoxb3/hoxb4* compound null mice display severe hematopoietic defects. *Exp. Hematol.* 35, 1421–1428 (2007).
163. Sauvageau, G. et al. Overexpression of HOXB4 in hematopoietic cells causes the selective expansion of more primitive populations in vitro and in vivo. *Genes Dev.* 9, 1753–1765 (1995).
164. Thorsteinsdottir, U. et al. Overexpression of the myeloid leukemia-associated *Hoxa9* gene in bone marrow cells induces stem cell expansion. *Blood* 99, 121–129 (2002).
165. Lawrence, H. J. et al. Loss of expression of the *Hoxa-9* homeobox gene impairs the proliferation and repopulating ability of hematopoietic stem cells. *Blood* 106, 3988–3994 (2005).
166. Bijl, J. et al. Analysis of HSC activity and compensatory Hox gene expression profile in *Hoxb* cluster mutant fetal liver cells. *Blood* 108, 116–122 (2006).

167. Bjornsson, J. M. et al. Reduced proliferative capacity of hematopoietic stem cells deficient in Hoxb3 and Hoxb4. *Mol. Cell. Biol.* 23, 3872–3883 (2003).
168. Brun, A. C. M. et al. Hoxb4-deficient mice undergo normal hematopoietic development but exhibit a mild proliferation defect in hematopoietic stem cells. *Blood* 103, 4126–4133 (2004).
169. Cheng, T. et al. Hematopoietic stem cell quiescence maintained by p21cip1/waf1. *Science* 287, 1804–1808 (2000).
170. van Os, R. et al. A Limited role for p21Cip1/Waf1 in maintaining normal hematopoietic stem cell functioning. *Stem Cells* 25, 836–843 (2007).
171. Yamazaki, S. et al. Cytokine signals modulated via lipid rafts mimic niche signals and induce hibernation in hematopoietic stem cells. *EMBO J.* 25, 3515–3523 (2006).
172. Matsumoto, A. et al. p57 is required for quiescence and maintenance of adult hematopoietic stem cells. *Cell Stem Cell* 9, 262–271 (2011).
173. Scandura, J. M., Boccuni, P., Massague, J. & Nimer, S. D. Transforming growth factor beta-induced cell cycle arrest of human hematopoietic cells requires p57KIP2 up-regulation. *Proc. Natl. Acad. Sci. U. S. A.* 101, 15231–15236 (2004).
174. Zou, P. et al. p57(Kip2) and p27(Kip1) cooperate to maintain hematopoietic stem cell quiescence through interactions with Hsc70. *Cell Stem Cell* 9, 247–261 (2011).
175. Domen, J., Gandy, K. L. & Weissman, I. L. Systemic overexpression of BCL-2 in the hematopoietic system protects transgenic mice from the consequences of lethal irradiation. *Blood* 91, 2272–2282 (1998).
176. Domen, J. The role of apoptosis in regulating hematopoiesis and hematopoietic stem cells. *Immunol. Res.* 22, 83–94 (2000).
177. Park, I. et al. Bmi-1 is required for maintenance of adult self-renewing haematopoietic stem cells. *Nature* 423, 302–305 (2003).
178. Iwama, A. et al. Enhanced self-renewal of hematopoietic stem cells mediated by the polycomb gene product Bmi-1. *Immunity* 21, 843–851 (2004).
179. Han, Y.-C. et al. microRNA-29a induces aberrant self-renewal capacity in hematopoietic progenitors, biased myeloid development, and acute myeloid leukemia. *J. Exp. Med.* 207,

- 475–489 (2010).
180. O’Connell, R. M. et al. MicroRNAs enriched in hematopoietic stem cells differentially regulate long-term hematopoietic output. *Proc. Natl. Acad. Sci. U. S. A.* 107, 14235–14240 (2010).
  181. Nakamura, M., Okano, H., Blendy, J. A. & Montell, C. Musashi, a neural RNA-binding protein required for drosophila adult external sensory organ development. *Neuron* 13, 67–81 (1994).
  182. Charlesworth, A., Wilczynska, A., Thampi, P., Cox, L. L. & MacNicol, A. M. Musashi regulates the temporal order of mRNA translation during *Xenopus* oocyte maturation. *EMBO J* 25, 2792–2801 (2006).
  183. Sakakibara, S. et al. Mouse-Musashi-1, a neural RNA-binding protein highly enriched in the mammalian CNS stem cell. *Dev Biol* 176, 230–242 (1996).
  184. Murayama, M. et al. Musashi-1 suppresses expression of Paneth cell-specific genes in human intestinal epithelial cells. *J Gastroenterol* 44, 173–182 (2009).
  185. Good, P. et al. The human Musashi homolog 1 (MSI1) gene encoding the homologue of Musashi/Nrp-1, a neural RNA-binding protein putatively expressed in CNS stem cells and neural progenitor cells. *Genomics* 52, 382–384 (1998).
  186. Okano, H. et al. Function of RNA-binding protein Musashi-1 in stem cells. *Experimental Cell Research* 306, 349–356 (2005).
  187. Sakakibara, S., Nakamura, Y., Satoh, H. & Okano, H. RNA-binding protein Musashi2: developmentally regulated expression in neural precursor cells and subpopulations of neurons in mammalian CNS. *J Neurosci* 21, 8091–8107 (2001).
  188. Clarke, R. B. et al. A putative human breast stem cell population is enriched for steroid receptor-positive cells. *Dev Biol* 277, 443–456 (2005).
  189. Szabat, M. et al. Musashi expression in beta-cells coordinates insulin expression, apoptosis and proliferation in response to endoplasmic reticulum stress in diabetes. *Cell Death Dis* 2, e232 (2011).
  190. Sakakibara, S. et al. RNA-binding protein Musashi family: roles for CNS stem cells and a subpopulation of ependymal cells revealed by targeted disruption and antisense ablation.

- Proc Natl Acad Sci U S A 99, 15194–15199 (2002).
191. Wang, X. Y. et al. Musashi1 modulates mammary progenitor cell expansion through proliferin-mediated activation of the Wnt and Notch pathways. *Mol Cell Biol* 28, 3589–3599 (2008).
  192. Keyoung, H. M. et al. High-yield selection and extraction of two promoter-defined phenotypes of neural stem cells from the fetal human brain. *Nat. Biotechnol.* 19, 843–850 (2001).
  193. Imai, T. et al. The neural RNA-binding protein Musashi1 translationally regulates mammalian numb gene expression by interacting with its mRNA. *Mol Cell Biol* 21, 3888–3900 (2001).
  194. Sugiyama-Nakagiri, Y., Akiyama, M., Shibata, S., Okano, H. & Shimizu, H. Expression of RNA-binding protein Musashi in hair follicle development and hair cycle progression. *Am J Pathol* 168, 80–92 (2006).
  195. De Andrés-Aguayo, L. et al. Musashi 2 is a regulator of the HSC compartment identified by a retroviral insertion screen and knockout mice. *Blood* 118, 554–564 (2011).
  196. Kharas, M. et al. Musashi-2 regulates normal hematopoiesis and promotes aggressive myeloid leukemia. *Nat. Med.* 16, 903–911 (2010).
  197. Hope, K. et al. An RNAi screen identifies Msi2 and Prox1 as having opposite roles in the regulation of hematopoietic stem cell activity. *Cell Stem Cell* 7, 101–114 (2010).
  198. Ito, T. et al. Regulation of myeloid leukaemia by the cell-fate determinant Musashi. *Nature* 466, 765–773 (2010).
  199. Hope, K. J. & Sauvageau, G. Roles for MSI2 and PROX1 in hematopoietic stem cell activity. *Curr Opin Hematol* 18, 203–207 (2011).
  200. Barbouti, A. et al. A novel gene, MSI2, encoding a putative RNA-binding protein is recurrently rearranged at disease progression of chronic myeloid leukemia and forms a fusion gene with HOXA9 as a result of the cryptic t(7;17)(p15;q23). *Cancer Res* 63, 1202–1206 (2003).
  201. Taggart, J. et al. MSI2 is required for maintaining activated myelodysplastic syndrome stem cells. *Nat. Commun.* 7, 10739 (2016).
  202. Byers, R. J., Currie, T., Tholouli, E., Rodig, S. J. & Kutok, J. L. MSI2 protein expression predicts unfavorable outcome in acute myeloid leukemia. *Blood* 118, 2857–2867 (2011).



203. Miyanoiri, Y. et al. Origin of higher affinity to RNA of the N-terminal RNA-binding domain than that of the C-terminal one of a mouse neural protein, musashi1, as revealed by comparison of their structures, modes of interaction, surface electrostatic potentials, and backbone . *J. Biol. Chem.* 278, 41309–41315 (2003).
204. Nagata, T. et al. Structure, backbone dynamics and interactions with RNA of the C-terminal RNA-binding domain of a mouse neural RNA-binding protein, Musashi1. *J. Mol. Biol.* 287, 315–330 (1999).
205. Ruth Zearfoss, N. et al. A conserved three-nucleotide core motif defines musashi RNA binding specificity. *J. Biol. Chem.* 289, 35530–35541 (2014).
206. Ohyama, T. et al. Structure of Musashi1 in a complex with target RNA: The role of aromatic stacking interactions. *Nucleic Acids Res.* 40, 3218–3231 (2012).
207. Kaneko, Y. et al. Musashi1: an evolutionally conserved marker for CNS progenitor cells including neural stem cells. *Dev. Neurosci.* 22, 139–153 (2000).
208. Sakakibara, S., Ueda, K., Chen, J., Okuno, T. & Yamanishi, K. Octamer-binding sequence is a key element for the autoregulation of Kaposi's sarcoma-associated herpesvirus ORF50/Lyta gene expression. *J Virol* 75, 6894–6900 (2001).
209. Cuadrado, A., Garcia-Fernandez, L. F., Imai, T., Okano, H. & Munoz, A. Regulation of tau RNA maturation by thyroid hormone is mediated by the neural RNA-binding protein musashi-1. *Mol. Cell. Neurosci.* 20, 198–210 (2002).
210. Nickerson, P. E. B., Myers, T., Clarke, D. B. & Chow, R. L. Changes in Musashi-1 subcellular localization correlate with cell cycle exit during postnatal retinal development. *Exp. Eye Res.* 92, 344–352 (2011).
211. Kawahara, H. et al. Musashi1 cooperates in abnormal cell lineage protein 28 (Lin28)-mediated let-7 family microRNA biogenesis in early neural differentiation. *J. Biol. Chem.* 286, 16121–16130 (2011).
212. Kawahara, H. et al. Neural RNA-binding protein Musashi1 inhibits translation initiation by competing with eIF4G for PABP. *J Cell Biol* 181, 639–653 (2008).
213. Wang, S. et al. Transformation of the intestinal epithelium by the MSI2 RNA-binding protein. *Nat. Commun.* 6, 6517 (2015).

214. Katz, Y. et al. Musashi proteins are post-transcriptional regulators of the epithelial-luminal cell state. *Elife* 3, e03915 (2014).
215. Park, S. M. et al. Musashi2 sustains the mixed-lineage leukemia-driven stem cell regulatory program. *J. Clin. Invest.* 125, 1286–1298 (2015).
216. Kwon, H. Y. et al. Tetraspanin 3 Is Required for the Development and Propagation of Acute Myelogenous Leukemia. *Cell Stem Cell* 17, 152–164 (2015).
217. Choudhury, N. R. et al. Tissue-specific control of brain-enriched miR-7 biogenesis. *Genes Dev.* 27, 24–38 (2013).
218. Salmena, L. et al. Review Tenets of PTEN Tumor Suppression. *Cell*, 403-414. (2008).
219. Yilmaz, H. et al. Pten dependence distinguishes haematopoietic stem cells from. *Nature*, 441(2006).
220. Zhang, Jiawang et al. PTEN maintains haematopoietic stem cells and acts in lineage choice and leukaemia prevention. *Nature*, 441 (2006).
221. Cabezas-Wallscheid, N. et al. Identification of regulatory networks in HSCs and their immediate progeny via integrated proteome, transcriptome, and DNA methylome analysis. *Cell Stem Cell* 15, 507–522 (2014).
222. Heng, T. S. P. & Painter, M. W. The Immunological Genome Project: networks of gene expression in immune cells. *Nat. Immunol.* 9, 1091–1094 (2008).
223. Morrison, S. J. & Scadden, D. T. The bone marrow niche for haematopoietic stem cells. *Nature* 505, 327–34 (2014).
224. Orkin, S. H. & Zon, L. I. Hematopoiesis: An Evolving Paradigm for Stem Cell Biology. *Cell* 132, 631–644 (2008).
225. Wilkinson, A. C. & Gottgens, B. Transcriptional regulation of haematopoietic stem cells. *Adv. Exp. Med. Biol.* 786, 187–212 (2013).
226. Vaux, D. L., Cory, S. & Adams, J. M. Bcl-2 gene promotes haematopoietic cell survival and cooperates with c-myc to immortalize pre-B cells. *Nature* 335, 440–442 (1988).
227. van Lohuizen, M. et al. Predisposition to lymphomagenesis in pim-1 transgenic mice: cooperation with c-myc and N-myc in murine leukemia virus-induced tumors. *Cell* 56, 673–682 (1989).
228. Robin, C., Ottersbach, K., Boisset, J.-C., Oziemlak, A. & Dzierzak, E. CD41 is developmentally regulated and

- differentially expressed on mouse hematopoietic stem cells. *Blood* **117**, 5088–5091 (2011).
229. Mikkola, H. K. A., Fujiwara, Y., Schlaeger, T. M., Traver, D. & Orkin, S. H. Expression of CD41 marks the initiation of definitive hematopoiesis in the mouse embryo. *Blood* **101**, 508–516 (2003).
230. Ferkowicz, M. J. et al. CD41 expression defines the onset of primitive and definitive hematopoiesis in the murine embryo. *Development* **130**, 4393–4403 (2003).
231. Pinto do O, P., Kolterud, A. & Carlsson, L. Expression of the LIM-homeobox gene LH2 generates immortalized steel factor-dependent multipotent hematopoietic precursors. *EMBO J.* **17**, 5744–5756 (1998).
232. Zhou, K. *et al.* Wnt and Notch signaling pathways selectively regulating hematopoiesis. *Ann. Hematol.* **89**, 749–757 (2010).
233. Ruiz-Herguido *et al.* Hematopoietic stem cell development requires transient Wnt/ $\beta$ -catenin activity. *J Exp Med.* **209(8)**:1457-68 (2012).
234. Magee, J. A. *et al.* Temporal changes in PTEN and mTORC2 regulation of hematopoietic stem cell self-renewal and leukemia suppression. *Cell Stem Cell* **11**, 415–428 (2012).
236. Perry, J. M. *et al.* Cooperation between both Wnt/ $\beta$ -catenin and PTEN/PI3K/Akt signaling promotes primitive hematopoietic stem cell self-renewal and expansion. *Genes Dev.* **25**, 1928–1942 (2011).
237. Huang, J., Nguyen-McCarty, M., Hexner, E. O., Danet-Desnoyers, G. & Klein, P. S. Maintenance of hematopoietic stem cells through regulation of Wnt and mTOR pathways. *Nat. Med.* **18**, 1778–1785 (2012).
238. Trotman, L. C. *et al.* Ubiquitination regulates PTEN nuclear import and tumor suppression. *Cell* **128**, 141–156 (2007).
239. Bassi, C. *et al.* Nuclear PTEN controls DNA repair and sensitivity to genotoxic stress. *Science* **341**, 395–399 (2013).
240. He, J., Kang, X., Yin, Y., Chao, K. S. C. & Shen, W. H. PTEN regulates DNA replication progression and stalled fork recovery. *Nat. Commun.* **6**, 7620 (2015).
241. Keene, J. RNA regulons: coordination of post-transcriptional events. *Nat. Rev. Genet.* **8**, 533–543 (2007).
242. Yousefi, M. *et al.* Msi RNA-binding proteins control reserve intestinal stem cell quiescence. (2016).
243. Li, N. *et al.* The Msi Family of RNA-Binding Proteins

- Function Redundantly as Intestinal Oncoproteins. *Cell Rep.* **13**, 2440–2455 (2015).
244. Ma, X. *et al.* Msi2 maintains quiescent state of hair follicle stem cells by directly repressing the Hh signaling pathway. *J. Invest. Dermatol.* (2017). doi:10.1016/j.jid.2017.01.012



